The role of human medial frontal cortex in cognition investigated by functional magnetic resonance imaging

PhD Thesis

in partial fulfillment of the requirements for the degree
"Doctor of Philosophy (PhD)/Dr. rer. nat."
in the Neuroscience Program at the Georg August University Göttingen
Faculty of Biology

submitted by

HENRY HARRY LÜTCKE

born in

EBERSWALDE-FINOW, GERMANY

Göttingen 2007

Advisor, first member of FAC:	Prof. Dr. Jens Frahm
Advisor, second member of FAC:	Prof. Dr. Stefan Treue
Third member of FAC:	Prof. Dr. Thomas Rammsayer

Date of submission of the PhD thesis:	September, 17th, 2007
Date of defense:	

I hereby declare that I prepared the PhD thesis “The role of human medial frontal cortex in cognition investigated by functional magnetic resonance imaging” on my own and with no other sources and aids than quoted.

Göttingen, September 17th, 2007 Henry Lütcke

The work presented here has been inspired by the thinking of Francis Bacon who, some 400 years ago, built the foundation of modern scientific enquiry. His profound insights have never been summarized more concisely and beautifully than by himself in Aphorism 95 of the *"The New Organon or True Directions Concerning The Interpretation of Nature"*. It is for the reader to decide if my thesis lives up to these aspirations.

> »Qui tractaverunt scientias, aut empirici, aut dogmatici fuerunt. Empirici, formicæ more, congerunt tantum et utuntur: rationales, aranearum more, telas ex se conficiunt : apis vero ratio media est, quæ materiam ex floribus horti et agri elicit; sed tamen eam propria facultate vertit et digerit. Neque absimile philosophiæ verum opificium est; quod nec mentis viribus tantum aut præcipue nititur, neque ex historia naturali et mechanicis experimentis præbitam materiam, in memoria integram, sed in intellectu mutatam et subactam reponit. Itaque ex harum facultatum (experimentalis scilicet et rationalis) arctiore et sanctiore fœdere (quod adhuc factum non est) bene sperandum est.«
>
> (from: The Works of Francis Bacon, Vol. 8, p. 49, London: England, 1819)

> »Those who have handled sciences have been either men of experiment or men of dogmas. The men of experiment are like the ant, they only collect and use; the reasoners resemble spiders, who make cobwebs out of their own substance. But the bee takes a middle course: it gathers its material from the flowers of the garden and of the field, but transforms and digests it by a power of its own. Not unlike this is the true business of philosophy; for it neither relies solely or chiefly on the powers of the mind, nor does it take the matter which it gathers from natural history and mechanical experiments and lay it up in the memory whole, as it finds it, but lays it up in the understanding altered and digested. Therefore from a closer and purer league between these two faculties, the experimental and the rational (such as has never yet been made), much may be hoped. «
>
> (translated by James Spedding, Boston: Taggard and Thompson, 1863)

Table of contents

1. Introduction

Throughout the 19th and large parts of the 20th century, neuroscientific thinking on the organization of the brain revolved around two opposing ideas. Localizationists argued that specific behavioral functions, or mental faculties, could be localized to distinct areas of the brain. Contrarily, the concept of holism, or equipotentiality, holds that any functional area in the brain has the capacity to carry out any behavior. Contemporary theories of brain function acknowledge the paucity of evidence for either of these two extreme positions and instead introduce the idea of functional specialization (Friston, 2002). Based on the principle of functional segregation (Zeki, 1990), which holds that neurons with common properties are grouped together, it is argued that cortical areas are specialized for some aspect of sensory, motor or cognitive computations. Different areas may be specialized for processing different aspects so that functions itself can be distributed.

Attempts to characterize functional specializations in various brain regions have met with mixed success. Primary sensory and motor cortices as well as their associated secondary areas were already well described by the middle of the 20th century. Large parts of the brain outside these regions (see Fig. 1), however, have been substantially more resistant to any straightforward functional organization. The so called association areas have been implicated in sensorimotor transformations, cognition or emotions. Interestingly, these parts of the cortex also develop late both in phylogeny and ontogeny (Fuster, 2002).

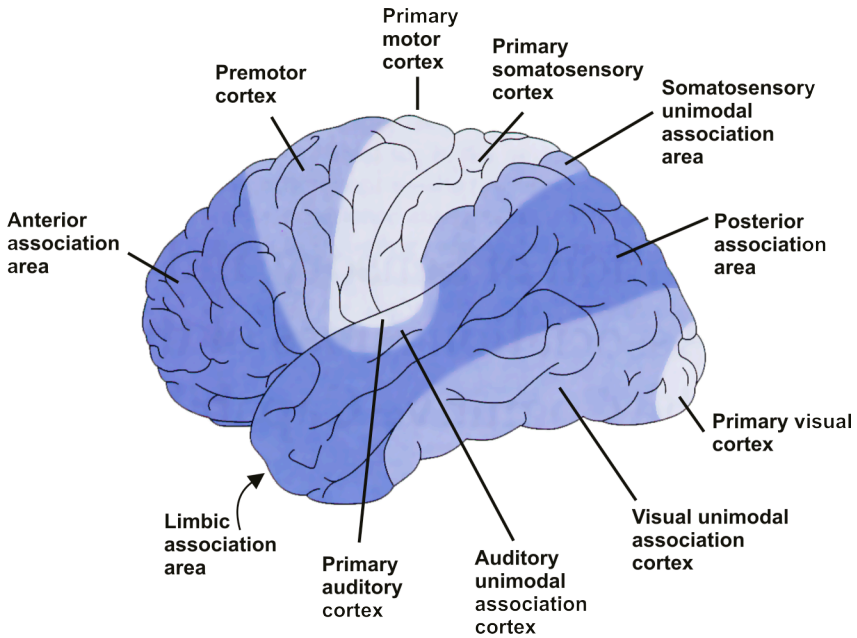

Fig. 1. Primary (light blue) and association (dark blue) areas in the human brain (from Kandel et al., 2000).

Association areas may be poorly understood because they are difficult to study with common model organisms. Whereas basic sensory and motor paradigms are easily transferable to experimental animals, the translation of cognitive tasks has proven to be substantially more complex. Even more problematically, a straightforward structural homology of association areas between organisms, for example rodents and primates, has been questioned (Brown and Bowman, 2002). Electrophysiological or lesion studies in non-human primates, usually rhesus monkeys, have partly addressed this concern since they are sufficiently similar to humans and allow investigation of complex cognitive paradigms (e.g. working memory; Funahashi *et al.*, 1989). Ironically it is precisely this similarity to humans which leads to ethical concerns about invasive primate experiments and forbids studying of large sample sizes. To investigate the neural mechanisms of cognitive functions in humans, patients with selective injuries to parts of the brain have been studied extensively (Luria, 1980). While patient studies have contributed immensely to our understanding of higher cognitive functions in man, especially with respect to organization of the prefrontal cortex (Shallice, 1982), they also suffer from serious shortcomings. First of all, lesions are rarely selective and, if they are, researchers are usually limited to studying a single patient. Secondly, potential reorganization of brain circuits after injury may limit the applicability of findings to the general population.

Given these limitations, the advent of modern neuroimaging techniques, such as functional magnetic resonance imaging (fMRI) and positron emission tomography (PET) in the early 1990s has considerably enhanced our ability to systematically study the functional organization of association areas in the healthy human brain. The introduction of fMRI has been particularly welcomed by the cognitive neuroscience community as it is essentially non-invasive (unlike PET) and therefore allows for the repeated measurement of large samples of volunteers. Further advantages of fMRI include its high spatial resolution, the ability to image the whole brain and the increasing availability of MR scanners. Consequently, it is no surprise that the first cognitive fMRI studies (e.g. McCarthy *et al.*, 1994) appeared shortly after the initial presentation of the technique (Ogawa *et al.*, 1992). Numerous investigations have been performed ever since and there can be no doubt that our understanding of human cognition has benefited substantially from this surge in neuroimaging studies (e.g. frontal cortex function; Duncan and Owen, 2000). On the other hand, it is also true that the multitude of studies has led to many discrepant results which are difficult to reconcile or even contradictory. The latter objection is particularly true for the medial frontal cortex (MFC), a brain region which has been suggested to play a role in a wide range of functions, from

cognition over emotions to social paradigms (see below). A number of reasons could account for these discrepancies, including lack of spatial resolution, substantial individual variability within the region or inappropriate and difficult to interpret experimental paradigms.

To address some of these concerns and reinvestigate the role of MFC in cognition, I used functional MRI to perform three experiments. After an overview of regional anatomy and function as well as methodological concerns has been given, the experiments will be described separately in the subsequent chapters. The first study reinvestigated the role of MFC in conflict and error processing by using a novel fMRI approach which allows for very high spatial resolution. This experiment addressed the issue of limited spatial resolution which may have led to discrepancies between previous studies. Secondly, we performed a direct comparison of the neural basis of conflict processing and anticipatory behavior, both of which have been implicated in MFC function. To investigate the extent of between-subject variability in MFC activation, we performed an extensive analysis of data from individual volunteers. Finally, in the third experiment, I developed a neurofeedback paradigm based on fMRI. The approach permits modulation of brain function in healthy volunteers and will allow a more direct test of hypotheses on MFC function in future experiments.

2. Anatomical organization of MFC

Medial frontal cortex may be broadly defined as the cortex dorsal and rostral to the corpus callosum. As such it is part of the frontal lobe and may be subdivided into two main regions (Rushworth *et al.*, 2004; see also Fig. 2). Anterior cingulate cortex (ACC), located directly adjacent to the corpus callosum, comprises roughly Brodmann's areas (BA) 24 and 32. Human homologue of macaque superior frontal gyrus (SFG) is located further dorsally, separated from ACC by the cingulate sulcus. SFG, which is also sometimes referred to as medial frontal gyrus (MFG), comprises the medial portion of BAs 6, 8 and 9. Based on functional imaging studies, ACC has been further subdivided into a dorsal (dACC) and a rostral (rACC) component (Polli *et al.*, 2005). Roughly, dACC corresponds to BAs 24' and 32' whereas rACC is located in the vicinity of BAs 24 and 32 proper (see Fig. 2). Functional areas within SFG include supplementary motor area (SMA, usually associated with BA 6), pre-SMA as well as the supplementary eye field (SEF). In fact, SEF is thought to mark the rostral boundary of SMA, separating it from the more anterior pre-SMA (Sumner *et al.*, 2007). Finally, a small portion of subcallosal cortex is usually included in MFC (BA 25 and part of BA 32; see Fig. 2), which however is not functionally relevant to the current investigation.

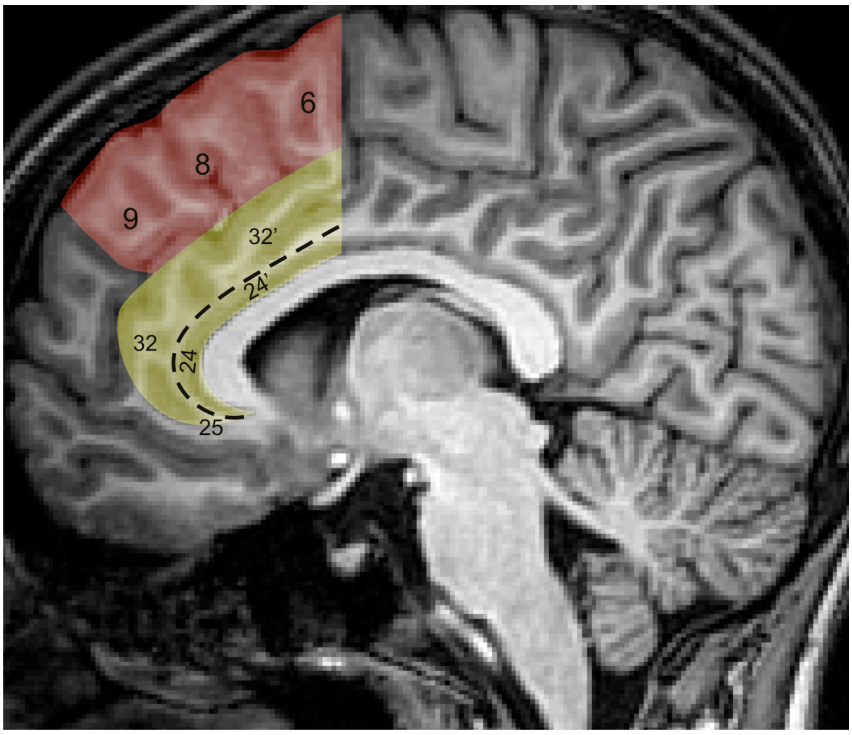

Fig. 2. Organization of medial frontal cortex with superior frontal gyrus (red) and anterior cingulate cortex (yellow). Approximate locations of Brodmann areas are indicated.

In a seminal anatomical MRI study of 247 volunteers, Paus and colleagues (Paus *et al.*, 1996) revealed a surprising degree of structural variability in the medial frontal region of the human brain. Most notably, the sulcal pattern in front of the corpus callosum (comprising ACC and more anterior cortex) was found to be highly ambiguous and difficult to classify. Furthermore, the authors reported a hemispheric asymmetry in sulcal organization (paracingulate sulcus was more developed in the left hemisphere) as well as sex differences.

To summarize, MFC presents as a structurally complex entity with a high degree of inter-individual variability, which suggests that discrepant functional attributions may, at least in part, be due to investigation of heterogeneous brain regions in different studies.

3. Functions of MFC in human behavior

In light of the plethora of studies aimed at a better understanding of MFC's role in the generation of behavior, a comprehensive review of the subject is in the interest of neither the reader nor the author of this thesis. The following section provides a selective overview of imaging studies implicating MFC in the domains of cognition, emotion, pain perception and social reasoning. In the interest of succinctness, important insights from other techniques, especially monkey electrophysiology, will not be considered. A more comprehensive summary of the available literature on MFC function in various processing domains can be found in several excellent reviews (emotion: Bush *et al.*, 2000; pain: Rainville, 2002; cognition: Botvinick *et al.*, 2004; social: Amodio and Frith, 2006). Finally, I will postpone the question, how these various findings may be integrated, to the discussion, where a unification of the results will be attempted in the light of current models of MFC function.

Cognition

With the onset of imaging studies of MFC function, the region has been implicated in various kinds of cognitive tasks. Among the most important are tasks in which subjects have to resolve conflict between competing responses, paradigms which involve a high degree of erroneous responses as well as anticipatory behavior. As these form the proper subject of the thesis, they will be discussed in detail in the respective chapters.

A few neuroimaging studies have associated visuospatial processing and memory retrieval with MFC. The evidence for a selective role of the region in these paradigms remains, however, inconclusive.

Emotion

It has been appreciated for quite some time that ACC is part of the limbic system, a circuit of brain regions involved in the generation of emotions (Papez, 1995). Not surprisingly then, a recent meta-analysis of 55 neuroimaging studies of emotion (Phan *et al.*, 2002) reported that MFC is recruited during various emotional paradigms, irrespective of affective type (positive or negative). Furthermore, ACC in particular seemed to be involved in emotional recall or imagery. In a PET study, Damasio and colleagues (Damasio *et al.*, 2000) observed strong ACC activation when subjects recalled and attempted to re-experience strong emotional episodes of sadness, anger and, to a lesser extent, happiness.

It is commonly accepted that emotions are associated with modulations of autonomic functions, such as increased heart rate and pupil dilation during fear. Interestingly, several recent imaging studies have reported a strong association between ACC and autonomic nervous system activity (Critchley *et al.*, 2003; Critchley *et al.*, 2005). Activation in ACC during emotional paradigms may therefore be due to concurrent variations in autonomic function, which are usually not accounted for.

Pain perception

Painful stimuli elicit strong and robust brain responses in ACC, as shown by both PET (Jones *et al.*, 1991) and fMRI (Ploghaus *et al.*, 1999). Further evidence suggests that rACC in particular plays a role in pain modulation and affect. A seminal study by Rainville and colleagues (Rainville *et al.*, 1997) used hypnosis to modulate perceived pain affect while physical stimulus intensity was kept constant. Surprisingly, rACC emerged as the only component of the pain matrix whose activity correlated significantly with perceived pain affect.

Social reasoning

The relatively young discipline of social cognitive neuroscience characterizes neural correlates of social processes, such as perception of the self, perception of others or thinking about others' thoughts (Amodio and Frith, 2006). Interestingly, in several neuroimaging studies, social cognitive paradigms have elicited surprisingly selective activation in MFC. In a recent fMRI study, subjects activated anterior rACC when they formed impressions of other people versus inanimate objects (Mitchell *et al.*, 2005). Mentalizing, the ability to form representations of other people's thoughts, also relies on MFC. Fletcher and colleagues (Fletcher *et al.*, 1995), using PET reported significantly elevated responses in the region when subjects had to judge other people's mental states in order to solve a story comprehension task.

Explaining the diversity of activations

A number of reasons could account for the observed multitude of activations in MFC. First of all, it is possible and given the evidence quite likely, that MFC is a heterogeneous structure, with subregions that are differentially selective for different task aspects. Conceivably, the spatial resolution of current functional imaging techniques may be too coarse to resolve all specializations within the region.

Secondly, the substantial inter-individual variability within MFC, both anatomical and functional, may contribute significantly to the discrepancies between different studies. The fact that neuroimaging studies have so far largely neglected variability in favor of group activation centers may conceal important information, as will be shown below. According to this view, ACC is indeed organized in different functional modules, specialized for cognitive, emotional or other processes, but these modules differ in their precise arrangement between individuals.

Thirdly, MFC may be specialized to process one specific task aspect which is common to the paradigms reported before, yet this 'meta-function' has so far remained elusive.

Finally, these reasons are certainly not exclusive of each other. It will be argued in the discussion that a combination of the above suggestions may best inform future studies of MFC function and give some leeway in understanding its role in behavior.

4. Methodological aspects concerning fMRI

Basic principles of magnetic resonance imaging

Functional MRI is essentially an adaptation of standard magnetic resonance imaging which has become widely used in clinical settings to obtain high resolution images of the interior of the human body. MRI exploits the magnetic properties of atomic nuclei (hence, it is also known as nuclear magnetic resonance, NMR). A detailed discussion of the fundamental principles underlying MRI is beyond the scope of the thesis and I will therefore only discuss some basic issues (see also Jezzard *et al.*, 2001, especially chapters 1 and 3 - 7). At the heart of the technique is a large permanent magnetic field (B_0; 3 Tesla in the current experiments). Protons that are placed into the field align their spins either parallel or antiparallel to B_0. The parallel state is energetically favorable compared to the antiparallel state. In other words, energy is required to move a proton from a state where its spin is parallel to B_0 into the antiparallel state. Consequently, if a proton falls from the antiparallel to the parallel state, energy is released. Due to thermal motion the total difference between protons in parallel and antiparallel states is very small, there are, however, an enormous number of protons in a tiny volume of tissue and it therefore becomes possible to exploit the effect of B_0 on them.

In order to obtain a signal, we briefly apply an electromagnetic pulse at a specific frequency (Lamor Frequency). This pulse provides sufficient energy to move a tiny portion of protons from the parallel to the antiparallel spin state. The macroscopic manifestation is a flipping of the magnetization vector (z) by a certain flip angle into the transverse plane. When the excitation pulse is switched off, protons with antiparallel spins gradually return to the parallel spin orientation. Macroscopically, this leads to a cycling of the z vector in the transverse plane (with the characteristic frequency) gradually approaching its original configuration in the longitudinal plane. This process is characterized by two relaxation times, the longitudinal relaxation time, T_1 and the transverse relaxation time, T_2. During the relaxation process, the cycling magnetization vector induces a current in the receiving coil which is recorded and then converted into an intensity signal. The signal decays rapidly with time depending, in theory, on the rate of transverse relaxation, given by $1/T_2$. In practice, however, signal decay occurs faster than would be expected from a T_2 - dependent decay. The reason for this can be seen when considering that the relaxation frequency is directly proportional to the strength of the magnetic field, B_0.

$$\omega = \gamma B_0 \tag{1}$$

In this equation ω represents the relaxation frequency and γ stands for the gyromagnetic moment (which is 42 $MHz*T^{-1}$ for protons). It follows from equation 1 that small but inevitable fluctuations in a magnetic field that is not perfectly homogeneous will lead to slightly different relaxation rates at different points in the tissue. This "dephasing" accumulates over time and leads to a progressive decrease in the signal. In order to take into account these effects, an effective transverse relaxation time (T_2^*) is usually stated. Thus, the amount of detectable signal is a function of the effective transverse relaxation time, T_2^*.

Spatial encoding in MRI is made possible by applying additional magnetic fields during the acquisition (and excitation) period using gradient coils. These gradients bring about systematic changes in the magnetic field which lead to excitation and emission variations. Analyzing and transforming these variations eventually yields spatially localizable information. As an example, consider the problem of slice selection. In this case, a magnetic field gradient is applied during the excitation pulse such that, for example, the anterior end of the body experiences a stronger B_0 field than the posterior end. As the Lamor frequency depends on the magnitude of B_0, giving an excitation pulse with a very precisely determined wavelength will only excite the protons in the part of the body which meets the resonance condition (equation 1). Consequently, a signal will only be recorded from the selected slice.

fMRI

Before the advent of human fMRI, animal experiments had shown that the use of exogenous contrast agents (e.g. Gadolinium) can alter the signal strength during magnetic resonance imaging. Subsequent research (e.g. Ogawa *et al.*, 1992) established that an endogenous contrast agent, deoxygenated hemoglobin (rHb), could be used to monitor brain activity. When oxygenated hemoglobin releases its bound oxygen into the tissue, it becomes a paramagnetic substance which causes local dephasing of the relaxation process leading ultimately to a loss of the water proton signal, as discussed above. In other words, if MRI sequences are chosen that are susceptible to changes in T_2^* (gradient echo sequences with a long echo time, TE) the amount of signal obtained will be inversely proportional to the concentration of rHb. This technique, known as "blood oxygen level dependent functional magnetic resonance imaging" (BOLD fMRI) can be used for functional investigations of the brain because neural activity and blood oxygenation level are tightly coupled. Unfortunately, this relationship is non-trivial as multiple parameters with an influence on blood oxygen level change in response to a change in neural activity. Most importantly, however, an increase in neural activity is accompanied by a swift increase in the rate of cerebral blood flow (CBF) by

approximately 40%, resulting in blood hyperoxygenation (reduced concentration of rHb). This effect leads to an fMRI signal gain, which is known as the BOLD response.

The BOLD response has been extensively characterized (e.g. Fransson *et al.*, 1998). In response to a brief visual stimulus, the signal increase can be detected 1.5 to 2 seconds after stimulus onset (due to hemodynamic latency) and achieves a maximum of around 4%, with respect to the previous baseline, by 5 to 7 seconds after stimulus onset. Most importantly, the signal does not return to the prestimulus baseline for more than one minute after stimulus onset. In paradigms that employ short interstimulus intervals (ISI) it is therefore vital to ensure that consecutive episodes are not contaminated by previous activation. Previous work (Rosen *et al.*, 1998) suggests that fast presentation paradigms (as low as 2 s ISI) are possible in fMRI if jittered stimulus presentation is employed.

While the temporal resolution of fMRI is limited by the BOLD response's sluggishness, the technique provides exquisite spatial resolution, ideally within the sub-millimeter range (Voit and Frahm, 2005). In practice, however, the majority of fMRI studies, especially when employing cognitive paradigms, have imaged at much lower spatial resolution (at best $3\times3\times3$ mm^3 but frequently worse) in order to gain signal-to-noise ratio (SNR) and achieve whole-brain coverage. As we have demonstrated, it is however perfectly feasible to perform cognitive fMRI with almost millimeter spatial resolution (see below as well as Lütcke and Frahm, in press).

Analysis of fMRI data

MR signal changes elicited by sensory, motor or cognitive challenges are extremely weak, amounting only to a fraction of a percent for some cognitive paradigms. Not surprisingly then, numerous strategies for the evaluation of fMRI data have been proposed (Jezzard *et al.*, 2001, chapters 11 - 16). In the following, I will outline a number of analysis techniques that were employed in the experiments to be presented. The majority of described procedures are available within the free fMRI analysis suite FSL (FMRIB's software library, www.fmrib.ox.ac.uk/fsl; Smith *et al.*, 2004) which was employed for most of the data processing during my thesis.

Prior to any statistical evaluation, reconstructed images are frequently preprocessed to remove artifacts and enhance the SNR. Low frequency components are common in fMRI time series and typically taken to reflect non-physiological signal components due to, for example, gradient coil heating. Consequently, they are removed by high-pass filters, such as a Gaussian-weighted straight line fit. In addition, images are frequently spatially low-pass

filtered in order to optimize SNR. The most common procedure involves convolution with a Gaussian kernel of a given full width at half maximum (FWHM) which determines the extent of image blurring. Gaussian smoothing reduces the effective spatial resolution and therefore should be used cautiously since extensive blurring may remove small activation foci. Promisingly, recent fMRI studies have employed non-linear, structure-preserving filtering algorithms that enhance SNR but do not smooth across anatomical boundaries (Smith and Brady, 1997).

The vast majority of fMRI studies follow a mass univariate strategy for statistical data evaluation. In this framework, the similarity of each image point's (voxel's) time series with a suitably adjusted reference vector, based on the stimulation paradigm (usually by convolution with a Gamma function which models the shape of the hemodynamic response), is determined. In the simplest case, this amounts to computation of the correlation coefficient (R) between each voxel's time series (Y) and the reference vector (X):

$$R = \frac{\sum_{t=1}^{N}(X_t - \overline{X})(Y_t - \overline{Y})}{\sqrt{\sum_{t=1}^{N}(X_t - \overline{X})^2 \sum_{t=1}^{N}(Y_t - \overline{Y})^2}} \tag{2}$$

To allow for multiple explanatory variables (predictors), the correlation analysis has been extended to the general linear model (GLM) which may be expressed as:

$$y_n = b_0 + b_1 X_{n1} + \cdots + b_k X_{nk} + e_n \tag{3}$$

The GLM minimizes the sum of squares of the error term (e) by determining optimal beta-weights ($b_1 \ldots b_k$) for each of the predictors ($X_1 \ldots X_k$). The first beta-weight (b_0) represents the baseline signal intensity around which the measured values fluctuate. The GLM permits direct comparison of the contribution of each predictor to the model fit by simple comparison of the associated beta-weights (contrasts). The statistical significance of the fitted model may be determined by the ratio between the variance of estimated ($\hat{y}$) and the variance of measured values (y):

$$R^2 = \frac{Var(\hat{y})}{Var(y)} \tag{4}$$

The multiple correlation coefficient R may then be used for an *F*-test with N-1 and N-k degrees of freedom, where N is the number of time points and k the number of predictors:

$$F = \frac{R^2(N-k)}{(1-R^2)(k-1)} \tag{5}$$

For easier communicability of findings, *F*-values are frequently converted to *z*-scores which are simply gaussianized representations of the statistic.

Assessment of the significance of statistical parameters is non-trivial as thousands of voxels need to be examined consecutively, yet they are not all strictly speaking independent, due to the inherent and imposed smoothness of the data set. Thus, statistical inference amounts to a multiple comparison problem with an unknown number of independent examinations. Numerous strategies for dealing with this situation have been proposed and are known as thresholding techniques (e.g. Worsley *et al.*, 1992; Genovese *et al.*, 2002; Baudewig *et al.*, 2003). In the present experiments, two techniques were employed in the majority of cases. Cluster thresholding (Worsley *et al.*, 1992) relies on initial determination of active voxels based on a liberal threshold (e.g. $z > 2.3$). Subsequently, the probability of occurrence of each cluster of activated voxels under the null hypothesis is determined within the framework of Gaussian Random Field (GRF) theory and clusters are eliminated if their probability exceeds a certain threshold (e.g. $p > 0.05$). Importantly, cluster thresholding demands that data are sufficiently smooth, which is not the case for unprocessed high-resolution fMRI data. Recently, thresholding based on the false discovery rate (FDR; Genovese *et al.*, 2002) has emerged as a new inference approach that does not rely on spatial smoothing. Intuitively, FDR controls the number of false positives at a given level, *q* (i.e. if $q \leq 0.05$, the number of voxels that are falsely considered active does not exceed 5%, on average).

Finally, to permit averaging of results across multiple subjects, comparison with published studies as well as to facilitate anatomic referencing, functional data are usually registered to subjects' anatomical scans as well as to a standard brain using linear registration techniques. We chose the Montreal Neurological Institute 152 (MNI152) referencing system as standard space for group analysis, as it is based on averaged MRI scans from a representative sample of the western population. Subsequent group analysis is commonly performed also in the framework of the GLM.

5. High-resolution fMRI of anterior cingulate function

5.1. Introduction

In a permanently changing environment, only few things seem to be more important for the pursuit of stable, long-term goals than the ability to constantly monitor one's own actions, initiate changes in the face of new external demands, or abandon unsuccessful strategies altogether. Such a capacity for cognitive control may well be one of the hallmarks of human behavior.

Architecture of cognitive control

Far from being a unitary concept, however, cognitive control mechanisms can be subdivided into a number of components (Ridderinkhof *et al.*, 2004). Prior to the exertion of control over a specific behavior, an action needs to be selected. Action selection is therefore the first step in the cognitive control cycle (see Fig. 3) and may be based either on internal deliberations or external stimulus – response mappings.

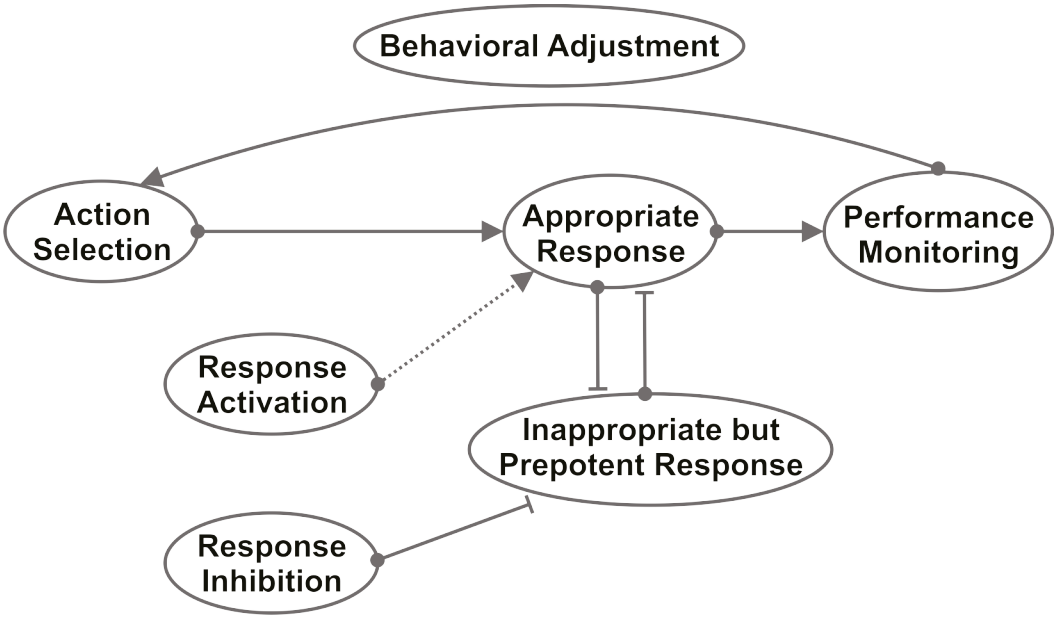

Fig. 3. Cognitive control cycle (based on Ridderinkhof *et al.*, 2004). Selected actions are thought to be reinforced by response activation processes. More importantly, inappropriate responses are strongly inhibited. Furthermore, competing responses inhibit each other. Once initiated, responses are monitored and, if necessary, behavior is adjusted accordingly. See text for details.

Selected actions frequently have to compete for activation with strong alternative responses, requiring cognitive control to resolve such response conflict. Inhibitory processes are thought to play a central role when resisting interference from alternative actions in order

to ensure timely and accurate execution of appropriate responses (see Fig. 3). In the context of the current work, inhibition may be defined as the suppression of inappropriate but prepotent response tendencies (Aron *et al.*, 2004). A number of tasks have been devised to assess inhibitory processes, most famously the Stroop test (Stroop, 1935). In this task, subjects have to suppress color word reading (prepotent response) in favor of naming the color in which the word is typed.

In order to ensure that actions and their outcome are in agreement with internal goals, performance needs to be continuously monitored (see Fig. 3). Errors have a particular relevance in this respect as they signal the need for modifications in current response pattern. Behavioral adjustments in response to errors may be the most prominent and easily measured signature of performance monitoring. It is clear, however, that a number of internal evaluation processes must be occurring even if subjects perform without errors.

Neural correlates of cognitive control in MFC

Numerous studies have identified medial frontal cortex, and especially its anterior cingulate part, as a reliable correlate of cognitive control in the human brain (reviewed in Botvinick *et al.*, 2004). Error processing was associated with MFC in an early electrophysiological study by Gemba and colleagues (Gemba *et al.*, 1986). They recorded characteristic potentials following errors in rhesus monkey's ACC. Subsequent electroencephalography (EEG) studies (Falkenstein *et al.*, 1991; Gehring *et al.*, 1993) revealed a typical fronto-median negativity which coincided with error occurrence and was therefore named error-related negativity (ERN). Functional imaging studies confirmed the importance of ACC for error processing in humans and demonstrated that internally as well as externally generated errors implicate MFC (Ullsperger and von Cramon, 2003; Holroyd *et al.*, 2004).

Evidence for a role of ACC in resolution of response conflict has been obtained in a number of functional neuroimaging studies (Carter *et al.*, 1998; Botvinick *et al.*, 1999; Barch *et al.*, 2001). Using a speeded response task, Garavan and colleagues (Garavan *et al.*, 1999) showed that MFC, together with a right-lateralized prefrontal network, is involved in inhibition of prepotent responses.

Although both conflict and error processing elicit brain responses in MFC, it is currently unknown if both involve similar networks or whether they may be localized to distinct subregions within the area. To this end, several researchers have proposed a functional subdivision of ACC (Polli *et al.*, 2005; Taylor *et al.*, 2006). Based on fMRI evidence, Taylor and colleagues (Taylor *et al.*, 2006) suggested that the dorsal part of ACC

plays a role in conflict monitoring, whereas its rostral component may be more involved in error-specific processing such as performance evaluation (reviewed in Lütcke, 2006). On the other hand, these authors also demonstrated a surprising degree of inter-subject variability for activation foci along the mesial wall, suggesting that discrepancies in the localization of conflict or error-related processing between previous studies may be due to differential clustering of the subjects' activation in the different samples.

High-resolution fMRI of conflict monitoring and error processing

In the present study, we used high-resolution fMRI to investigate the functional anatomy of ACC and determine potential differences between error and inhibition processes at a previously unaccomplished spatial scale. While earlier fMRI studies have employed voxel sizes on the order of $3 \times 3 \times 3$ mm^3, the technique itself allows for acquisitions with at least an eight times smaller voxel size of $1.5 \times 1.5 \times 1.5$ mm^3. Additionally, uncritical use of post-processing procedures, such as spatial smoothing, introduced further spatial inaccuracies in previous studies.

We employed a GoNogo task, which was designed to generate high proportions of errors on Nogo trials and therefore allowed us to compare putative neural correlates of conflict as well as of error monitoring processes. Whereas successful conflict resolution implicates only conflict monitoring, error trials involve both conflict and error-related mechanisms.

Functional MRI at high spatial resolution has previously been used to study early sensory processes, mainly in the visual system (Schneider *et al.*, 2004; Schwarzlose *et al.*, 2005; Grill-Spector *et al.*, 2006). These studies benefited from the good functional contrast-to-noise ratio (CNR) as well as limited inter-subject variability in sensory areas. Cognitive neuroimaging, on the other hand, suffers from low CNR and high variability, making it apparently unsuitable for high-resolution fMRI. Thus, a more general aim of the current study was to investigate the feasibility of a new strategy for cognitive neuroimaging combining low and high spatial resolution.

5.2. Materials and Methods

Subjects

Eleven right-handed volunteers (3 male and 8 female; mean age 27 ± 6 years) participated in two experimental sessions (separated by more than 1 day). One data set was excluded due to excessive motion (relative displacement in any direction of more than 1 mm). In each experimental session, subjects performed between 4 to 6 repetitions of the experiment. Thus, we obtained a total of 50 standard and 64 high-resolution runs for analysis. Given the substantial variability in activation between subsequent runs, partly attributable to factors such as fatigue, motivation or hardware changes, each experiment was treated independently for the purpose of statistical analysis. To investigate reproducibility of high-resolution activation maps, one male subject took part in two high-resolution sessions (separated by 6 months). All participants were informed about the purpose of the study as well as possible risks associated with MRI. Written consent was obtained prior to each experimental session. After the end of the second session, subjects were debriefed about the staircase procedure (see below). Participants earned 10 Euros per hour plus a bonus depending on their performance (see below). All experimental procedures conformed fully to institutional guidelines.

Task

We used a visual letter-based GoNogo task where subjects had to press a button with their right thumb or index finger whenever a Go (target) stimulus (A, J, S, O) appeared in the center of the screen (see Fig. 4). Subjects were instructed to refrain from pressing the button upon presentation of a Nogo (non-target) stimulus (X).

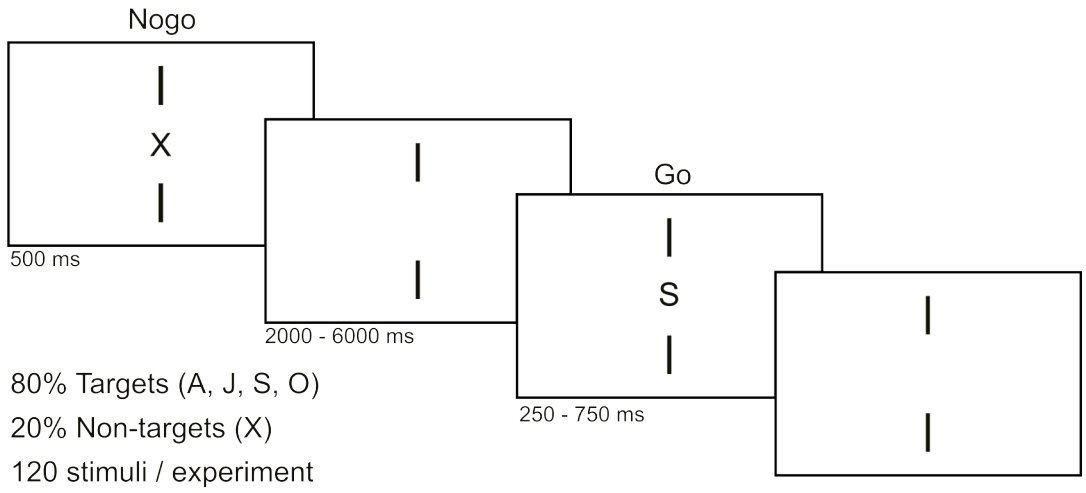

Fig. 4. Schematic representation of the GoNogo paradigm. See text for details.

All stimuli were presented in black color on a grey background. Two yellow vertical bars were continuously presented above and below the stimulus location, in order to direct subjects' attention to the center of the screen and to provide feedback (see below).

A total of 120 stimuli were presented per run (20% Nogo) with jittered stimulus onset asynchrony (2, 4, 6 s; mean 4 s) using a dedicated projection setup (Schäfter & Kirchhoff, Hamburg, Germany) or MRI-compatible liquid crystal display goggles (Resonance Technology Inc., Northridge, CA, USA). Corrective lenses were applied if necessary.

The initial presentation duration for all stimuli was 500 ms and subjects were instructed to respond within this time frame. Subjects were informed about an error (late response to target or response to non-target) immediately after a trial by briefly changing the color of the vertical bars to red. Usually subjects achieve high performance accuracy on this task (less than 10% false alarms), which makes the analysis of errors virtually impossible. Therefore we modified the presentation time of targets over the course of each run depending on subjects performance on Nogo trials. More precisely, two consecutive successful inhibitions led to a reduction of the Go stimulus duration by 50 ms (minimum presentation time 250 ms), whereas two consecutive responses to Nogo stimuli increased target duration by 50 ms (maximum presentation time 750 ms). These values were found to yield approximately 50% errors during pre-testing. Importantly, the presentation duration of Nogo stimuli was always 500 ms. Participants received a small bonus for correct trials, whereas errors incurred a financial penalty.

Magnetic Resonance Imaging

All studies were conducted at 2.9 T (Siemens Tim Trio, Erlangen, Germany) using a 12-channel receive-only head coil in combination with the whole-body coil for radiofrequency pulse transmission. Each session comprised T_1-weighted MRI using a 3D FLASH sequence at $1 \times 1 \times 1$ mm^3 resolution for anatomic referencing. For fMRI we employed a single-shot gradient-echo EPI sequence (TR/TE = 2000/36 ms, flip angle 70°, 244 volumes per run). Scans with a voxel size of $2 \times 2 \times 4$ mm^3 were based on a 84×96 acquisition matrix (192 mm FOV, 7/8 partial Fourier phase encoding, bandwidth 1336 Hz/pixel, echo spacing 0.81 ms) and comprised 22 transverse-to-coronal slices, covering the whole cerebrum. High-resolution fMRI with a voxel size of $1.5 \times 1.5 \times 1.5$ mm^3 was achieved using a 90×128 matrix (180×192 mm rectangular FOV, 6/8 partial Fourier phase encoding, bandwidth 1396 Hz/pixel, echo spacing 0.86 ms) with 18 slices, positioned so as to achieve good coverage of the previously determined active region in ACC.

Data Analysis

Evaluation of fMRI data was performed using tools from the FMRIB Software library (FSL, www.fmrib.ox.ac.uk) and MATLAB (The MathWorks, Natick, Massachusetts). After initial motion correction in k-space (Siemens, Erlangen, Germany) residual motion was accounted for by image-based registration (Jenkinson *et al.*, 2002). Data at standard resolution were smoothed using a Gaussian kernel of FWHM 5 mm. Non-brain tissue was removed (Smith, 2002) and all volumes were intensity normalized by the same factor and temporally high-pass filtered (Gaussian-weighted least-squares straight line fitting, with high-pass filter cut-off at 30 s). High-resolution data were preprocessed in a similar way but, instead of Gaussian smoothing, the images were filtered with the smallest univalue segment assimilating nucleus (SUSAN) noise reduction algorithm, also part of FSL (Smith and Brady, 1997). Briefly, the SUSAN algorithm performs 3D edge detection to identify anatomical regions and subsequently smoothes the image with a standard Gaussian kernel but only within anatomical areas, not across their boundaries. Intensity thresholds for the definition of anatomical regions were set to one tenth of the maximum image intensity, separately for each volume, and smoothing was performed within regions of similar intensity using a 5 mm Gaussian kernel.

To compare brain responses associated with correctly resolved and erroneous Nogo trials, we created models for correct rejections (CR) and false alarms (FA) by convolving relevant events with a Gamma function which takes into account temporal properties of the hemodynamic response to neural activation. Model fit was determined by statistical time-series analysis in the framework of the general linear model and with local autocorrelation correction (Woolrich *et al.*, 2001).

Standard resolution images were spatially normalized to the MNI152 template brain and mixed-effects group analysis was performed (Beckmann *et al.*, 2003; Woolrich *et al.*, 2004). Significant activations based on z statistic (Gaussianised T/F) images were obtained by first determining clusters of $z > 3.1$ and then applying a corrected cluster threshold of $p = 0.05$, as described above (Worsley *et al.*, 1992).

High-resolution images were spatially normalized to their respective anatomic scan as well as to the MNI152 template brain (Jenkinson and Smith, 2001; Jenkinson *et al.*, 2002) and summarized for each subject using a fixed effects model. Statistical inference was restricted to an anatomically defined region of interest (ROI) covering the entire MFC. We considered voxels active that surpassed an uncorrected threshold of $p \leq 0.01$ and had at least five activated neighbors. This rather liberal thresholding was motivated by the less severe multiple

comparison problem due to spatial restrictions on statistical inference as well as the fact that maps of individual subjects were analyzed. A second higher level analysis examined effects across all subjects and over the whole volume covered. Thresholded activation maps were obtained by controlling the false discovery rate (FDR), discussed above, at $q \leq 0.01$ (Genovese *et al.*, 2002).

Subsequently, ROIs in dACC and rACC were defined individually for each subject by drawing a line at the anterior boundary of the genu of the corpus callosum that was at right angles to the intercommissural plane (Devinsky *et al.*, 1995; Polli *et al.*, 2005; see Fig. 5). Rostral and dorsal parts were further subdivided according to hemisphere, yielding four ROIs. Normalized mean parameter estimates (beta-weights) from these regions as well as the number of activated voxels in each ROI were subjected to statistical analysis (all p values Bonferroni corrected for multiple comparisons).

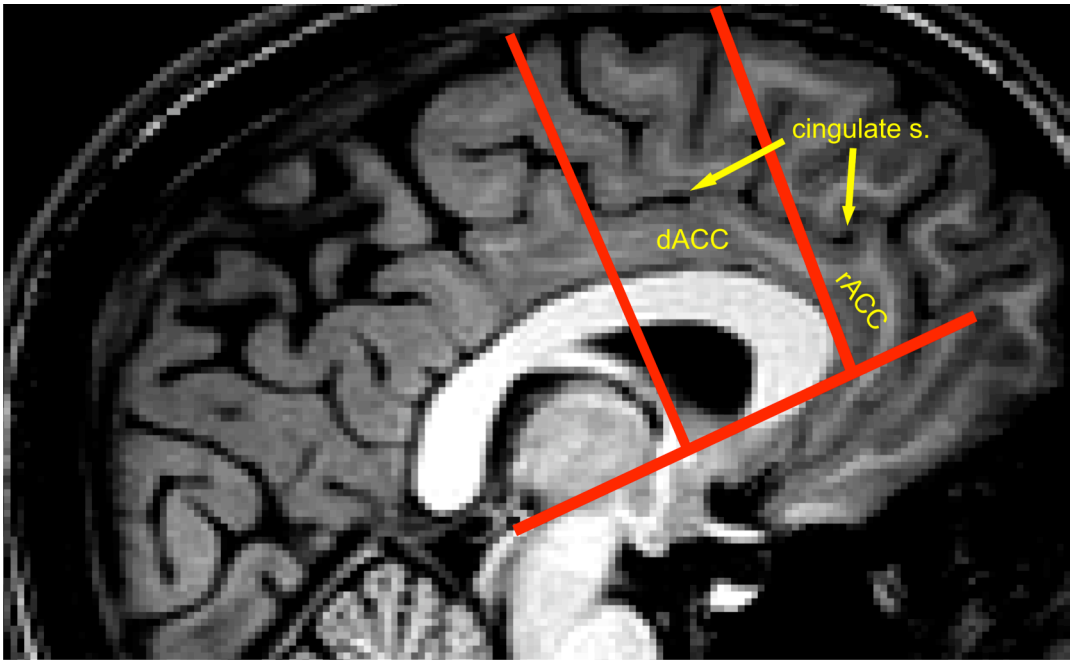

Fig. 5. ROI definition in ACC according to Polli and colleagues (Polli *et al.*, 2005). ROIs were defined individually for each subject based on the respective high resolution anatomical scan. A line perpendicular to the intercommissural plane and crossing it at the anterior commissure defines the posterior boundary of ACC. The border between dACC and rACC is marked by a second line at the anterior boundary of the genu of the corpus callosum that was at right angles to the intercommissural plane.

5.3. Results

Psychophysics

There were no significant differences for any of the behavioral measures (reaction time, accuracy) between the standard and high-resolution sessions (see Fig. 6). The error rate on Nogo trials was high (57 ± 7% correct rejections), demonstrating validity of the staircase procedure. Furthermore, errors proved to be behaviorally relevant, as shown by significantly slower reaction times (RT) after a FA, compared to responses before FAs (372 ms versus 348 ms, $t_{(20)} = 5.74$, $p < 0.001$, see Fig. 7). Conversely, subjects did not adjust their RT after a correct rejection (359 ms versus 357 ms, $t_{(20)} = 0.83$, $p = 0.42$).

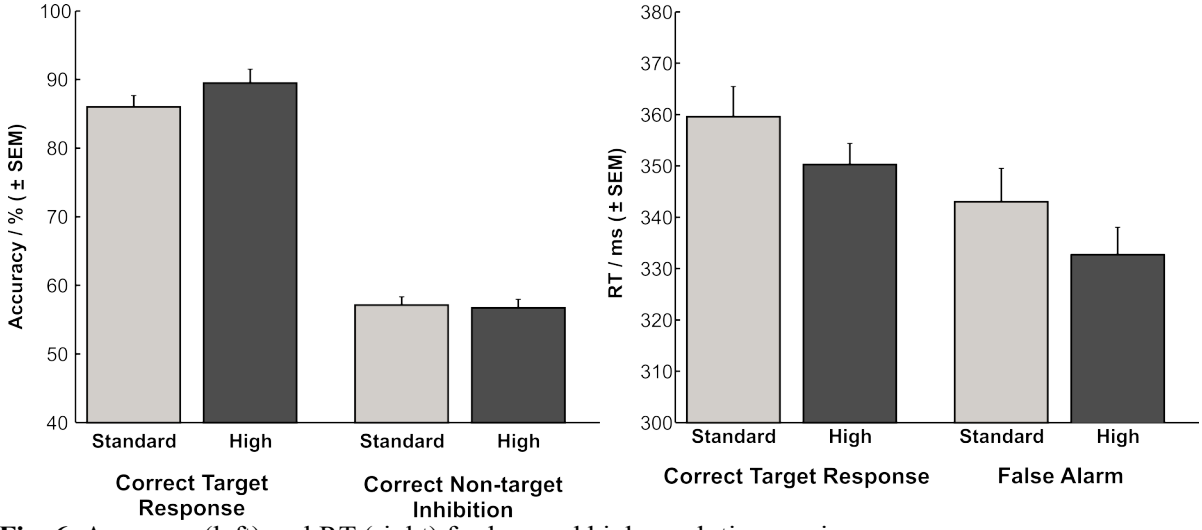

Fig. 6. Accuracy (left) and RT (right) for low and high resolution sessions.

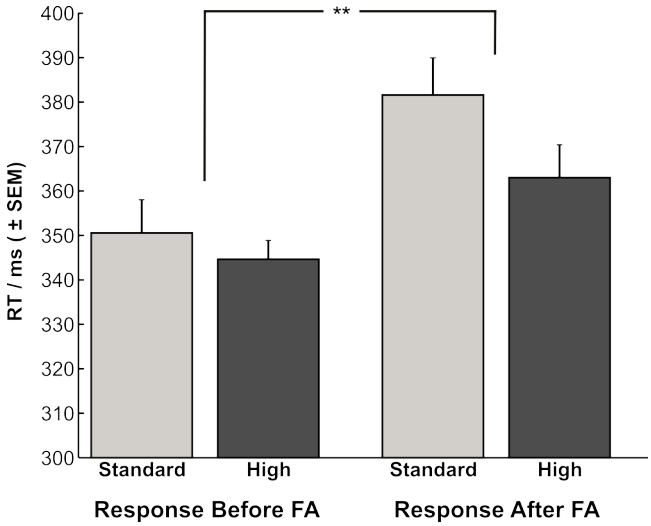

Fig. 7. RT increased significantly after a false alarm, compared to correct responses before FA.

Neuroimaging: Standard Resolution

Linear contrasts between CR and FA were calculated from their model parameter estimates. As expected, contrasting FA and CR (FA > CR) revealed a significant ($z > 3.1$ and corrected cluster $p \leq 0.05$) activation cluster in MFC as shown in Fig. 8 (left panel; see also Table 1). To explore the individual variability of this group activation cluster, we summarized individual runs for each subject and projected the center-of-gravity (COG) of the largest cluster in MFC into standard space. While subjects' activation scattered around the cluster obtained from group analysis, there was also a considerable degree of variability, most notably along the dorsal–rostral axis of the MFC (see Fig. 8 top left panel). In addition, error-related brain responses were detected in insular, extrastriate and motor cortex bilaterally, right postcentral gyrus, thalamus as well as midbrain (see Table 1). Specific activation due to successful resolution of conflict (as measured by contrasting CR > FA, Fig. 8 right panel) was detected in a cluster in right inferior parietal lobule as well as right orbitofrontal cortex (see Table 1). No MFC activation was observed for this contrast.

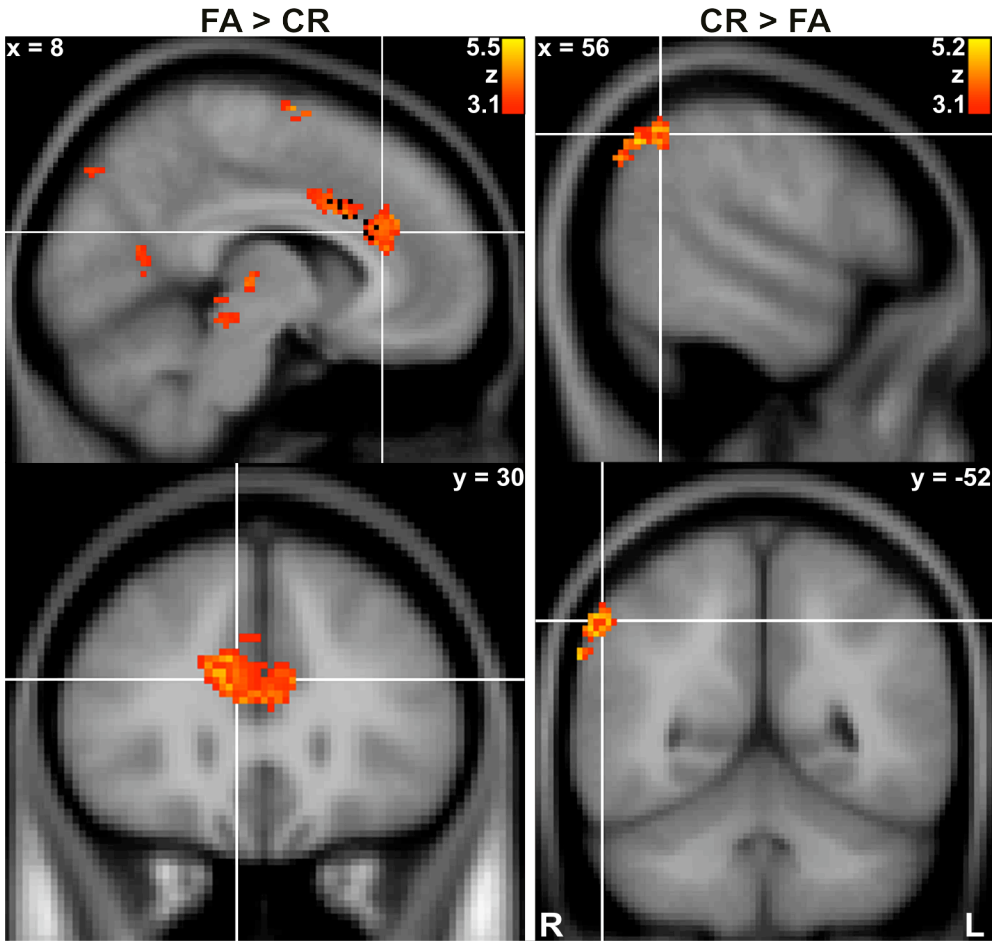

Fig. 8. Brain responses to false alarms (left) and correct rejections (right). Centers of gravity for individual subjects' responses to FA are indicated in the top left panel.

Table 1: Atlas coordinates (in MNI space) and maximum *z*-scores for the centers-of-gravity (COG) of clusters significantly activated in contrasts between False Alarms (FA) and Correct Rejections (CR) at standard resolution.

Contrast	Brain region	COG Coordinates (x, y, z)	*z*-score
FA > CR	MFC	3, 19, 33	5.32
	Left insular cortex	-40, -4, -2	5.48
	Right insular cortex / Postcentral gyrus	54, -17, 24	4.89
	Left / right extrastriate cortex	±34, -79, 22	5.23
	Right motor cortex	35, -34, 60	4.22
	Left motor cortex	-26, -41, 68	4.90
	Thalamus	-2, -24, 0	5.37
	Midbrain	6, -30, -12	4.22
CR > FA	Right inferior parietal lobule	53, -62, 43	4.96
	Right orbitofrontal cortex	42, 44, -20	5.16

Neuroimaging: High Resolution

To examine shared and distinct regions of error and conflict processing in MFC, we calculated linear contrasts between FA and rest (FA > Rest) as well as CR and rest (CR > Rest), respectively. Significant error-related brain responses at the preset criteria ($p \leq 0.01$, 5 connected voxels) were detected in 9/10 subjects. Activation maps of two representative volunteers, displayed on their respective anatomic scans, are shown in Fig. 9. While there appears to be "less activation" compared to conventional acquisitions at lower resolution, all significant voxels are located in the cortical grey matter and respect sulcal architecture. Interestingly, activation in response to impulse errors appears to be more pronounced in the ACC of the right hemisphere, although small foci are also present in left ACC. Note also that active clusters scatter along the whole length of ACC, even for single volunteers. To assess reliability of these maps, the high-resolution session was repeated in one subject. Individual foci co-localized to a surprising degree for these two sessions as demonstrated in Fig. 10. Taken together, these findings suggest that the ACC foci obtained by high-resolution fMRI represent actual centers of neural activity which are blurred across anatomical borders by standard fMRI acquisition and analysis.

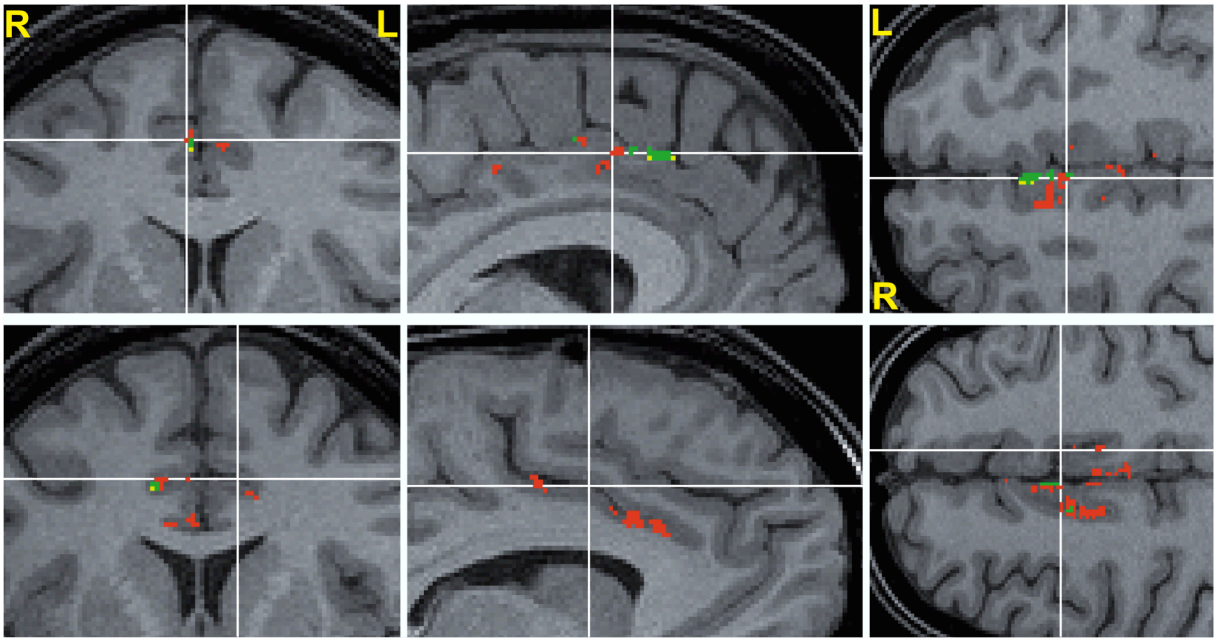

Fig. 9. High resolution activation maps for two representative volunteers presented on their respective anatomical scan (red … false alarms, yellow … correct rejections, green … overlap).

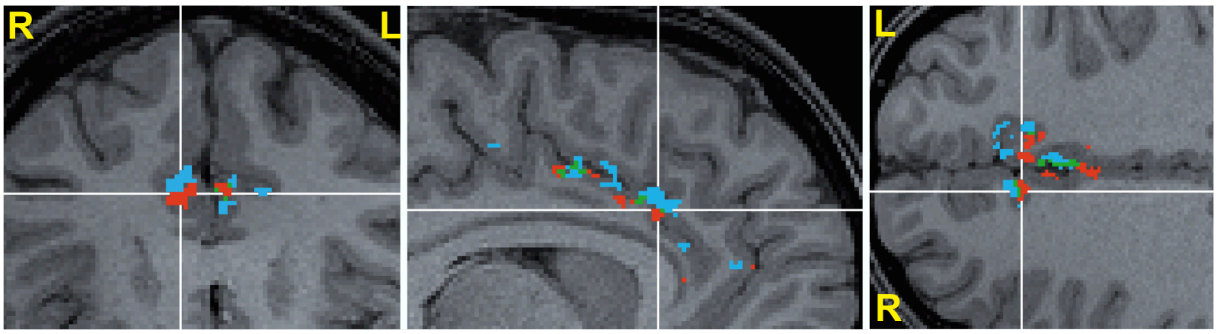

Fig. 10. Reproducibility of brain responses to false alarms for one volunteer (red … session 1, blue … session 2. green … overlap).

While ACC responded very strongly to FA, we could also detect a weak but significant activation for successful inhibitions in 8/10 subjects (as assessed by CR > Rest; see Fig. 9). CR foci were exclusively localized in the right ACC and largely overlapped with error-responsive activation clusters.

Results obtained from the evaluation of individual volunteers were confirmed and extended by a multi-subject analysis. Significant ($q \leq 0.01$, FDR) and overlapping brain responses to FA > Rest and CR > Rest were detected in MFC (see Fig. 11). The error-related activation cluster was predominantly localized in the right ACC although activation was also seen in the left hemisphere (center-of-gravity, COG: x = 2, y = 17, z = 34; z_{max} = 5.1). In agreement with single subject results, activation for successful inhibitions was exclusively right lateralized (COG: 5, 21, 34; z_{max} = 3.8). Apart from activation in MFC, this analysis

revealed a region in the right frontopolar cortex that responded significantly to both CR > Rest (COG: 36, 48, 20; z_{max} = 4.6) and FA > Rest (COG: 37, 43, 23; z_{max} = 4.4; see Fig. 11).

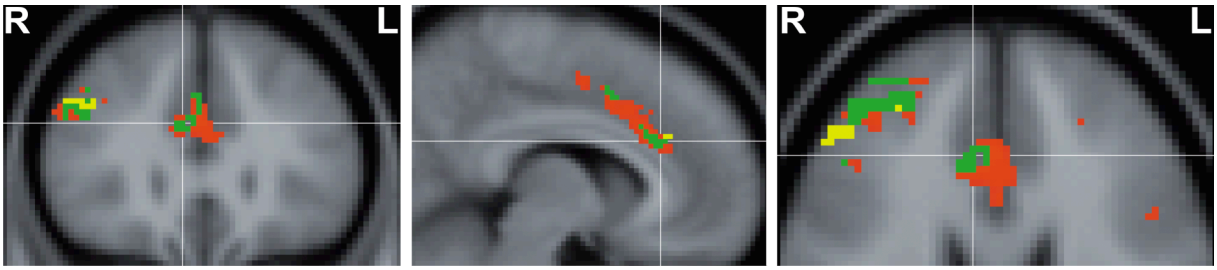

Fig. 11. High resolution results averaged across 10 volunteers and presented on the MNI standard brain (red … false alarms, yellow … correct rejections, green … overlap).

To exclude the possibility that error and conflict-related activations in MFC and prefrontal cortex are unspecific effects of stimulus presentation, we analyzed brain responses to correctly resolved target responses (compared to rest). As expected, an active cluster in left motor cortex (COG: -46, -17, 53; z_{max} = 6.4) could be detected in this case. Furthermore, erroneous button presses on Nogo trials also elicited activation in left motor cortex (COG: -47, -14, 50; z_{max} = 5.3), whereas successful inhibitions failed to do so.

A direct comparison of standard and high resolution activation maps is impeded by the latter's low SNR. To nevertheless illustrate the correspondence between standard and high resolution fMRI, we calculated group activation maps for the FA > CR contrast (Fig. 12) for both acquisitions. To account for the SNR difference, the standard resolution maps were required to pass a more stringent threshold ($q \leq 0.01$ versus $q \leq 0.1$, FDR). An overlapping activation cluster in ACC was detected with standard and high resolution acquisition, demonstrating the correspondence between the two approaches (Fig. 12).

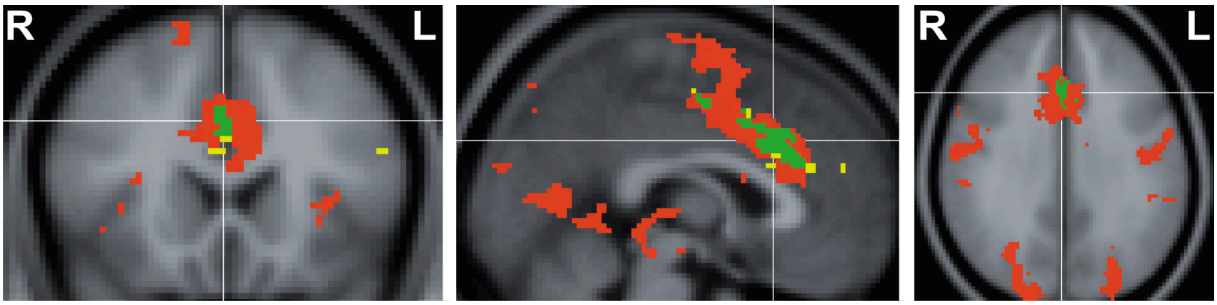

Fig. 12. Overlap (green) between low (red) and high (yellow) resolution brain responses to false alarms, displayed on MNI standard brain. Note that different thresholds were employed for low and high resolution maps (see text for details).

To quantify the high resolution fMRI results, we determined the number of active voxels in response to FA, CR and correct target responses for each experiment separately (thresholded at $p \leq 0.01$, 5 connected voxels) in four subregions of ACC (see Materials and Methods). A 2 × 3 (hemisphere: left – right; trial type: correct target response – CR – FA) analysis of variance (ANOVA) was carried out separately for dorsal (dACC) and rostral (rACC) anterior cingulate cortex (see Fig. 13). Significant main effects for hemisphere and trial type were obtained in both dACC ($F_{(1,63)} = 5.6$, $p < 0.05$; $F_{(1,78)} = 19.7$, $p < 0.001$ respectively) and rACC ($F_{(1,63)} = 6.7$, $p < 0.05$; $F_{(1,82)} = 10.5$, $p < 0.01$ respectively). A significant interaction between both factors, indicating a differential modulation of the two hemispheres by CR and FA, was evident in rACC ($F_{(2,114)} = 3.6$, $p < 0.05$) but not dACC ($F_{(2,107)} = 0.2$, $p > 0.1$). As shown in Fig. 13, FA activated significantly more voxel than correct target responses in all 4 ROIs (all $p \leq 0.05$, Bonferroni corrected for multiple comparisons). Furthermore, only rACC in the right hemisphere responded stronger to CR than to correct target responses ($t_{(63)} = 2.7$, $p = 0.05$, Bonferroni corrected for multiple comparisons) whereas the number of voxels activated by FA did not differ from CR in this ROI ($t_{(63)} = 2.3$, $p = 0.1$). Such a pattern of activation would be expected if right rACC were to play a role in conflict monitoring, which is implicated by both CR and FA.

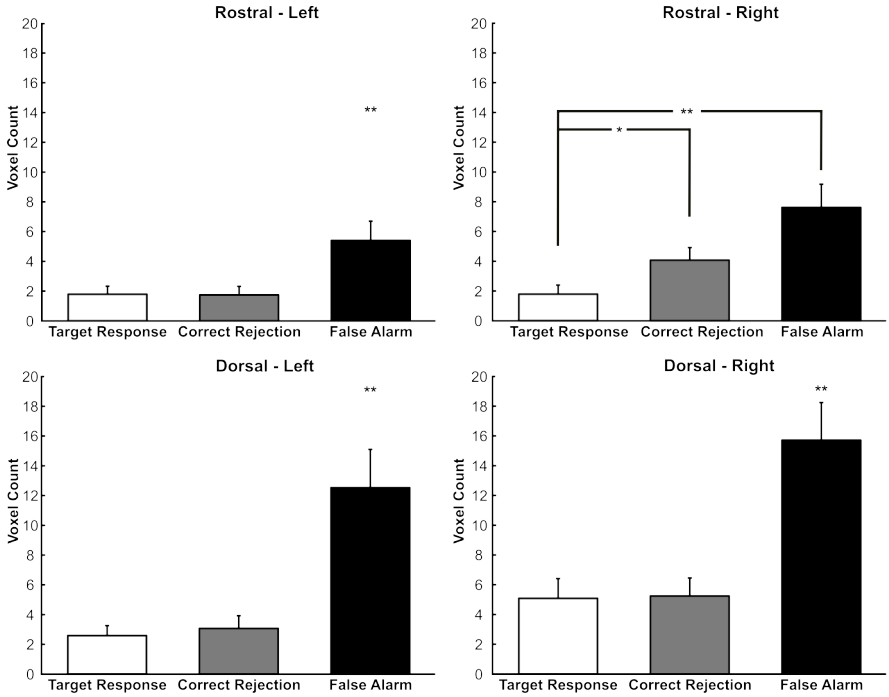

Fig. 13. Mean number of activated voxels (single experiments) in dorsal and rostral as well as left and right ACCs. Whereas dACC as well as left rACC responded significantly stronger to FAs than to either correct target responses or CR, right rACC was activated by both CRs and FAs. ** $p \leq 0.01$, * $p \leq 0.05$; Bonferroni corrected

We obtained further evidence for a hemispheric specialization in ACC by calculating a 'laterality index' for each subject from the number of activated voxels in right and left ACC (averaged across dorsal and rostral ROI):

$$laterality = \frac{Vox_{right} - Vox_{left}}{Vox_{right} + Vox_{left}} \tag{6}$$

This index shows a strongly right-lateralized ACC response for correct rejections (0.73 ± 0.09), whereas false alarms elicit a more bilateral response, though skewed to the right (0.27 ± 0.12).

Since the number of activated voxels only takes into account a very small fraction of the information that is available (and depends on the particular technique and cut-off used for thresholding) we additionally extracted and compared the normalized mean parameter estimates (beta-weights) of the fitted model for FA, CR, and correct target responses from the four ROIs (see Fig. 14). In accordance with the previous analysis, FA was associated with significantly stronger brain activation than correct button presses in all four ROIs (all $p \leq 0.01$, Bonferroni corrected for multiple comparisons). Furthermore, both left and right dACC responded stronger to FA than to CR ($t_{(63)} = 5.1$, $p < 0.01$; $t_{(63)} = 4.6$, $p < 0.01$ respectively) while these comparisons failed to reach significance in rACC ($t_{(63)} = 2.1$, $p > 0.1$ and $t_{(63)} = 1.4$, $p > 0.1$ respectively). As before, right rACC responded significantly stronger to CR than to correct target responses ($t_{(63)} = 2.9$, $p < 0.05$), supporting a role for the region in conflict related processes.

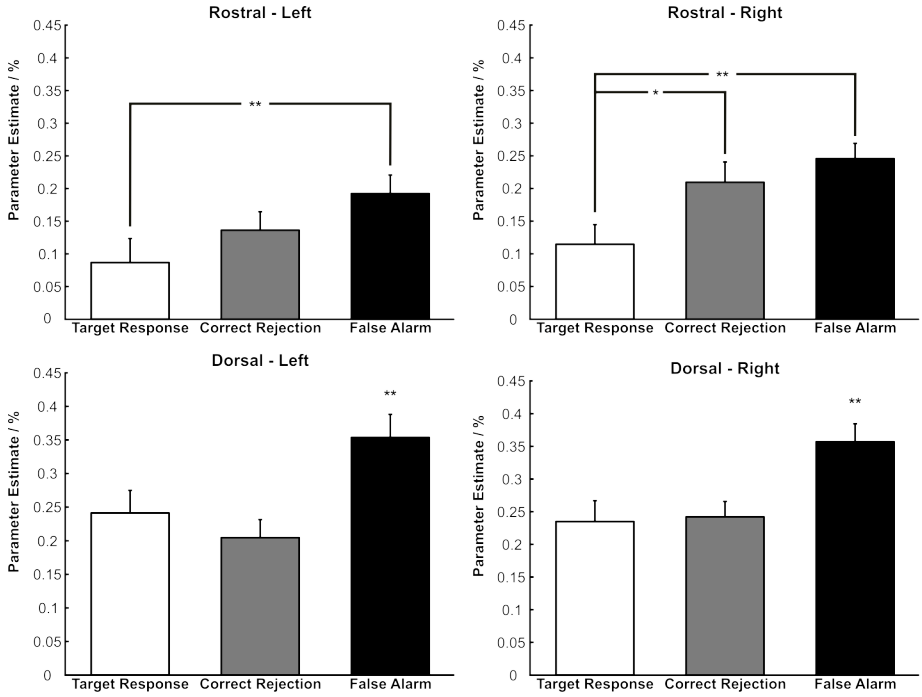

Fig. 14. Mean parameter estimates of the fitted model in dorsal and rostral as well as left and right ACC. Whereas activation in dACC was associated with impulse errors, rACC in the right hemisphere responded significantly to errors as well as successful inhibitions. Left rACC responded significantly stronger to FAs than to target responses whereas responses to CRs did not differ from either FAs or target responses. ** $p \leq 0.01$, * $p \leq 0.05$; Bonferroni corrected

As shown in the behavioral data, subjects responded significantly slower after they committed an error. We calculated the difference in RT for correct responses before and after a FA ($RT_{postFA} - RT_{preFA}$) as behavioral index of error processing and correlated this index with the normalized mean parameter estimates for FA and CR in ACC (see Fig. 15). Surprisingly, at standard resolution, the slow-down after a FA correlated significantly with CR ($r = 0.46$, $p < 0.001$) but not FA activation ($r = 0.26$; $p = 0.07$). At high resolution, this correlation failed to reach significance for both CR and FA ($r = 0.1$; $p = 0.42$ and $r = 0.08$; $p = 0.53$, respectively), possibly due to the low SNR. To address this issue, we extracted parameter estimates from the most significantly activated voxels only (top 10%), which revealed a similar correlation pattern as for standard acquisition (CR: $r = .34$; $p < .01$; FA: $r = 17$; $p = .19$).

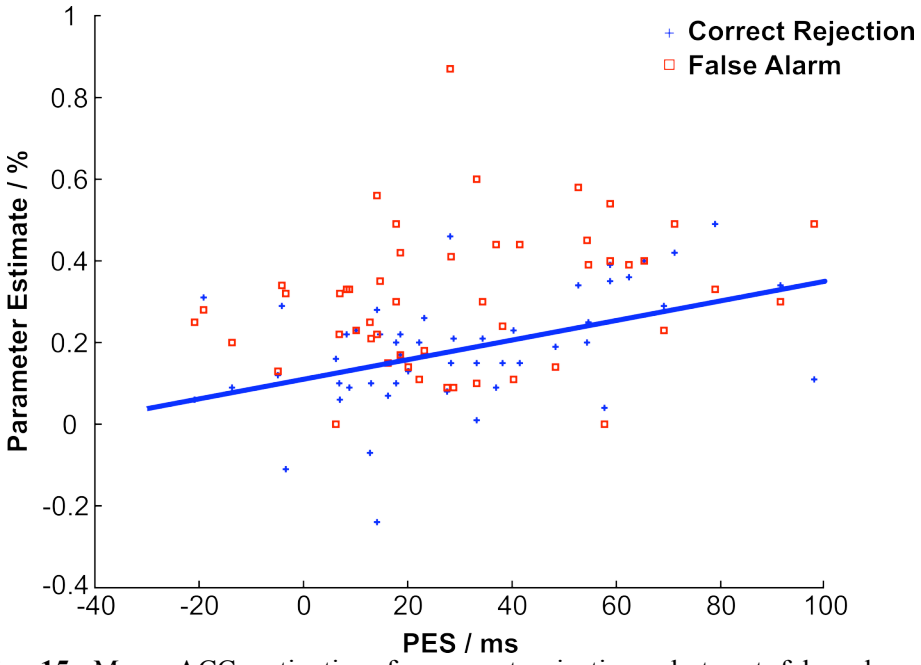

Fig. 15. Mean ACC activation for correct rejections, but not false alarms, correlates significantly with degrees of slow-down after a false alarm. Data shown are for standard resolution. At high resolution, similar results were obtained with the most significantly activated voxels.

5.4. Discussion

In this study, we used fMRI at high spatial resolution to uncover the functional microanatomy of human ACC during conflict monitoring and error processing. In line with previous studies, standard fMRI demonstrated a stronger ACC response for erroneous trials than for successful inhibitions. Based on these results, we imaged activated regions in MFC with higher spatial resolution and were able to obtain highly localized activation maps of neural foci both for conflict and error processing in the majority of subjects. Furthermore, these maps proved to be surprisingly reproducible. A multi-subject analysis demonstrated bilateral error and right-lateralized conflict-associated processing in MFC as well as a cluster in right frontopolar cortex which responded significantly to Nogo trials. Subsequent ROI analysis largely agreed with the conclusions derived from high-resolution activation maps. Left rostral ACC, as well as dorsal ACC, responded significantly to incorrect Nogo trials only and presumably plays a role in error-related processes, such as error detection or evaluational aspects of error commission. Conversely, right rACC was activated both for successful and unsuccessful inhibition, albeit more strongly for the latter. This suggests that the region plays a role in monitoring and resolving cognitive conflict.

Further evidence for hemispheric specialization in ACC

While a number of previous GoNogo studies have reported conflict and error-related ACC activation (Konishi *et al.*, 1998; Menon *et al.*, 2001; Garavan *et al.*, 2003), they remained inconclusive with respect to a differential involvement of the two hemispheres. While lateralization was not mentioned in the majority of studies, some groups reported a specialization of either the left (Rubia *et al.*, 2001) or right hemisphere (Garavan *et al.*, 1999) for conflict monitoring. In agreement with our results, Taylor and colleagues (Taylor *et al.*, 2006) found that in a Flanker task, high conflict activation foci of individual subjects tended to cluster in the right MFC, whereas brain responses to errors were distributed more bilaterally. Stephan and coworkers (Stephan *et al.*, 2003) showed, by analyzing effective connectivity, that ACC in the hemisphere that was occupied with the task at hand, also mediated the influence of cognitive control on the involved regions. Accordingly, for a visuospatial interference task which involved the right hemisphere, right ACC was also involved in monitoring for conflict, whereas left ACC mediated cognitive control when subjects processed verbal stimuli. These results seem to be at odds with the findings in our study because we used letter stimuli but nevertheless found conflict-related activation in the

right ACC. It is, however, unclear to what extent subjects processed single letters verbally. Indeed, when we contrasted successful inhibition with false alarms at standard resolution, the active cluster in inferior parietal cortex was close to the visuospatial activation reported by Stephan and colleagues (Stephan *et al.*, 2003) yielding maximum voxel coordinates of 46, -76, 34 vs. 54, -64, 42. This suggests that our subjects may have been relying more on configurational cues in solving the task than on verbal information about the letters. Further evidence for such a speculation derives from several subjects' introspective report that they did not verbalize the letters during the experiment.

Taken together, our results are in broad agreement with two previous studies which investigated the hemispheric lateralization of cognitive control in ACC. Using high-resolution fMRI, however, we were able to show for the first time directly that the right part of rostral ACC mediated cognitive control in a letter-based GoNogo task, whereas left rACC as well as dorsal ACC were more concerned with error processing. It remains a question for future research whether dissociation between right and left ACC can be shown for tasks that are explicitly verbal or spatial (such as word or spatial GoNogo paradigms). Furthermore, it would be interesting to see if the opposite hemisphere always continues to process error-related information (as in our study). Such a scenario would be in accordance with current models of conflict monitoring and error processing (Yeung *et al.*, 2004). Thus, the ACC in the task-dominant hemisphere is implicated in cognitive control and monitors for conflict. Once conflict rises above a certain threshold, an error is assumed and the contralateral ACC is activated to initiate error-related processing. This interpretation would also explain why, in our study, right rACC was stronger activated for errors than for correct rejections, because errors simply are envisaged as situations of very high conflict.

Why did so many previous imaging studies detect no or inconsistent lateralization results in ACC? Considering the close proximity of both cortices as well as standard fMRI methodology, the failure to reliably identify lateralization is not very surprising. The average distance between left and right ACC, which are only separated by the interhemispheric fissure, is on the order of 1 cm. It can be shown that, with an image resolution of 3 × 3 × 3 mm^3 and the use of substantial spatial smoothing (Scouten *et al.*, 2006), such as a Gaussian kernel of 5 mm FWHM, focal neural activations in left and right ACC may become at least partly indistinguishable. Inaccuracies introduced by imperfect spatial normalization (Hellier *et al.*, 2003) as well as group averaging and the considerable variability of ACC anatomy (Paus *et al.*, 1996) may have further contributed to the discrepancies in previous studies.

Frontopolar cortex implements behavioral readjustment

Although the primary aim of our study was to investigate the functional anatomy of ACC at high spatial resolution, we also detected a region in right frontopolar cortex that responded significantly to successful inhibitions as well as false alarms and therefore presumably plays a role in conflict monitoring processes. Previously, Carlson and colleagues (Carlson *et al.*, 1998) observed frontopolar activation when contrasting conditions of high and low memory load in a visuospatial *n*-back task. Furthermore, in a Stroop task, activation of right frontopolar brain areas was associated with the incongruent condition (Zysset *et al.*, 2001). These experiments, together with results from the current study, provide support for the idea that lateral prefrontal cortex plays an important role in neural processes associated with cognitive conflict. Furthermore, the similar patterns of activation in right ACC and frontopolar cortex are in line with the conflict monitoring hypothesis of anterior cingulate function (Botvinick *et al.*, 2001; Botvinick *et al.*, 2004). In this model, ACC is thought to monitor for cognitive conflict and recruit other brain regions, such as lateral prefrontal cortex, which bring about behavioral readjustments to minimize subsequent conflict.

Perhaps surprisingly, behavioral parameters such as reaction time remained relatively constant throughout the two experimental sessions. While there were small improvements in performance as well as a trend for faster responses in the high-resolution session, these turned out to be non-significant. One reason for this might be that we chose a relatively long time delay between the two experiments (at least several days), so that any practice effects gained over the first session would essentially be lost. It is important to remember, however, that subjects might still have changed their strategy individually throughout the experiment, without a noticeable effect on RT on the group level. Such strategy changes would nevertheless contribute to the large inter-individual variability of activation centers in ACC.

In accordance with previous studies on error processing (Rabbitt, 1966), we detected a significant slowing of the RT after the occurrence of a false alarm but not after a correct rejection. This effect probably reflects a compensatory mechanism aimed at improving performance on subsequent trials (Gehring and Fencsik, 2001). Surprisingly, the degree of slowing was significantly correlated across subjects with the amount of activation in ACC for correct rejections but not false alarms. A possible explanation for this finding may be that ACC is always implicated for FAs since behavioral readjustment is mandatory after such trials in order to be rewarded again in the future. On the other hand, CRs do not necessitate readjustments of current action schemata. It is nevertheless conceivable that some subjects still evaluate the correctness of their responses after CRs and consequently stronger activate

ACC than those who do not. Individuals with such a 'tentative' strategy may also be the ones who slow down significantly following an error. Such an interpretation receives support from analysis of single subject data which shows that the degree of RT adjustment after an error is quite stable for the same volunteer across different repetitions of the experiment and may therefore be an index of a 'tentative' trait or predisposition.

High-resolution fMRI in cognitive neuroscience

Functional MRI at an effective resolution (including post-acquisition smoothing) comparable to that employed in the present study has previously been used solely to investigate the functional organization in subregions of the early visual system (Schneider *et al.*, 2004; Schwarzlose *et al.*, 2005; Grill-Spector *et al.*, 2006). Here we demonstrate the feasibility of such an approach for brain regions involved in higher level processes, such as cognitive control. Improving the spatial resolution by a factor of 8 enabled us to explore the functional organization of ACC at a previously unaccomplished spatial scale and to reveal a dissociation between left and right ACC that has not been directly observed with standard techniques. Consequently, it may turn out fruitful to revisit a number of paradigms which have been reported to elicit ACC activation including pain stimulation (Jones *et al.*, 1991; Koyama *et al.*, 2005) or emotional processing (Whalen *et al.*, 1998; Bush *et al.*, 2000). One would predict that at high resolution a number of regional specializations will become apparent for stimuli and tasks which have so far been mapped to overlapping locations. Furthermore, given the high functional and anatomical variability in ACC, extensive analysis of single subject data would be recommendable, in addition to traditional group approaches.

Importantly, high-resolution fMRI should be considered as a complementary technique to standard neuroimaging rather than as a replacement. While standard approaches provide the benefits of whole-brain coverage in a reasonable time frame, good signal-to-noise ratio, and also offer the opportunity to estimate functional connectivity, high-resolution fMRI is limited in these respects. Indeed, the technique may be envisaged as 'zooming into' a region which was previously identified as active by established imaging strategies. While this approach has been used routinely to study early visual processing, we present the first successful attempt, to our knowledge, of mapping a higher level brain area in this way. We believe that the 'zooming in' fMRI strategy will provide a powerful new tool for cognitive neuroscientists. It may help bridging the gap between neuroimaging and electrode recording and thereby contribute to our understanding of the neural basis of cognition.

In summary, the findings presented here demonstrate a functional specialization in anterior cingulate cortex: while the right rostral ACC is selectively involved in conflict processing, its left part as well as dorsal ACC play a role in error-related computations. In the following chapter, a third putative cognitive function of MFC, response anticipation, will be investigated more closely. Furthermore, the experiments focused on examining the relationship between the neural basis of response conflict and anticipation in ACC.

6. Neural basis of response conflict and anticipation

6.1. Introduction

The experiments described in the previous chapter, together with many other investigations, demonstrate a crucial role for MFC, and especially ACC, in the neural processes underlying resolution of conflicting responses. Furthermore, we showed that distinct aspects of cognitive control, such as error or conflict monitoring, may be localized to specific subregions of ACC. On the other hand, processing of cognitive conflict is certainly not the only task of MFC, as has been discussed in the general introduction. Interestingly, a cognitive function that is closely related to response conflict, namely response anticipation, also relies on neural systems within the medial wall of the frontal lobe (Nagai *et al.*, 2004). Effective anticipation of future responses based on past stimuli presents obvious survival advantages since the organism may pre-activate resources required for dealing with a given situation. Preparatory anticipation processes would be especially useful in a context were future responses remain partly underdetermined and allocation of sufficient attentional resources will be crucial for efficient decision making. Consequently, top-down control processes must constitute a major aspect of response anticipation, as has been argued previously (Tecce, 1972). Equally, when dealing with two or more conflicting responses, as in the GoNogo task, allocation of top-down attentional resources becomes essential for mastering the situation. Given that both response conflict and anticipation implicate top-down control processes, the experiments described in the current chapter aimed at comparing and contrasting the neural structures underlying these two cognitive functions. In line with the previous study, we focused mainly on MFC and hoped to identify both shared and distinct activated areas for the two processes.

Contingent negative variation as neuroelectric signature of expectancy

When a warning signal is presented prior to a target response, reaction times improve. The underlying anticipation process is reflected in a characteristic slow cortical potential (SCP) termed the contingent negative variation (CNV). Its discovery as a neuroelectric signature of expectancy more than 40 years ago (Walter *et al.*, 1964), has initiated a long and successful research enterprise yielding a detailed understanding of properties as well as cellular mechanisms underlying the generation of the CNV (reviewed in Tecce, 1972; Tamas and Shibasaki, 1985; Birbaumer *et al.*, 1990).

Classically, response anticipation and the CNV have been investigated using a two-stimulus paradigm in which the first stimulus (warning signal; S_1) indicates that a second

(imperative; S_2) stimulus will occur after a given time interval (Birbaumer *et al.*, 1990). Usually, presentation of S_2 requires subjects to make some kind of response (e.g. a button press). The original CNV study (Walter *et al.*, 1964) as well as the vast majority of subsequent experiments employed rather short interstimulus intervals (ISI) of around 1 second which give rise to a sustained negativity over the entire interval. Surprisingly, longer ISIs (6 – 9 s) give rise to a more complex, biphasic wave form (Loveless and Sanford, 1974). Immediately after presentation of S_1, the characteristic negative potential is observed which, however, returns to baseline by about one second. Two to three seconds before presentation of the imperative stimulus, a further negativity appears which peaks around the time of onset of S_2. Referring to their respective time of occurrence within a trial, Birbaumer and colleagues (Birbaumer *et al.*, 1990) proposed the terms initial (iCNV) and terminal (tCNV) contingent negativity. There is considerable evidence that iCNV and tCNV reflect dissociable neural processes which are, at least to some degree, confounded in the monophasic wave of the short ISI paradigm. Whereas the iCNV is usually strongest at bilateral frontal electrodes, tCNV has a maximum at the vertex (Cz electrode). Furthermore, while iCNV is thought to reflect activation of stored stimulus representations together with their past content, tCNV is more closely associated with a possible upcoming response. Unlike iCNV, the amplitude of the terminal wave increases with uncertainty over the response to the imperative stimulus, compared to when the nature of the response is already determined by S_1 (van Boxtel and Brunia, 1994). Consequently, tCNV is not simply a reflection of motor preparation but refers to more general preparatory and anticipatory processes.

A neurophysiological model of CNV generation

The substantial amount of research on CNV generation has culminated in a detailed neurophysiological model (Birbaumer *et al.*, 1990) which is now widely accepted within cognitive neuroscience (Kotchoubey, 2006). Briefly, in this model the CNV is generated by a potential sink due to non-specific thalamic afferents synapsing on dendritic trees in layer 1 of cortical pyramidal neurons, leading to a reduction of firing thresholds in networks required for the response to the imperative stimulus S_2. Tuning of the thalamic input to the cortex is achieved by 'bottom-up' signals from the midbrain reticular formation as well as 'top-down' influences from the prefrontal cortex, via the mediothalamic frontocortical system (MTFCS).

As this model is mainly based on EEG evidence, which suffers from poor spatial resolution and 3-D localization, it has been difficult to elaborate and specify the precise functional architecture underlying anticipatory behavior. Furthermore, the involvement of

subcortical structures in humans has remained largely speculative as respective parts of the model are based almost exclusively on extracellular recording studies in animals. It is surprising therefore that only a few functional imaging studies have tried to overcome these limitations and addressed the question of preparatory activity in human subjects.

In a combined EEG – fMRI study, Nagai *et al.* (2004) demonstrated that anticipation in a S_1 – S_2 paradigm leads to strong activation in the ACC which is correlated to CNV amplitude. They furthermore reported the correlated involvement of subcortical centers, such as the thalamus, in CNV generation. Due to the short ISI employed in this study (3.5 – 4.5 s) it seems likely that their results pertain mainly to the generation of the early wave or even a superposition of iCNV and tCNV. In a subsequent experiment, even shorter ISIs (1 s) were employed in a mixed event-related and blocked fMRI study designed to reveal neural processes of task preparation (Fassbender *et al.*, 2006). Besides not taking into account tCNV, interpretation of these findings is difficult due to the slow hemodynamic response, which makes it hard to separate regularly spaced events which occur within 1 s of each other. Finally, these authors did not obtain EEG measurements from any of their subjects which makes it difficult to relate their complex paradigm to the existing electrophysiological literature.

In a very recently published study, Fan *et al.* (2007) investigated the relationship between conflict and anticipation processes in the human brain using both EEG and fMRI. The authors employed a cued / uncued Flanker task paradigm in order to investigate preparatory brain activity (cued versus uncued), response conflict (incongruent versus congruent Flanker trials; see below) as well as the interaction between these two processes. In line with previous studies, response conflict was associated with increased activation in ACC as well as regions in frontal and parietal cortex. Cues reliably elicited a CNV which corresponded to activity in a thalamo-cortico-striatal network including ACC. Importantly, cue and conflict effects did not interact with each other, which was interpreted by the authors as a partial independence of the networks subserving the two functions. Since this study also employed a relatively fast paradigm (ISI: 2.25 s; less than 1 TR) the early and late components of the CNV could not be resolved. Furthermore, due to the slow hemodynamic response, it seems doubtful whether anticipation and conflict could be separated in the same brain region if both processes always occur within 1 – 2 seconds of each other.

Objectives of the experiment

In the present experiment, we set out to investigate more closely the link between response conflict and anticipation. Specifically, we hoped to identify neural structures associated with the late wave of the CNV, which has been neglected in previous studies but which is thought to reflect stimulus independent response preparation and anticipation (Birbaumer *et al.*, 1990). To this end, we employed a continuous performance test (CPT; Heinrich *et al.*, 2004) with long ISI (6 s) in order to generate the full biphasic CNV as well as take into account hemodynamic response properties. The CPT corresponds in fact to a slightly modified $S_1 - S_2$ paradigm, where a cue letter is followed by a target to which subjects should respond by pressing a button. Alternatively, a distracter may be presented. Crucially, the distracter may also be presented in place of a cue, signifying to the subject that any subsequent letter is irrelevant, as no response would be required on the next trial (see below for a detailed description of the paradigm). Since tCNV amplitude increases with uncertainty about the response to S_2 (van Boxtel and Brunia, 1994), we reasoned that cues would produce substantially stronger response anticipation compared to distracters (non-cues). The crucial contrast reflecting anticipatory processes was therefore obtained by comparison of brain activity during the 3 – 6 s time interval following a cue versus a non-cue.

In order to measure response conflict, a standard Flanker paradigm was employed (Eriksen and Eriksen, 1974) which has been used in previous fMRI studies to investigate the neural mechanisms of conflict related processing (Taylor *et al.*, 2006). The Flanker task allows a more efficient assessment of cognitive conflict than the GoNogo experiment because virtually all trials (and not only Nogos) may be used for analysis. Furthermore, the contrast of interest (incongruent versus congruent trials; see below) in general does not stand out subjectively for naïve participants.

In the present study, the same pool of subjects performed several runs of both CPT and Flanker experiments. In addition to group comparisons, we therefore had the opportunity to investigate activation differences between anticipation and conflict at the level of individual subjects. Furthermore, our approach made it possible to assess both within and between subject variability for the two processes. Finally, since participants performed several runs for each task, we were interested in putative practice effects as well as their neural correlates.

6.2. Materials and Methods

Subjects

Twelve right-handed volunteers (3 male and 9 female; mean age 28 ± 6 years) participated in both Flanker and CPT experimental sessions (carried out on separate days). In each experiment, subjects performed 4 or 5 repetitions of the task, leaving us with a total of 53 CPT and 47 Flanker runs for analysis. Given the substantial variability in activation between subsequent runs, partly attributable to factors such as fatigue, motivation or hardware changes, each experiment was treated independently for the purpose of statistical analysis. For logistic reasons, we generally performed the CPT experiments prior to the Flanker session. This order was reversed for three subjects. All participants were informed about the purpose of the study as well as possible risks associated with MRI. Written consent was obtained prior to each experimental session. Participants earned 10 Euros per hour plus a bonus depending on their performance. All experimental procedures conformed fully to institutional guidelines.

CPT Task

We employed a cued version of the CPT which has been shown to reliably elicit a CNV in previous EEG studies (Heinrich *et al.*, 2004). Subjects were presented with the letters O, X or H and instructed to press the response button with their right thumb or index finger only for an X (target), if it was preceded by an O (see Fig. 16).

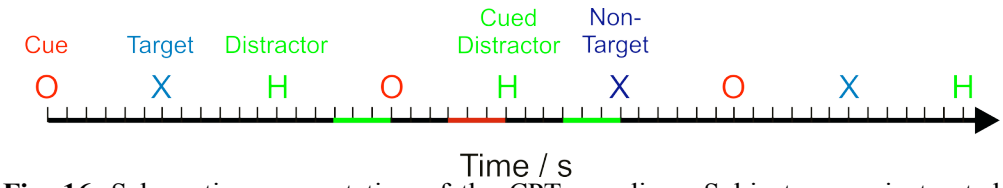

Fig. 16. Schematic representation of the CPT paradigm. Subjects were instructed to press the response button upon presentation of the letter X (target) if it was preceded by the letter O (cue) but refrain from responding if the X was preceded by an H. See text for details.

Therefore, the O acted as a cue to orient subject's attention to a possible target. However, only in 50% of the cases an X actually followed the cue whereas an H (distracter) was presented in the remaining trials. Over the whole experiment, the probability of an O-X pair (cue-target) as well as O-H (cue-distracter) was 20% each. Additionally, there was a 10% probability of an uncued X (non-target) or H being shown. In order to encourage fast responses, letters were shown very briefly (250 ms). Correct responses to targets had to occur

within 1000 ms of stimulus presentation. All stimuli were presented in black color on a white background. Two black vertical bars were continuously presented above and below the stimulus location, in order to direct subjects' attention to the center of the screen.

Based on EEG results (see below), we hypothesized that subjects build up a tCNV indicating response anticipation approximately 1-2 s before the occurrence of a cued stimulus. Due to the sluggish hemodynamic response, it is not possible to separate this time interval from activity due to a target response. We therefore modeled cue-related processing as the 3 s time interval prior to a cued distracter stimulus (Cue). As a reference, the equivalent time interval preceding an uncued distracter was chosen (Non-cue). For both tasks (CPT and Flanker), only correct trials were included in the analysis.

Flanker Task

A letter version of the Eriksen flanker task was used in the present study (Eriksen and Eriksen, 1974; Taylor *et al.*, 2006). Stimuli consisted of a string of four distracter and one target letter, presented in the centre of the screen (see Fig. 17). Subjects had to identify the odd letter and make a response: right hand button press for "C" or "H" and left hand button press for "K" or "S". Crucially, the distracters consisted of letters from this same set of four letters. On congruent trials, both targets and distracters indicated the same response whereas on incongruent trials distracters were associated with the opposite hand as the target (see Fig. 17).

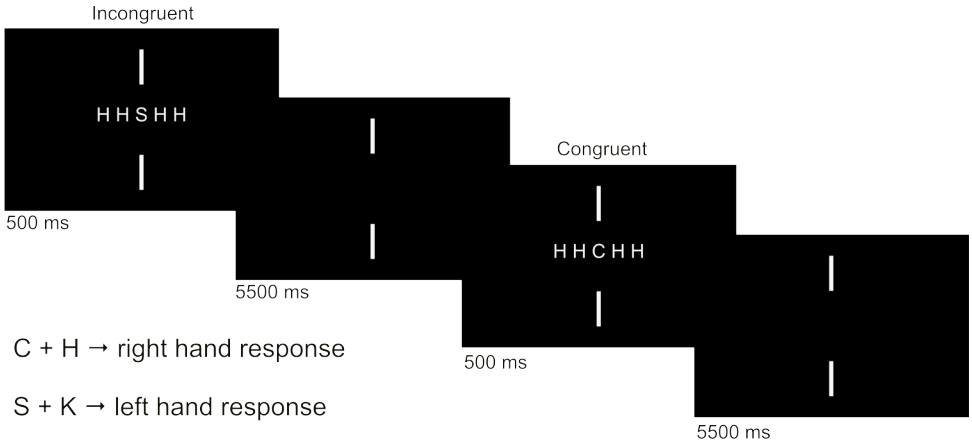

Fig. 17. Schematic representation of the Flanker paradigm. Subjects were instructed to respond to the odd-one-out letter (target) as indicated. For congruent trials, distracters were associated with the same hand as targets. During incongruent trials, distracters and targets were associated with different responses. See text for details.

Target letters were allowed to occur in one of the three central positions of the five letter string. Pseudo-random stimulus sequences were generated such that the same number of congruent and incongruent as well as left and right-hand trials was presented during a run. Furthermore, the occurrence of more than three consecutive congruent or incongruent and left or right-hand trials was not allowed. Stimuli were presented for 500 ms and appeared in white color on a black background. Subjects were required to respond within 1500 ms of stimulus presentation. As in the CPT task, two vertical bars were continuously presented to focus subjects' attention. Congruent and incongruent trials were modeled as 1 s boxcar function following the onset of a respective trial.

In both CPT and Flanker task, a total of 80 stimuli were presented with a stimulus onset asynchrony of 6 s using a computer running Presentation (Neurobehavioral Systems, Albany, CA, USA) and interfaced with a dedicated projection setup (Schäfter & Kirchhoff, Hamburg, Germany) or MRI-compatible liquid crystal display goggles (Resonance Technology Inc., Northridge, CA, USA). Corrective lenses were applied if necessary. Button presses were recorded with custom-built MRI-compatible response boxes. For each experiment, the sequence of stimuli to be presented was randomly selected from a list of four possible sequences which had been previously generated to fulfill the aforementioned criteria. The duration of a single experimental run was about 8 minutes.

Magnetic Resonance Imaging

All studies were conducted at 2.9 T (Siemens Tim Trio, Erlangen, Germany) using a 12-channel receive-only head coil in combination with the whole-body coil for radiofrequency pulse transmission. For each subject we acquired a T_1-weighted MRI using a 3D MPRAGE sequence at 1.3 × 1 × 1.3 mm^3 resolution for anatomic referencing as well as cortical reconstruction. For fMRI we employed a single-shot gradient-echo EPI sequence (TR/TE = 2000/36 ms, flip angle 70°, 244 volumes per run) with a voxel size of 2 × 2 × 4 mm^3 (84 × 96 acquisition matrix, 192 mm FOV, 7/8 partial Fourier phase encoding, bandwidth 1336 Hz/pixel, echo spacing 0.81 ms). We acquired 22 slices without gap, positioned in the transverse-to-coronal plane approximately parallel to the corpus callosum and covering the whole cerebrum. At the end of each session, one EPI volume was acquired with the same specifications as the functional series but covering the whole brain (36 slices) in order to facilitate registration of fMRI data to the anatomical scan.

Data Analysis

Evaluation of fMRI data was performed using tools from the FMRIB Software library (FSL, www.fmrib.ox.ac.uk) and MATLAB (The MathWorks, Natick, Massachusetts). Scans were corrected for subject motion both in k-space (Siemens, Erlangen, Germany) as well as by image-based registration (Jenkinson *et al.*, 2002). Data were smoothed using a Gaussian kernel of FWHM 5 mm. Non-brain tissue was removed (Smith, 2002) and all volumes were intensity normalized by the same factor and temporally high-pass filtered (Gaussian-weighted least-squares straight line fitting, with high-pass filter cut-off at 30 s).

Boxcar models (see above) were convolved with a Gamma function to take into account temporal properties of the hemodynamic response. Model fit was determined by statistical time-series analysis in the framework of the general linear model and with local autocorrelation correction (Woolrich *et al.*, 2001). For CPT experiments, contrasts between Cue and Non-cue trials were calculated as an index of response anticipation (RA). Correspondingly, the contrast of incongruent and congruent trials in the Flanker task presented a measure of response conflict (RC).

Functional images were spatially normalized to the MNI152 template brain as well as their respective anatomical scan. To summarize results across all subjects, mixed-effects group analysis was performed (Beckmann *et al.*, 2003; Woolrich *et al.*, 2004). Unless otherwise indicated, significant activations based on z statistic (Gaussianized T/F) images were obtained by cluster thresholding (Worsley *et al.*, 1992) with an initial threshold of $z > 3.1$ and then applying a corrected cluster threshold of $p = 0.05$.

To assess the variability of activations for RA and RC both between and within subjects, we determined two complementary parameters. The centre-of-gravity (COG, defined as the average position of activated voxels) is a point measure indicating the approximate location of a subject's active cluster in MFC. It does not provide any information, however, about the extent and amount of activation. To quantify the latter two parameters, we calculated the spatial correlation coefficient between raw z statistic images (excluding structures outside MFC) within individual subjects (correlation of maps for different runs) as well as across subjects. The spatial correlation coefficient provides an estimate of the similarity between two activation maps.

EEG

In addition to the fMRI experiments, three subjects performed an additional session of CPT experiments during which EEG recording took place (carried out by the Department of Child and Adolescent Psychiatry at the University Hospital Göttingen). The EEG was recorded with Ag/AgCl electrodes and Abralyt 2000 electrode cream from 23 sites according to an extended 10-20 system using a BrainAmp amplifier. The electrooculogram (EOG) was recorded from two electrodes placed above and below the right eye and at the outer canthi. Impedances were kept below 10 kΩ. EEG and EOG were recorded simultaneously using FCz as recording reference at a sampling rate of 500 Hz with low and high cutoff filters set to 0.016 Hz and 100 Hz respectively and a 50 Hz notch filter. The ground electrode was placed at the forehead. Further analyses were computed with the Vision Analyzer 1.05 software.

6.3. Results

CPT task validation

Subjects responded very accurately (99 ± 0.35 % correct) as well as fast (393.77 ± 6.21 ms) and performance did not change throughout the experiment. As shown for two subjects in Fig. 18, a contingent negative variation (CNV) was evident at the Cz electrode, which confirms that the classical neuroelectric signature of response anticipation is indeed present in the modified CPT paradigm. As expected, we obtained a biphasic wave form with iCNV lasting from 0.5 – 1.5 s and tCNV from 4 – 6 s.

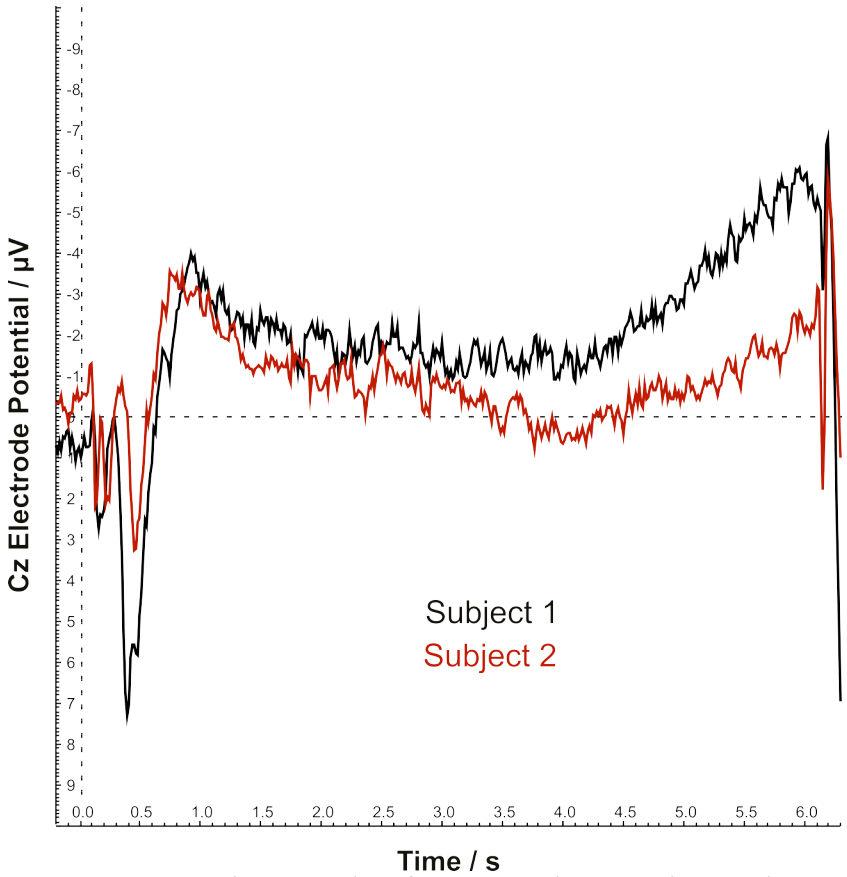

Fig. 18. Representative EEG data from two volunteers show a clear early (≈ 0.5 – 1.5 s) and late (≈ 4 – 6 s) CNV component.

Flanker task validation

As expected, responses were more accurate as well as faster on congruent compared to incongruent trials (see Fig. 19). A 2 × 4 repeated-measures analysis of variance (ANOVA) with congruency (congruent – incongruent) and practice (runs 1 – 4) as factors revealed that subjects responded significantly faster on congruent compared to incongruent trials ($F_{(1,10)}$ = 79.98, $p < 0.001$). This so called positive compatibility effect (PCE) proved to be extremely

robust, being present in every run and every volunteer. Reaction times did not change with increased practice on the task and there was no evidence for an interaction between the two factors (both $F_{(3,30)} < 1$). An equivalent ANOVA was performed for accuracy, also revealing the PCE ($F_{(1,10)} = 21.73$, $p = 0.001$). Subjects' accuracy improved slightly over the four runs ($F_{(3,30)} = 2.68$, $p = 0.065$) which was mainly due to improvements on incongruent trials, as shown by a significant interaction ($F_{(3,30)} = 2.96$, $p = 0.048$, see also Fig. 19).

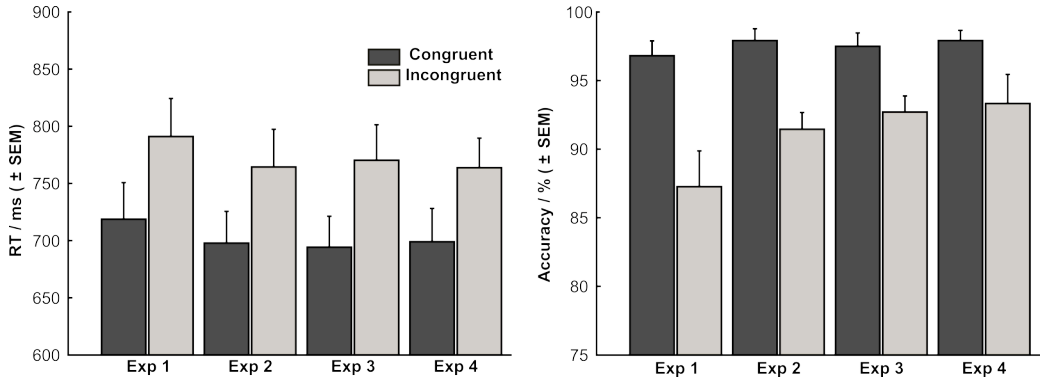

Fig. 19. RT and accuracy over four successive Flanker runs show a significant positive compatibility effect (PCE) as well as increased response accuracy on incongruent trials over the course of the experiment. Surprisingly, practice on the task did not lead to faster responses.

CPT – Flanker Imaging

Both response anticipation (RA) and response conflict (RC) elicited reliable and robust activation in MFC. At the single subject level, we summarized data across multiple runs for each task and presented thresholded activation maps (cluster thresholding at $z > 2.3$ and $p \leq 0.05$) on each volunteer's high-resolution anatomical scan. Representative results from four subjects are displayed in Fig. 20, both for RA and RC. At single subject level, only one volunteer did not activate MFC in response to anticipation while four subjects failed to show conflict-related activation in this brain region. Inspection of Fig. 20 immediately shows that RA activated MFC more strongly and extensively then RC. Furthermore, anticipation involved a more extensive network of additional brain areas, most notably thalamic and midbrain structures.

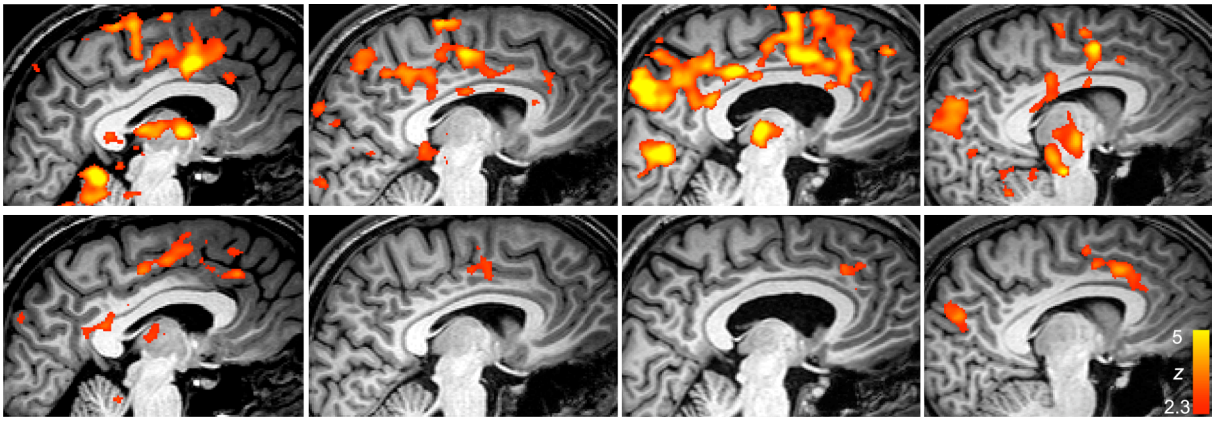

Fig. 20. Brain responses to RA (top) and RC (bottom) for 4 volunteers displayed on their respective anatomical scan. Both tasks elicit activation in MFC but response anticipation clusters are more widespread and stronger than RC foci. Note the substantial between-subject variability in the extent and strength of activations.

Results from single subjects were confirmed and extended by a multi-subject group analysis (see Fig. 21). In line with the previous analysis, RA activated a more extensive network of cortical and subcortical brain regions. Within ACC, conflict-related activation largely overlapped with activation due to RA (COG: 3, 26, 36 and 2, 27, 28 respectively). Differential brain responses for anticipation and conflict processing where observed in the superior portion of MFC, especially superior frontal gyrus (SFG). Conflict activated a region in posterior SFG (COG: -1, 21, 54), presumably pre-supplementary motor area (pre-SMA). Contrarily, RA activation was detected in a more anterior region along the SFG (COG: 3, 32, 44).

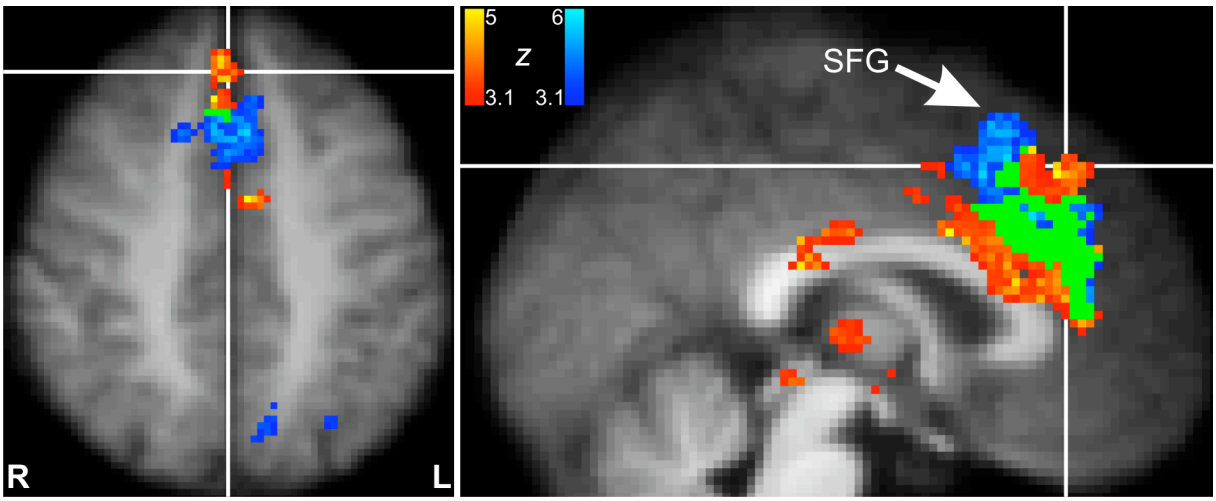

Fig. 21. Cortical activations for response anticipation (red) and conflict (blue) as well as overlap (green). Note the differential involvement of SFG in both processes. Left intra-parietal sulcus was only activated for RC (left panel)

Outside MFC, response anticipation activated an extensive network of brain regions (see Fig. 22; COG coordinates are reported in Table 2). Cortical activations were observed in right and left dorsolateral prefrontal cortex (DLPFC) as well as right insular cortex. Subcortical regions modulated by the RA contrast included thalamus, striatum (including putamen and pallidum) as well as focal midbrain activation, very likely corresponding to the substantia nigra. Conflict-related brain responses outside MFC largely overlapped with RA activation in anterior thalamus, right insular cortex and right DLPFC (middle frontal gyrus). A small cluster in left intra-parietal sulcus (IPS) was activated for conflict but not response anticipation (see Fig. 21).

Table 2: Atlas coordinates (in MNI space) and maximum *z*-scores for the centers-of-gravity (COG) of clusters significantly activated for response anticipation, conflict or both.

Contrast	Brain region	COG Coordinates (x, y, z)z	*z*-score
RA	subcortical cluster (incl. insula)	-5, 0, -1	6.29
	MFC / ACC	2, 27, 28	5.61
	right / left DLPFC	33, 53, 19 / -32, 48, 21	5.11 / 5.47
	SFG	3, 32, 44	5.06
	right / left substantia nigra	12, -16, -14 / -8, -15, -14	4.85 / 4.62
RC	MFC / ACC	3, 26, 36	5.18
	right anterior insula	35, 23, -7	4.49
	right / left (anterior) thalamus	12, 0, 3 / -10, 1, 8	4.14 / 4.01
	right frontopolar cortex (FPC)	36, 45, 18	4.04
	left intra-parietal sulcus (IPS)	-28, -62, 39	4.35
	right DLPFC (inferior frontal gyrus)	50, 15, 22	4.23
	SFG	-1, 21, 54	5.18
Overlap	ACC	4, 31, 29	5.24
	right / left anterior thalamus	12, -1, 3 / -10, 3, 6	5.51 / 4.87
	right insula	35, 23, -5	4.56
	right FPC	30, 52, 18	4.55

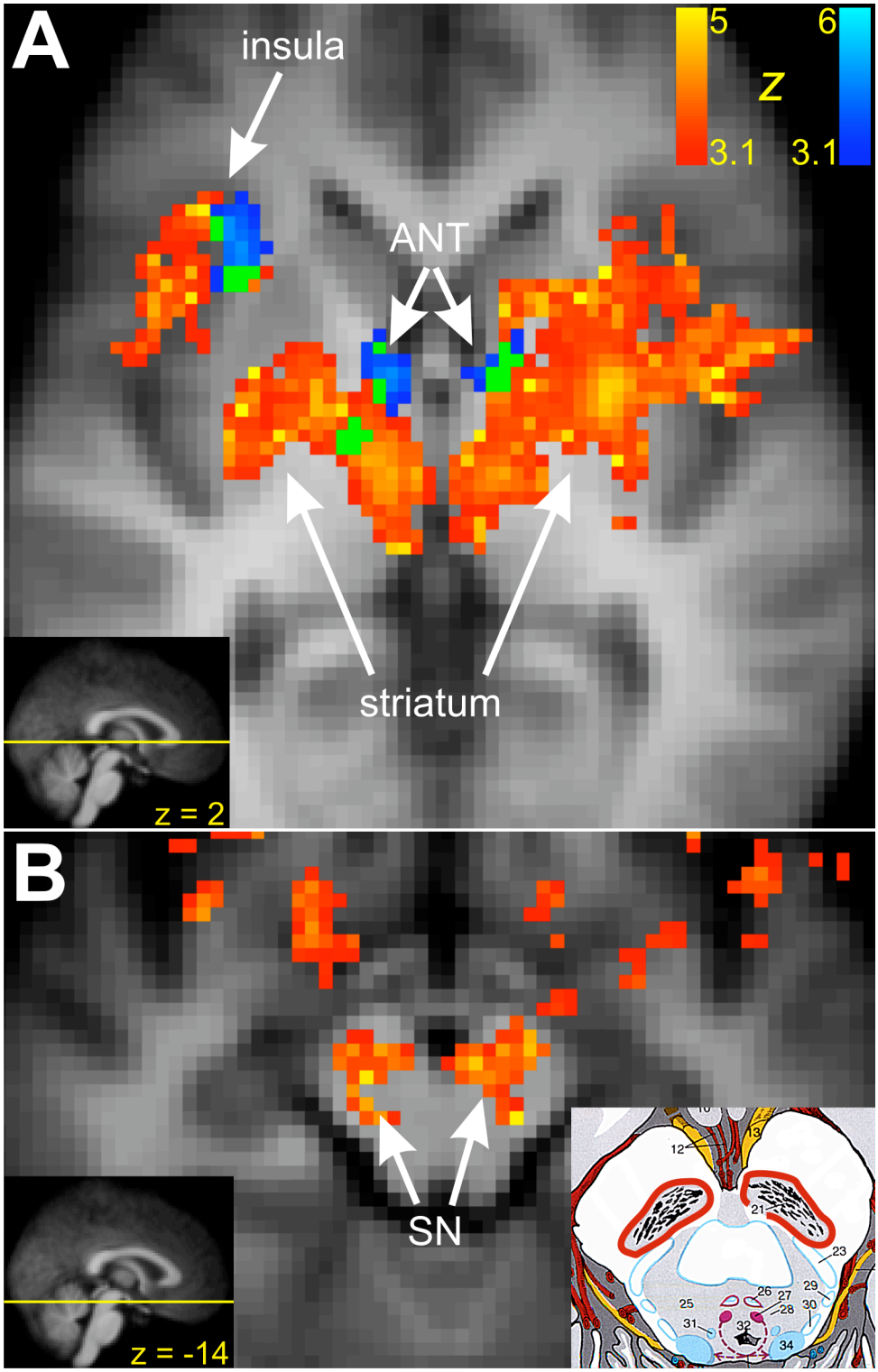

Fig. 22. Cortical activations for response anticipation (red) and conflict (blue) as well as overlap (green). A: Horizontal section through the thalamus and striatum (compare left inset) reveals overlapping brain responses for RA and RC in insular cortex as well as the anterior nucleus of the thalamus (ANT). Anticipation activates a more wide-spread network including medial thalamus and striatum. B: Horizontal section at the upper midbrain level (compare left inset) reveals activation associated with anticipatory behavior in the substantia nigra (SN). The right inset shows a schematic drawing of the midbrain at the corresponding level. The substantia nigra is labeled with number 21 (red circles; from Kretschmann and Weinrich, 2003). Note that right and left are reversed, in accordance with the radiological convention.

Linear contrasts were calculated for the two cognitive processes (RA > RC and RC > RA) and the resulting maps thresholded using the false discovery rate (FDR) at a threshold of $q \leq 0.05$ (minimum of 20 connected voxels). As shown in Fig. 23 (see also Table 3), RA responses were significantly stronger than RC in dorsal ACC, thalamus, striatum as well as left and right DLPFC. The opposite contrast (RC > RA) revealed a range of brain regions putatively stronger activated for response conflict than anticipation (see Fig. 23 and Table 3). Interestingly, the majority of these areas (posterior cingulate, orbitofrontal, frontopolar as well as left / right sensorimotor cortex and SMA) were in fact strongly deactivated during response anticipation. Truly stronger conflict responses were detected only in the previously described SFG cluster as well as left inferior frontal gyrus.

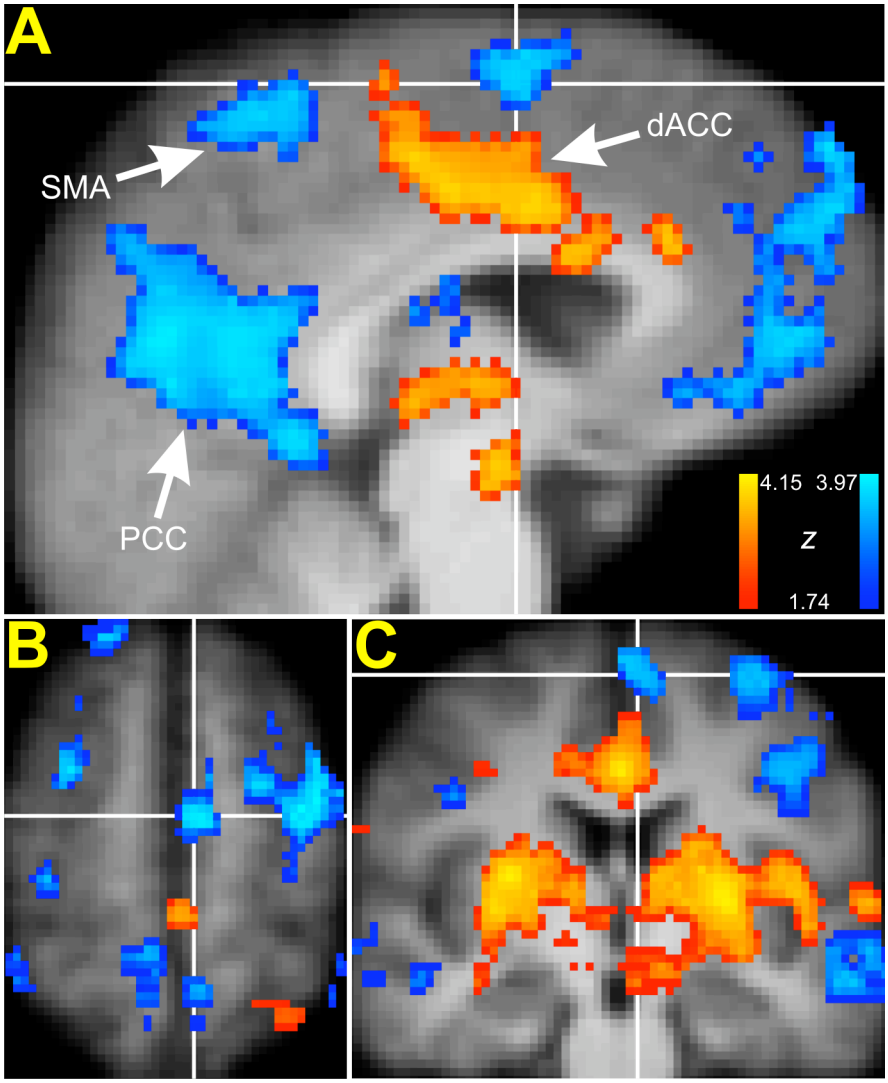

Fig. 23. Contrast activation maps between response anticipation and conflict, showing regions putatively stronger activated for RA (red) and RC (blue). Note that the standard brain was rotated by -25° around the x-axis to visualize the differential activation along SFG (panel B). PCC … posterior cingulate cortex

Table 3: Atlas coordinates (in MNI space) and maximum *z*-scores for the centers-of-gravity (COG) of clusters significantly stronger activated for RC than RA or vice versa.

Contrast	Brain region	COG Coordinates (x, y, z)	*z*-score
RA > RC	subcortical cluster	-8, 0, -1	4.15
	MFC / ACC	-1, 11, 35	3.97
	left motor / premotor cortex	-17, -29, 62	3.37
	left supramarginal gyrus	-61, -30, 20	3.27
	left / right DLPFC	-35, 47, 21 / 38, 55, 22	3.41 / 2.69
RC > RA	left anterior SFG	-4, 23, 55	3.52
	left DLPFC	-47, 21, 20	3.76
	PCC	-3, -53, 31	3.87
	orbitofrontal cortex	1, 42, -17	3.27
	FPC	-8, 64, 8	3.43
	right / left sensorimotor cortex	46, -22, 58 / -44, -22, 60	3.97 / 3.29
	SMA	3, -25, 66	3.25

Variability analysis

The previous analysis demonstrated that MFC plays an important role in both response anticipation and response conflict processes. Furthermore, subregions within MFC may be selectively processing different aspects of the tasks. While information on mean activation patterns for a group of subjects is no doubt valuable, estimating the variability between different individuals seems to be equally important. Though few cognitive fMRI studies have so far addressed the issue of inter-individual variation (for examples see Taylor *et al.*, 2006; Lütcke and Frahm, in press), those that have, relied on calculation of centers-of-gravity for each subject. Accordingly, we determined COGs from subjects' activation maps, as shown exemplarily in Fig. 20. In order to take into account the global difference in activation level between response anticipation and conflict, RA maps were thresholded more stringently ($z > 3.1$, $p < 0.05$) while RC maps had to pass a rather lenient threshold ($z > 2.1$, $p < 0.05$). Using these criteria, we were able to obtain significant RA and RC clusters in MFC for 11 and 8 subjects, respectively. As shown in Fig. 24, individual subjects' COGs varied considerably for both tasks, most notably along the dorsal-rostral axis of MFC. Mean and standard deviations of COGs for both tasks (in MNI standard space coordinates) are presented in Table 4. COGs during response anticipation were significantly right lateralized (mean x-coordinate 1.7 mm, $t_{(10)} = 3.07$, $p = 0.01$, two-tailed) whereas conflict COGs were distributed more bilaterally (mean x-coordinate 0.5 mm, $t_{(7)} = 0.38$, $p = 0.72$). Moreover, inspection of Fig. 24 as well as

Table 4 shows that Flanker COGs tended to be located somewhat more superiorly ($y_{RC} > y_{RA}$), although this trend failed to reach significance ($t_{(6)} = 1.3$, $p = 0.2$).

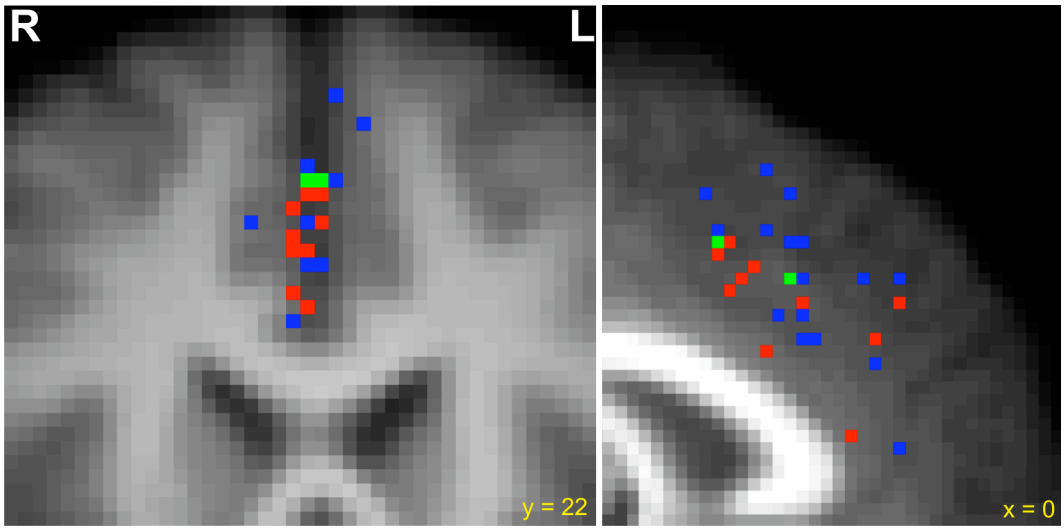

Fig. 24. Centers of gravity for individual subjects in MFC for RA (red) and RC (blue). Overlapping COGs are indicated in green. Note the variability in COG location, especially along the dorsal-rostral axis of MFC (right).

Table 4: Atlas coordinates (in MNI space) for COGs in MFC for individual subjects (means and standard deviations).

	COG - x	COG - y	COG - z
CPT Mean (± SD)	1.73 (1.87)	18.95 (9.68)	38.07 (7.02)
Flanker Mean (± SD)	0.48 (3.61)	23.71 (10.77)	41.59 (10.21)

To estimate the spread of COGs and compare them between the two tasks, mean and standard deviation of the Euclidean pairwise distance between all COGs were calculated. The Euclidean distance between two vectors, x_r and x_s is defined as:

$$d_{rs}^2 = (x_r - x_s)(x_r - x_s)' \quad (7)$$

Whereas the mean of the Euclidean distance indicates how far, on average, two COGs are from each other, its standard deviation provides an estimate of the uniformity of a distribution of points (i.e. if some are located more closely than others). Both mean and standard deviation of the Euclidean distance between COGs did not differ substantially between response anticipation and conflict (RA: mean distance 3.80 mm / standard deviation 3.04; RC: mean distance 4.32 mm / standard deviation 3.33).

Whereas COGs provide a convenient way for describing individual activation centers in a group of subjects, the amount of information captured by this parameter is limited. In addition to localization variability (which is measured by COG-based analysis), subjects' activations may differ for example in extent or shape. To date, however, no standard approach has emerged on how to quantify these parameters. One promising parameter appears to be the overall similarity of activation maps, which may be simply quantified by the correlation coefficient. Accordingly, we calculated subject-wise spatial correlations between unthresholded statistical *z*-maps in MFC and collected the results in a subject correlation matrix (see Fig. 25).

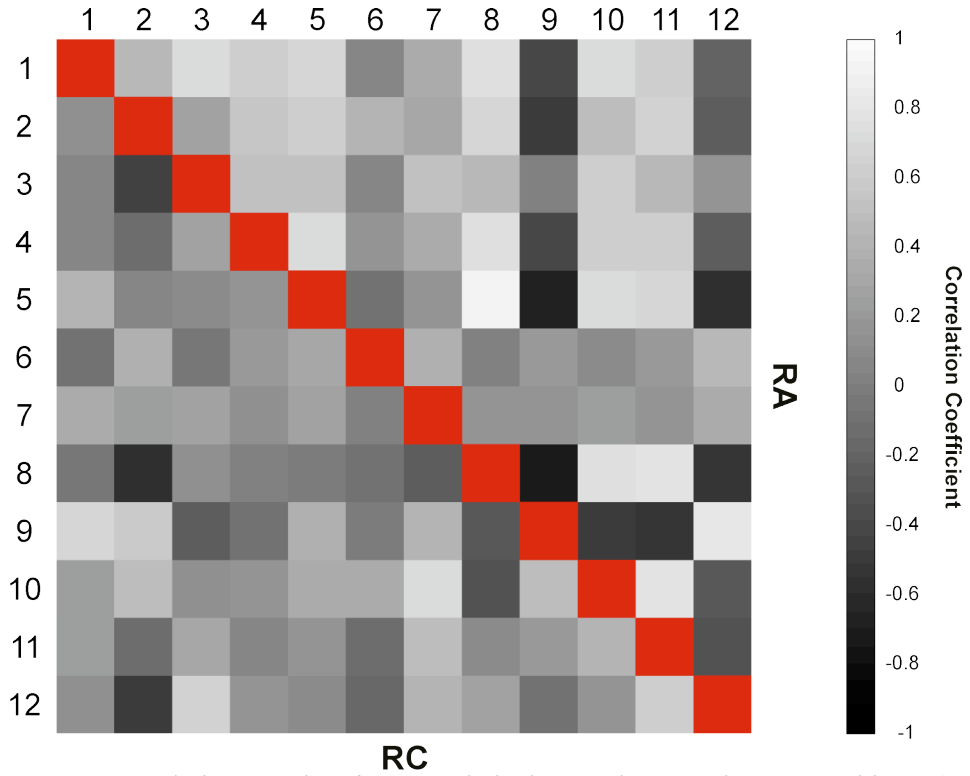

Fig. 25. Correlation matrix of raw statistical maps in MFC between subjects (1 – 12) for response anticipation and conflict. Note the overall higher between-subject similarity of RA maps, compared to RC. Subject 9 (and possibly subject 12) shows very dissimilar activation compared to other volunteers during RA, as indicated by negative correlation coefficients.

Interestingly, RA statistical maps were slightly more similar to each other than RC maps ($r_{RA} = 0.27 \pm 0.05$ versus $r_{RC} = 0.14 \pm 0.03$; $t_{(65)} = 1.79$, $p = 0.08$). In Fig. 25, note also that one volunteer (subject 9) shows very dissimilar RA statistical maps to virtually all other subjects (as shown by very low correlation coefficients). Interestingly, subject 9 is also the only volunteer that failed to show significant activations for the response anticipation contrast

(see above). Once excluded, the difference in map similarity between RA and RC becomes even more pronounced ($r_{RA} = 0.37 \pm 0.05$ versus $r_{RC} = 0.14 \pm 0.04$; $t_{(54)} = 3.69$, $p < 0.001$).

Finally, we investigated the variability of activation maps across multiple runs for the same volunteer. For each subject, we calculated correlation coefficients between unthresholded statistical maps (restricted to MFC) for the first versus the second, third and fourth run (see Fig. 26). A 2 × 3 repeated-measures ANOVA (CPT / Flanker × Correlation distance) revealed significantly stronger intra-subject correlations for response anticipation than conflict ($F_{(1,11)} = 6.67$, $p = 0.025$). While the mean correlation between CPT statistical maps seemed to be quite stable across several runs, there was a sharp drop in the correlation from third to fourth session for the Flanker task. However, due to the large inter-subject variability in this analysis neither the main effect for correlation distance nor the interaction between the two factors reached statistical significance ($F_{(2,22)} = .28$, $p = 0.8$ and $F_{(2,22)} = .47$, $p = 0.6$, respectively).

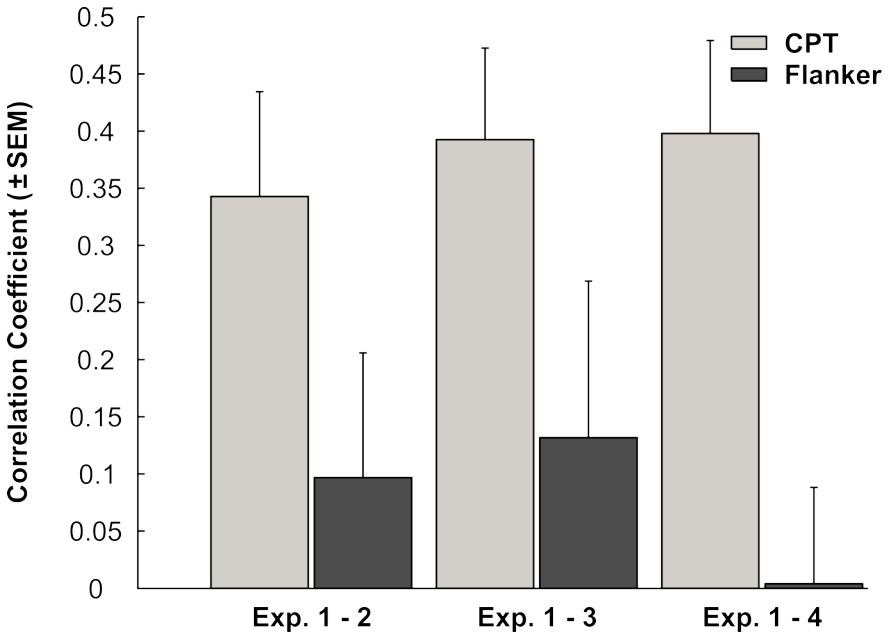

Fig. 26. Correlation of raw statistical maps in MFC within subjects between successive runs for CPT and Flanker tasks. Response anticipation (CPT) elicits more reproducible brain responses than conflict (Flanker).

6.4. Discussion

The previous experiment employed a conflict eliciting Flanker task as well as the continuous performance test to compare and contrast neural mechanisms underlying response conflict and anticipation. Analysis of behavioral data from the Flanker task demonstrated a clear PCE both for accuracy and reaction times, providing strong evidence that incongruent trials indeed elicited more response conflict than congruent trials. Separate EEG experiments in a subset of subjects showed that the CPT elicited a classic biphasic negativity with a pronounced late wave, which was the focus of the current study.

Neural basis of response anticipation

Our results are in line with previous studies and support the hypothesis of a thalamo-cortico-striatal network underlying anticipatory behavior (Birbaumer *et al.*, 1990). While initial claims for a role of subcortical structures in the generation of the CNV in humans were based largely on speculation and indirect evidence, recent neuroimaging studies, together with the current data, have firmly established the importance of thalamus and striatum for successful response anticipation (Nagai *et al.*, 2004; Fan *et al.*, 2007). Based on the previous literature, our results suggest that thalamic afferents facilitated at least two distinct cortical areas: the anterior part of the superior frontal gyrus (medial portion of Brodmann areas 8 / 9) as well as anterior cingulate cortex. Interestingly, motoric regions such as premotor or supplementary motor cortex appeared not to be modulated during response anticipation. A likely reason is that the response to S_2 was not precisely specified in the paradigm and subjects could therefore not prepare for an action. Instead, anticipation equated to a generally attentive and alert state in order to effectively make a decision upon presentation of the imperative stimulus.

In addition to activation along the medial frontal wall, we observed significant brain responses bilaterally in dorsolateral prefrontal cortex. The precise location of this activation was in frontopolar cortex (BA 45 / BA 10 lateral) somewhat more inferior and anterior to the prefrontal foci reported in previous studies (Nagai *et al.*, 2004; Fan *et al.*, 2007). Speculatively, this region may exert top-down control on thalamic nuclei via the mediothalamic frontocortical system (MTFCS).

Activation of ACC was pronounced during response anticipation. Examination of individual subjects' COGs in MFC revealed a significant right lateralization, which is in line with a previous EEG study (Brunia and Damen, 1988) that reported right-sided predominance

of sources specifically for tCNV and independent of the response modality. Based on correlation evidence, Nagai and colleagues (Nagai *et al.*, 2004) speculated that ACC underlies the generation of the CNV early wave. While this may be true, the results from the current study provide strong evidence that ACC is additionally involved in processes underlying tCNV generation. Future studies should attempt combined EEG / fMRI acquisition in a long ISI paradigm. While technically challenging, this would allow correlation of early and late CNV amplitude with activity in ACC.

As expected, response anticipation was associated with activation in a large network of subcortical structures, including thalamus, putamen, pallidum as well as caudate nucleus. In a strict sense, the high activation level observed at our chosen threshold does not allow a finer distinction, for example of individual thalamic nuclei (see Fig. 22). If thresholds are adjusted *post hoc* to higher levels ($z > 4$, $p \leq 0.05$), however, individual clusters are located in insular cortex, putamen as well as medial thalamus. Interestingly, based on anatomical considerations, the medial thalamus has been isolated as the primary source of projections to the cortex underlying CNV generation (Birbaumer *et al.*, 1990). A functional involvement of medial thalamus in the generation of tCNV in humans, however, has not yet been demonstrated. In this context, it is interesting to note that the two previous fMRI studies pertaining to iCNV generation (Nagai *et al.*, 2004; Fan *et al.*, 2007), have reported activation maxima in lateral thalamus and pulvinar. Future studies employing high-resolution fMRI specifically of subcortical nuclei may be capable of resolving this issue.

The neostriatum (especially putamen) plays a prominent role in the previously discussed model of CNV generation. It receives extensive input from the medial thalamus, probably via collateral projections of thalamo-cortical fibers. The neostriatum further receives contextual information from the cortex and is thought to modulate thalamic 'gating' based on current task demands (Birbaumer *et al.*, 1990).

Activation of the substantia nigra in relation to anticipatory behavior is in line with the well-known role of the dopaminergic system in CNV generation. It has been speculated that dopamine neurons activate thalamic afferents by inhibition of GABAergic interneurons in the reticular nucleus of the thalamus, thereby contributing to the CNV. Loss of dopaminergic neurons in the substantia nigra, as in Parkinson's disease, leads to a strong attenuation of the CNV while the biphasic wave form remains unaltered (Pulvermüller *et al.*, 1996). Reassuringly, direct evidence for a projection of dopamine neurons from the substantia nigra to the reticular nucleus has recently been obtained by tract tracing in rodents, rhesus monkeys as well as humans (Freeman *et al.*, 2001).

Neural basis of response conflict

Cortical conflict-related activation was observed in ACC, right frontal cortex as well as posterior SFG. These results are in accordance with the general model of conflict processing and error monitoring outlined in the previous chapter (Yeung *et al.*, 2004). ACC is thought to act as a detector of conflict which then recruits areas in frontal cortex to exert top-down control on posterior brain regions involved in task-specific conflict resolution processes. One possible target region for specific resolution of competing responses in the Flanker task may be in the posterior SFG, an area commonly defined functionally as pre-supplementary motor area (pre-SMA; Picard and Strick, 1996). While the tasks which have been reported to activate pre-SMA are numerous and diverse, recent evidence suggests that they may amount to multiple manifestations of one fundamental function, namely the competitive interaction for a unitary output channel between neural representations of incompatible motor responses (Nachev *et al.*, 2007). This idea is elaborated within a framework for MFC function in the general discussion.

Finally, we observed conflict-related activation in the right anterior insular cortex and in the anterior nucleus of the thalamus bilaterally. Together with ACC, these regions are part of the limbic system (Papez, 1995; originally published 1937), a network of brain areas underlying the modulation of emotional and motivational aspects of behavior as well as autonomic function (Morgane *et al.*, 2005). Strong interconnection between these three regions has been demonstrated previously by deep brain stimulation of the thalamus for epilepsy treatment (Zumsteg *et al.*, 2006). In this study, stimulation of anterior, but not dorso-medial or centro-medial, thalamic nuclei elicited strong cortical responses in both insular cortex and ACC.

Comparison of neural responses to conflict and anticipation

The results of the present study suggest that response anticipation (RA) and conflict (RC) are subserved by distinct but overlapping brain networks. With respect to areas involved in both processes, similar regions were identified as in a previous study (Fan *et al.*, 2007): ACC, (right) anterior insular and frontal cortex as well as anterior thalamus. Because our study was designed to assess both anticipation and conflict processing in the same volunteers but in different sessions, we could also calculate contrasts for RA and RC. A large subcortical network, including thalamus, pallidum and caudate nucleus, as well as dorsal ACC responded significantly stronger for anticipatory behavior. Contrarily, pre-SMA showed a greater activation during conflict processing.

Overlapping activation in ACC, anterior thalamus as well as anterior insular cortex suggests that both anticipatory behavior and conflict processing involve increased activity in the limbic system. While traditionally seen as a neural substrate for emotions (Morgane *et al.*, 2005), a number of components in the limbic system (including the aforementioned regions) are crucially involved in the regulation of autonomic functions (Critchley *et al.*, 2003). Interestingly, both response anticipation and conflict have been linked to changes in autonomic arousal, albeit in opposite directions. Tecce (1972) provided a comprehensive review of studies showing a generalized decrease of autonomic activity, as indexed for example by lower heart rate or reduced tonic muscle activity, with elevated CNV amplitude. Conversely, response conflict increases arousal as shown by acceleration of heart rate (Freyschuss *et al.*, 1988) as well as increased skin conductance (Kobayashi *et al.*, 2007) on high conflict trials. It seems reasonable to assume, therefore, that the observed common activation of a limbic network reflects modulation of autonomic function in both conditions. This hypothesis awaits future confirmation by studies combining imaging and measurement of physiological parameters.

Further overlap between anticipatory and conflict processes was detected in the right frontopolar cortex (FPC). Strikingly, this activation corresponded precisely to the FPC cluster detected in the previous GoNogo experiment (see Fig. 27) and has been associated with conflict processing in this context. While right lateralized for response conflict (Flanker and GoNogo tasks), FPC activation was observed bilaterally for anticipatory behavior.

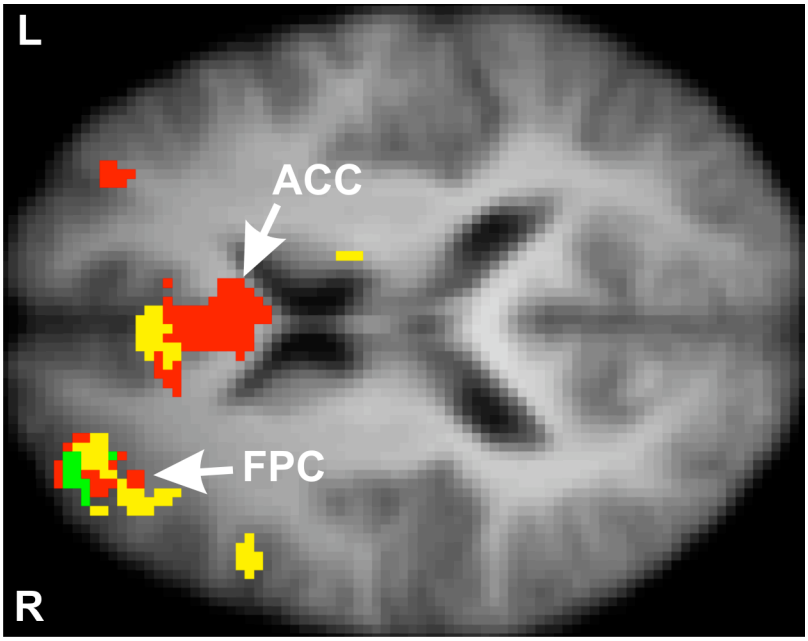

Fig. 27. Consistent right frontopolar activation on three different tasks (CPT … red, Flanker … yellow, GoNogo … green)

Speculatively, FPC may be the source of top-down control which modulates task-specific regions such as pre-SMA in the Flanker experiment or thalamus (via the MTFCS) during anticipation. Although left sided activation in FPC was only observed for RA, *post hoc* analysis of individual subjects' Flanker results using reduced thresholds ($z > 2$; uncorrected) revealed increased activity in left FPC for ten out of twelve volunteers. We conclude therefore that FPC provides various task-specific brain regions with top-down attentional resources and, in line with other authors (Corbetta and Shulman, 2002), we observed a right hemispheric preference of this inferior frontal control system.

In summary, the current study provides evidence for two distinct networks underlying both response conflict and anticipation. The first, comprising anterior thalamus and insular cortex, presumably plays a role in modulation of autonomic function. Secondly, an inferior frontal attentional system provides top-down processing resources to task-specific regions involved in either anticipation or conflict resolution. ACC functions as a link between the two networks, and is thought to perform a domain-general evaluation of the organism's internal state. Upon deviations from the desired internal state, as brought about for example by changing task demands, ACC recruits cognitive, autonomic or even emotional brain systems specialized for dealing with the task at hand. The idea that ACC acts as an interface between distinct processing networks has received considerable attention in recent years (Bush *et al.*, 2000; Rushworth *et al.*, 2004; Amodio and Frith, 2006; Rushworth *et al.*, 2007) and will be discussed more extensively in the final section of this thesis.

Neural mechanisms of tCNV generation

Previously, two studies have investigated the neural mechanisms underlying generation of the CNV using fMRI (Nagai *et al.*, 2004; Fan *et al.*, 2007). Both of them used too short ISIs for separating early and late components of the negativity. In the present experiment, we therefore focused on mechanisms pertaining to generation of the terminal wave, which has previously been neglected. Overall, a very similar network of brain regions emerged as in the previous studies. There were, however, some important differences. As outlined above, we detected thalamic activation largely in medial nuclei, whereas previously lateral and pulvinar activations have been reported. Given the limited spatial resolution in all three experiments, these differences must be taken as very preliminary and await future confirmation by high-resolution imaging. Secondly, we observed activation of the inferior frontal attention system whereas previous studies reported increased brain responses along the middle frontal gyrus. The precise reason for this discrepancy is currently not clear. Finally, unlike previous

investigations, we observed increased activity in a midbrain region which very likely corresponds to the substantia nigra. A possible explanation for this finding is that tCNV indexes movement preparation whereas iCNV has a stronger association with stimulus processing.

Within and between-subject variability

An advantage of our experimental design, which incorporated repeated measurements of each task on the same subjects, is the ability to assess variability of evoked brain responses both within and between individuals. In line with previous investigations of cognitive processing in MFC (Taylor *et al.*, 2006; Lütcke and Frahm, in press), we observed substantial variability in activation centers between subjects. These variations were of similar magnitude for CPT and Flanker experiments and also most pronounced along the dorsal-rostral axis of MFC. With respect to overall similarity of activation maps, however, these proved to be more variable for conflict processing, compared to response anticipation, both within and between subjects. An explanation for this difference may be that subjects employ different strategies for solving the Flanker task, which might result in different patterns of brain activation. Contrarily, the CPT as a relatively simple task does not afford substantial changes in strategy. Interestingly, since we did not observe profound behavioral changes over the course of four runs, different strategies must be, on average, equally effective in solving the task.

Our comprehensive analysis of variability demonstrates the importance of going beyond single point measures of localization. Furthermore, it provides additional evidence for strong between and within subject variability, a finding which has so far been neglected in theories of MFC function.

7. Real-time fMRI and BOLD neurofeedback

7.1. Introduction

From observation to modulation of brain activity

The experiments discussed in the previous chapters are both examples of the current standard approach in cognitive neuroimaging where a stimulus, task or, more broadly, some function is manipulated and the effect of this manipulation on brain activation is observed. Strictly speaking, however, such an approach allows only very limited conclusions to be drawn. At best one may argue that the identified brain systems can be considered sufficient for performing the investigated function (Price *et al.*, 1999), while more usually, it is not possible to exclude that some undetected regions also play an important role. On the other hand, no matter how strong the observed association, neuroimaging provides no evidence pertaining to the structure's necessity for performing a given function.

To illustrate this point, consider the following analogy between a car and the brain[1]. Observation of one of the car's parts, for example the speedometer, suggests that it may be involved in the car's function (driving) since there is a systematic covariation between the two. It would, however, be invalid (and in this case false) to conclude that there is a causal relation between the speedometer's activity and the car's function. More formally (Sarter *et al.*, 1996), let Ψ be a certain cognitive function and Φ a brain structure underlying this function, so that $\Psi = f(\Phi)$. Neuroimaging investigates the activity of brain regions, given a certain function. That is, it attempts to determine the probability of Φ, given Ψ [$P(\Phi/\Psi)$]. Problematically, experimental manipulation of cognitive function Ψ also influences certain brain activities φ_1, φ_2, … Consequently, if Ψ associates with φ_1 it is impossible to conclude a causal link, since undetected additional brain structures, such as φ_2, might be causal mediators. Contrarily, observing the effect of manipulating Φ on function Ψ [determining $P(\Psi/\Phi)$] permits causal inferences about structure-function relations. With respect to the previous example, manipulation of the speedometer has no influence on the car's ability to drive, demonstrating that there is no causal link between the two. On the other hand, breaking the engine impairs the car's function and therefore allows the conclusion that the engine's activity is directly linked to driving.

The inability to infer causal links between a structure and its function presents one of the major limitations of neuroimaging techniques (in fact, it applies not only to imaging, but

[1] *While this example has been widely publicized to illustrate the point that correlation does not imply causation, its original source is unknown to the author.*

to all observational methods such as EEG, MEG or single-unit recording). Moreover, neuroimaging is also limited in deducing causal links between different brain areas (Paus, 2005). While the previous statement that frontopolar cortex is recruited by ACC during cognitive conflict (see above) may be consistent with the data and previous knowledge, from a logical point of view it is not a valid conclusion (even ignoring certain methodological constraints, such as low temporal resolution of fMRI). Recently, a number of groups have attempted to circumvent this problem by evoking the concept of Granger causality, which is based on the idea that effects cannot precede their causes in time (Eichler, 2005; Roebroeck *et al.*, 2005). Given the speed of information transfer in the brain (feedback signals may reach early visual areas from PFC in less than 400 ms after stimulus presentation; Dale *et al.*, 2000) as well as the low temporal resolution of fMRI, however, robust inference of Granger causality becomes very difficult and may be limited to certain systems.

Consequently, techniques for direct interference with brain regions are highly desirable in order to determine causal structure – function as well as structure – structure interactions. Obviously, while common in animal experiments, ethical and practical considerations limit the applicability of such techniques in studies of human subjects. Traditionally, studies of patients with circumscribed brain injuries have been the most popular interference method in cognitive neuroscience (reviewed in Moses and Stiles, 2002). The approach, however, suffers from several major disadvantages, as has been described in the introduction. In contrast to permanent lesions due to brain damage, reversible or 'virtual' lesions may be induced in healthy volunteers using transcranial magnetic (TMS; reviewed in Hallett, 2007) or transcranial direct current stimulation (TDCS; reviewed in Nitsche *et al.*, 2002; Floel and Cohen, 2007). While more flexible compared to brain injuries, both TMS and TDCS suffer from poor localizability as well as limited depth, making them unsuitable for disruption of subcortical tissue. Although recent attempts to combine lesions (Price *et al.*, 1999) or TMS (Bestmann *et al.*, 2003) with functional imaging have addressed some of the disadvantages, other problems have emerged in this way.

Clearly then, our ability to interfere with brain function in healthy human volunteers in order to determine causal structure – function relations is currently very limited. Interestingly, recent methodological developments in real-time analysis of fMRI data have suggested a new technique for non-invasive and reversible interference with localized brain regions. Using neurofeedback, subjects can learn to modulate the activity level of a specified brain region over the course of several experiments. After training, this ROI may be selectively activated

or deactivated while the researcher concurrently assesses the influence of regulation on behavior as well as other brain areas.

The following section will provide a brief overview of real-time fMRI (rtfMRI) as well as neurofeedback. Subsequently, a study will be described which was designed to establish neurofeedback based on rtfMRI and demonstrates the feasibility of voluntary regulation of MFC activity.

Real-time fMRI

Owing to the large matrix size of a standard fMRI experiment (typical 4D-image dimensions of 96 × 96 × 22 × 244), data analysis has traditionally been performed offline. Recent advances in computing hardware as well as the development of more efficient evaluation algorithms have made the real-time analysis of images feasible. More specifically, rtfMRI requires that image reconstruction from k-space, data transfer, preprocessing as well as statistical analysis are performed in the time it takes to acquire a single volume (typically 2 s), so that no time lag builds up over the course of the experiment. Today, the main challenge lies in the implementation of online reconstruction algorithms on the scanner hardware, as these require special software which is not provided by manufacturers. Commercially available computers easily fulfill criteria for rtfMRI analysis.

Real-time analysis of fMRI data was pioneered by Cox and colleagues (Cox *et al.*, 1995) although acquisition was limited to a single slice in their study. Considerably later (Gembris *et al.*, 2000), feasibility of multi-slice rtfMRI was reported, based on continuous sliding-window correlation analysis. Recently, even more sophisticated evaluation techniques, such as general linear modeling (Nakai *et al.*, 2006) or independent component analysis (Esposito *et al.*, 2003), have been developed for rtfMRI. An overview of the rtfMRI literature as well as specific methodological aspects is provided by Weiskopf and colleagues (Weiskopf *et al.*, 2007).

Neurofeedback using rtfMRI

Once the activation level in a pre-determined brain region can be calculated with minimal time delay, it is possible to inform subjects about their brain activity using a suitable graphical representation as well as standard stimulus projection devices. Subjects can then learn to up- or down-regulate this activity intentionally if they are given appropriate instructions (see below). An initial study (Weiskopf *et al.*, 2003) demonstrated this principle by providing evidence for selective regulation of both dorsal and rostral ACC in a single volunteer.

Subsequently, other brain regions were shown to be amenable to self-regulation, including somatomotor cortex (deCharms *et al.*, 2004), anterior insula (Caria *et al.*, 2007) and auditory cortex (Yoo *et al.*, 2006). Strikingly, a recent study demonstrated that regulation of ACC activity modulated perceived pain intensity in both healthy volunteers and chronic pain patients (deCharms *et al.*, 2005), suggesting that BOLD neurofeedback may be a promising new treatment strategy for disorders which involve hyper- or hypoactivity of a circumscribed brain region. Finally, a recent study (Bray *et al.*, 2007) showed that subjects are able to modulate activity in motor cortex without immediate feedback, simply by being rewarded for correct self-regulation.

Selection of the appropriate ROI may be one of the most critical aspects of BOLD neurofeedback experiments. Previous studies usually employed ROI definition based on anatomical information. Given the strong inter-subject variability of activations for cognitive tasks, functional determination (using localizer tasks) of ROIs may be more appropriate. In addition to the target ROI, a second region in another brain area is frequently chosen and feedback is calculated by subtracting the background signal from the target ROI signal (see below). In this way, global intensity variations due to uncorrected head motion or changes in breathing pattern cannot contribute to the feedback signal. Finally, instructions given to subjects may be a major contributor to success or failure of a feedback experiment. While instructing volunteers is trivial for regulation of early sensory or motor areas (e.g. *"Imagine moving your right hand."*), it becomes more complex in the case of higher brain areas which are thought to subserve very abstract functions, such as conflict monitoring. In our experience, provision of general instructions together with encouragement to develop an individual strategy seems to work best. In any case, subjects should be made aware of the temporal characteristics of the hemodynamic response which will lead to a delay of voluntarily induced changes of brain activity by several seconds.

Physiological self-regulation of functional subregions in MFC

In the present study, our primary goal was to establish rtfMRI and BOLD neurofeedback as new paradigms in the laboratory. Subsequently, we performed a proof-of-principle experiment which demonstrated that subjects can learn to regulate brain activation in small subregions of MFC. Unlike previous studies, we defined target ROIs based on a functional localizer task (Flanker; see above). Thus, we were able to determine regions in MFC that are likely to be involved in conflict-related processing. BOLD neurofeedback of functionally defined ROIs is a prerequisite for using the technique to perturb or enhance cognitive brain

areas since one would like to modulate only those regions truly involved in the task. Furthermore, it addresses the issue of inter-subject variability. Finally, we investigated which brain systems outside the target ROI contributed to feedback success.

7.2. Materials and Methods

Subjects

Six female subjects (mean age 28.5 ± 0.5 years) participated in proof-of-principal experiments to demonstrate the feasibility of BOLD neurofeedback in cognitively driven brain regions. Two subjects were asked to return for a second neurofeedback session on a separate day. Two volunteers failed to achieve significant and reproducible self-regulation over the course of two sessions and were excluded from data analysis. All participants were informed about the purpose of the study as well as possible risks associated with MRI. Written consent was obtained prior to each experimental session. Participants earned 10 Euros per hour. All experimental procedures conformed fully to institutional guidelines.

rtfMRI Setup

Real-time fMRI was based on a custom-built extension of the MRI scanner environment (see Fig. 28).

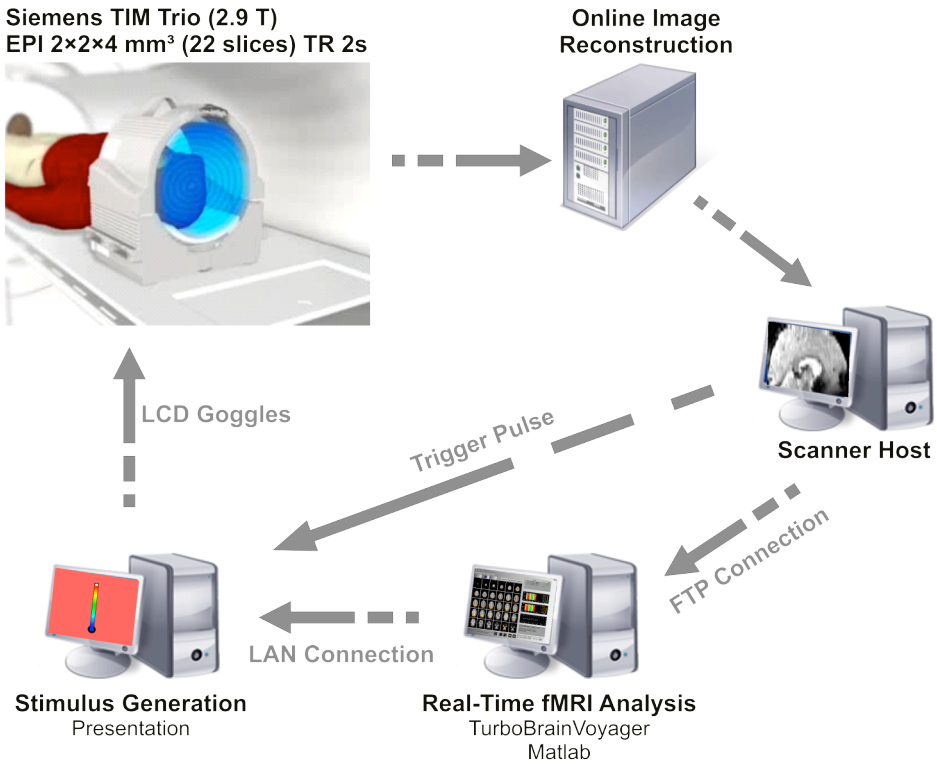

Fig. 28. Graphical representation of setup for rtfMRI and neurofeedback in our laboratory. Processing time for a single EPI volume does not exceed the acquisition time (2 s).

Imaging was performed using a standard single-shot gradient echo EPI sequence, as in previous experiments (TR/TE = 2000/36 ms, flip angle 70°, voxel size of 2 × 2 × 4 mm^3, 84 × 96 acquisition matrix, 192 mm FOV, 7/8 partial Fourier phase encoding, bandwidth 1336 Hz/pixel, echo spacing 0.81 ms). Again, we acquired 22 contiguous slices which covered the whole cerebrum. Online reconstruction of fMRI data was achieved using dedicated software developed at the Department of Medical Psychology and Behavioral Neurology, University of Tübingen (Weiskopf *et al.*, 2004; Weiskopf *et al.*, 2007) and adapted for our system by Dr. Dirk Voit. The algorithm reconstructs the k-space matrix for each slice into image space immediately after a slice has been acquired. After acquisition of the last slice in a volume, the individual slice images are merged into a 3D-image file (Analyze 7 format) and saved on the scanner's host computer, where they can be accessed by separate analysis hardware via a standard local area network (LAN) connection. Real-time fMRI analysis was performed using TurboBrainVoyager software (Brain Innovation, Maastricht, The Netherlands).

BOLD Neurofeedback Setup

Images were reconstructed using the same algorithm as described above. To optimize the communication rate between scanner host and analysis hardware, images were transferred via file transfer protocol (FTP) during feedback experiments. Furthermore, TurboBrainVoyager proved to be unsuitable for the online calculation of the neurofeedback signal. We therefore developed a toolbox based on the MATLAB programming environment (The MathWorks, Natick, Massachusetts) which transforms the signal intensity in ROIs into a suitable form for neurofeedback display (see below). The toolbox communicates with a separate computer running Presentation software (Neurobehavioral Systems, Albany, CA, USA) for generation of visual stimuli which were presented to subjects via MRI-compatible liquid crystal display goggles (Resonance Technology Inc., Northridge, CA, USA).

Feedback Paradigm

Participants were trained to achieve control over a brain region using a simple block design (see Fig. 29). A red background screen indicated to subjects that they should attempt to activate the region using specific activation strategies (see below) whereas a white background instructed them to pursue an alternative (deactivation) strategy. Activation and rest blocks lasted for 30 s each and one training run comprised 18 activation-rest cycles. Prior to each run, we included a 30 s baseline period to allow for initial signal normalization. The total scan duration per run was 9.5 minutes (285 volumes) and subjects performed three

training runs, during which they gradually learned to control their brain activity. A fourth run served as control experiment during which subjects were instructed to simply watch the screen and not to perform any regulation strategies.

Feedback was provided by means of a thermometer displayed in the centre of the screen (see Fig. 29). The thermometer allowed us to present subjects with 21 'feedback levels' ranging from blue (very low activation) to red (very high activation). Raw ROI signal intensity was converted to 'feedback level' (1-21) by first normalizing it to the mean ROI intensity during the preceding rest period. In a second step, negative and positive cut-offs were determined which corresponded to 'feedback levels' 1 and 21, respectively. Negative and positive cut-offs were determined adaptively according to subjects' performance. Initial values were set to +3% and -2%, respectively. Normalized signal intensities between the two cut-offs were mapped linearly to the 'feedback level' scale.

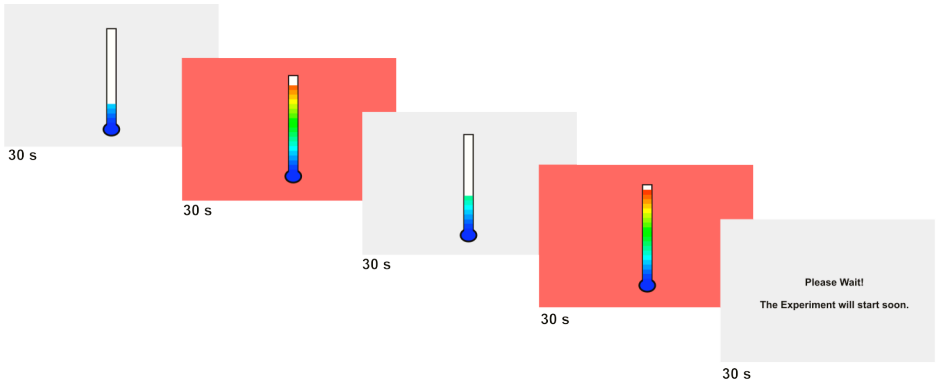

Fig. 29. Graphical representation of the feedback paradigm. Subjects were instructed to upregulate activation in a ROI when a red background screen was presented. The thermometer reflects the current activation level in the target ROI (compared to the preceding rest period).

Subjects were instructed to increase brain activity by mentally focusing on some event, by elevated concentration or by preparation for a specific action. Instructions for the rest period included relaxation and 'mind wandering'. Subjects were urged to develop individual cognitive strategies based on these general instructions. We informed participants that a change in strategy would lead to putative changes in the feedback signal some seconds later, due to the slow hemodynamic response. Finally, subjects were instructed not to move or close their eyes throughout the experiment.

Functional localizer

Determining the correct ROI is a crucial step in every BOLD neurofeedback experiment. We employed the Flanker task (described above) as functional localizer. Subjects performed one or several runs of the test, usually in a separate session. Statistical maps for the contrast of incongruent versus congruent trials were calculated (see above) and thresholded based on individual subject thresholds. The largest active cluster within MFC was then chosen as target ROI. To prevent that subjects could influence the global signal intensity over the whole brain, for example by adjusting breathing rate, we determined a background ROI of approximately same size and composition (in terms of tissue content) as the target ROI. The background ROI was normally localized in parietal cortex in a region which did not respond significantly to the incongruent versus congruent contrast. The feedback signal was based on the difference between target and background ROI intensity.

Statistical analysis

Image-based motion correction was carried out for all runs as previously described (Jenkinson *et al.*, 2002). To evaluate the success of feedback, ROI difference time courses were low-pass filtered (2-point running average) and detrended (removal of the best straight-line fit). The feedback paradigm was shifted by 2 volumes to take into account the hemodynamic delay and mean intensity values were calculated for active and rest periods. The difference between signal intensity during active and rest periods was chosen as index of feedback success and submitted to statistical analysis.

To identify regions outside the target ROI associated with successful feedback, a model of the feedback paradigm was created by convolving it with a double-gamma function which also takes into account the post-stimulus undershoot. Data were preprocessed as described above (section 6.2, high-pass filter cut-off at 60 s). Model fit was determined by statistical time-series analysis in the framework of the general linear model and with local autocorrelation correction (Woolrich *et al.*, 2001). Significant activations based on z statistic (Gaussianised T/F) images were obtained by cluster thresholding (Worsley *et al.*, 1992) with an initial threshold of $z > 3.1$ and then applying a corrected cluster threshold of $p = 0.05$. To allow for group analysis, functional images were transformed into MNI152 standard space, as described above. Due to the low number of subjects, we summarized across experiments using a fixed-effects model. Linear contrasts were calculated between the first and the last neurofeedback run, to reveal brain areas associated with successful regulation.

7.3. Results

ROI Definition

Functional definition of target ROIs using the conflict-contrast of the Flanker task (see above) was achieved in all six subjects. Exemplary target and background ROIs for one subject are displayed in Fig. 30.

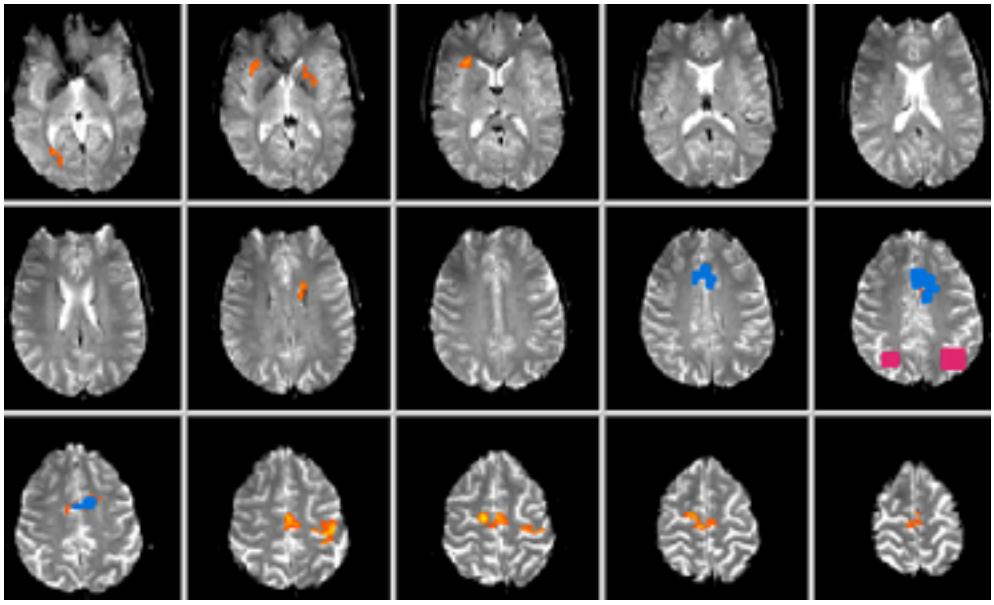

Fig. 30. Sample target (blue) and background (purple) ROIs for neurofeedback. ROIs are based on the incongruent > congruent contrast from a Flanker functional localizer experiment (underlying activation map).

Neurofeedback training

Control of brain activity in a small, functionally defined ROI improved in four of six subjects over three consecutive training runs. Exemplary target and background ROI signal time courses for runs 1 and 3 are presented in Fig. 31. Compared to the background ROI, the signal time course in the target region shows a more pronounced fluctuation, even during the first run. To take into account the baseline fluctuation of the signal, we calculated the difference between target and background ROI signal intensity. The difference time course correlated significantly with the feedback paradigm on the third ($r = 0.26$, $p < 0.001$) but not on the first ($r = -0.02$, $p = 0.71$) run, providing evidence for successful regulation of brain activity in the target ROI. Correlation coefficients and associated probabilities across the four runs for all subjects are presented in Table 5.

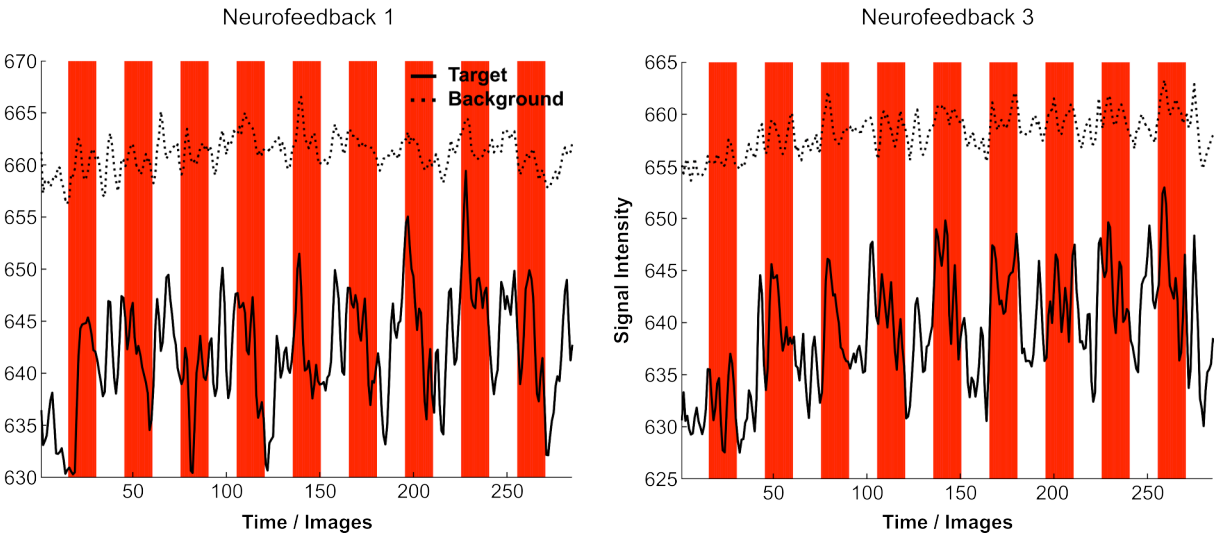

Fig. 31. Time courses from first and final neurofeedback training sessions for one representative volunteer. Note the increased target ROI signal intensity during active periods (red) in the third neurofeedback session (right).

Table 5: Correlation of difference time course with shifted neurofeedback paradigm. Correlation coefficients / associated probabilities (two-tailed) are presented.

	Run 1	Run 2	Run 3	Control
Subject 1	-0.02 / 0.71	0.15 / 0.01	0.26 / <0.001	-0.06 / 0.32
Subject 2	-0.18 / 0.002	0.18 / 0.003	0.23 / <0.001	0.01 / 0.87
Subject 3	0.19 / 0.002	-0.21 / <0.001	0.32 / <0.001	0.1 / 0.09
Subject 4	0.12 / 0.04	0.15 / 0.01	0.12 / 0.04	-0.03 / 0.62

To quantify feedback success, we calculated the difference between mean activation and rest period signal intensity (see Materials and Methods), adjusted by two image volumes in order to account for the hemodynamic delay. Representative data from one subject are displayed in Fig. 32 and demonstrate clearly that control of brain activation improved over the course of three training runs. Furthermore, activation levels returned to baseline in the final control session.

Feedback success of the group of four subjects over the course of three training and one control run is summarized in Fig. 33 and suggests that these subjects achieved control over target ROI activation at least partially by the third run. The low sample size in this proof-of-principle experiment precludes application of parametric statistical techniques to interrogate the significance of feedback success. Consequently, we performed a non-parametric one-way ANOVA (Friedman test) on the normalized signal intensities for three training and one control run, which revealed a significant main effect ($\chi^2_{(3)} = 8.4$, $p = 0.038$). Post-hoc testing using Wilcoxon's signed ranks statistic provided supportive evidence that

signal intensities were indeed elevated during activation periods of run 3, compared to both the first and the control experiment (Z = 1.83, p = 0.068, uncorrected for multiple comparisons).

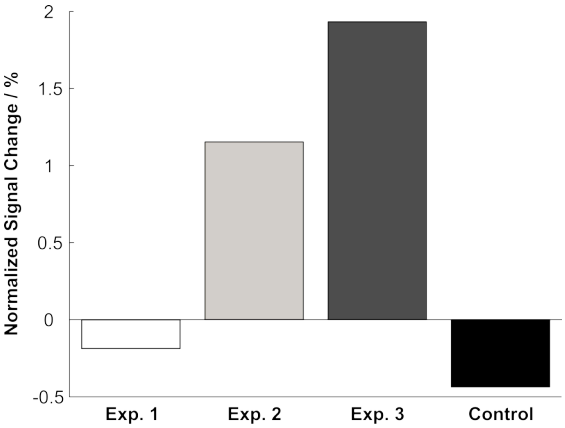

Fig. 32. Mean signal change during activation periods, normalized to rest periods based on target – background ROI difference. Results from one representative volunteer (same as Fig. 31).

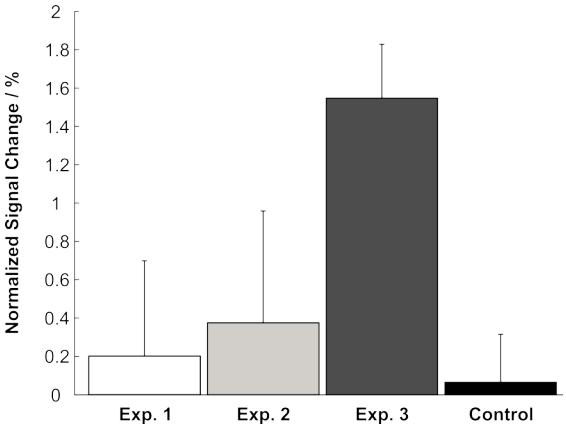

Fig. 33. Same data as in Fig. 32, but for the whole group of four subjects (error bars represent 1 SEM).

Brain regions involved in neurofeedback

Finally, we performed an exploratory whole-brain analysis to identify regions associated with successful regulation of activation in the target ROI by contrasting the first and last training run (see Materials and Methods). As shown in Fig. 34, this analysis revealed a surprisingly selective network of brain regions associated with neurofeedback success. We observed two substantial clusters of activation in medial prefrontal cortex (COG: -11, 58, 14; z_{max} = 4.7) and posterior cingulate cortex (COG: 0, -50, 35; z_{max} = 4.6). Smaller activations were located in the right superior temporal gyrus (COG: 53, -33, 3; z_{max} = 4.2) as well as along the inferior temporal gyrus bilaterally (COG left: -59, -10, -23; z_{max} = 5.1; COG right: 64, -7, -20; z_{max} = 5.5).

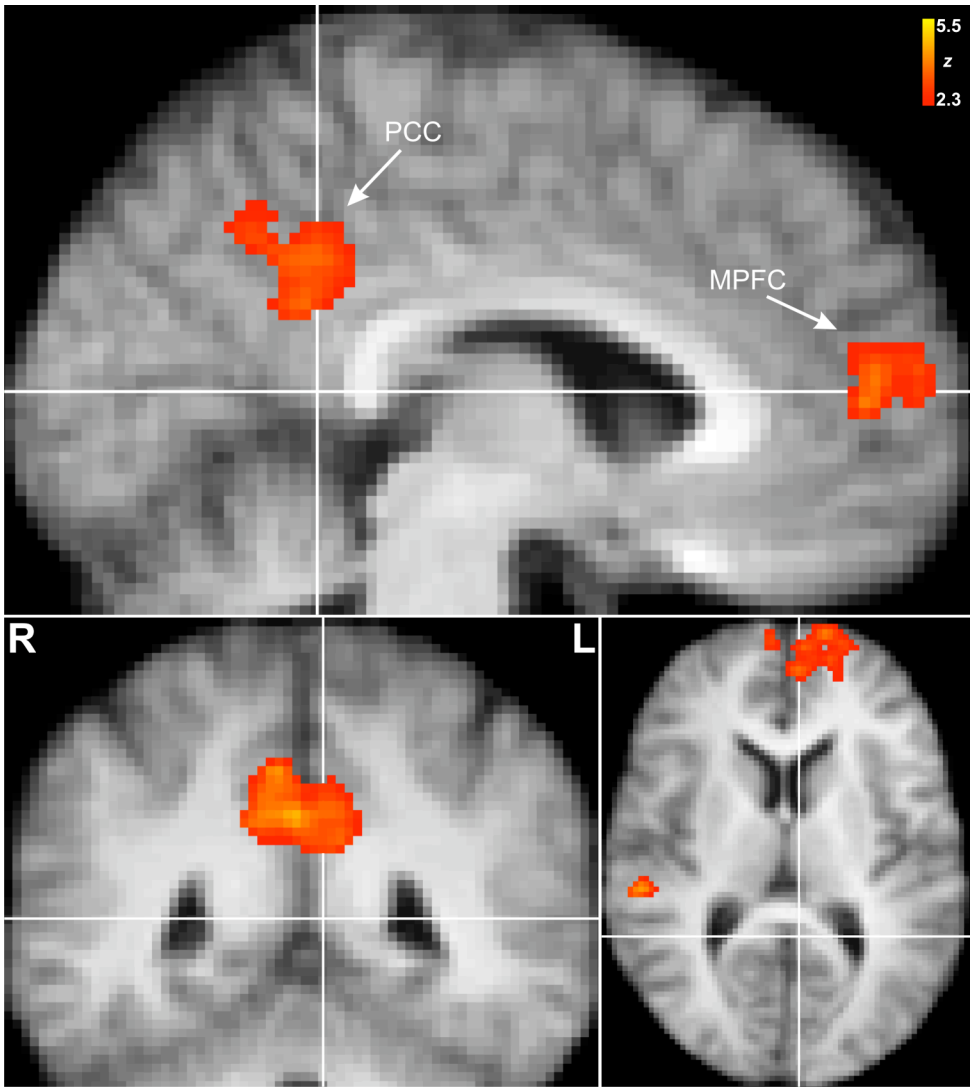

Fig. 34. Significantly stronger brain responses during activation period on third compared to first neurofeedback session. PCC … posterior cingulate cortex, MPFC … medial prefrontal cortex

7.4. Discussion

Real-time fMRI has been successfully established in our laboratory and is now in routine use. Besides neurofeedback, rtfMRI provides a number of additional benefits. Currently, it is used for monitoring of subject's head movement, for exclusion of BOLD non-responders and for the rapid evaluation of fMRI screening experiments.

Preliminary evidence for MFC self-regulation

The current study demonstrates an implementation of a neurofeedback design based on the BOLD signal. Using BOLD neurofeedback, we provide initial evidence for successful modulation of activity in MFC. These results confirm previous findings that the activation level of MFC, and ACC in particular, may be self-regulated (Weiskopf *et al.*, 2003; deCharms *et al.*, 2005). Importantly, our results also extend previous work by using a functionally defined ROI with a putative role in conflict processing as target region for neurofeedback. Furthermore, while previous studies focused on the modulation of brain areas involved in sensorimotor and emotional functions, here we provide initial evidence that higher cognitive regions may also be amenable to self-regulation.

The present proof-of-principle experiment still suffers from a number of shortcomings. Most notably, we observed a very large inter-individual variability in subjects' ability to self-regulate. Some volunteers achieved control over the target region very rapidly, whereas others did not succeed at all. Despite substantially larger sample sizes, previous studies also suffered from considerable inter-subject variability (Bray *et al.*, 2007; Caria *et al.*, 2007). Furthermore, in EEG neurofeedback (see below) only a subset of participants typically achieves self-regulation (*personal communication H. Gevensleben*). It remains unclear why there is such strong variability but possible reasons include differences in ROI definition, subtle variations in task instructions or motivational factors. A second shortcoming becomes evident upon close inspection of Fig. 31 (right graph). Target ROI signal intensity usually increases quite sharply at the beginning, or even before an activation period, but then drops to baseline before the start of the next resting phase. This evidence, which is representative for all participants, suggests that subjects had no difficulty in initiating a successful regulation strategy but found it challenging to sustain their approach throughout a 30 s activation interval. It seems likely that this may be a specific problem of neurofeedback using cognitive strategies. Unlike motor imagination or self-induction of emotional states, mental focusing for an extended period of time, especially given the distracting information from the feedback display, seems to be

surprisingly difficult, even for experienced subjects. This problem could be addressed by shorter activation intervals or event-related self-regulation (see below).

Despite several shortcomings, the current study provides the basis for experiments in which BOLD neurofeedback is combined with a cognitive task in order to observe the effect of modulated brain function on cognitive processing. Such an experiment would require that subjects are able to up- or down-regulate the target ROI in an event-related manner. Subsequently, after given a cue to regulate, a trial of the cognitive task will be presented once a certain signal intensity threshold (e.g. +1% with respect to the previous baseline) is exceeded. In this way, performance on up- and down-regulation trials may be compared.

Alternative neurofeedback approaches

Previous approaches to self-regulation of brain activity have relied mainly on EEG signals. In fact, a number of studies have made use of characteristic slow cortical potentials, such as the CNV (described above), to achieve neurofeedback (Lutzenberger *et al.*, 1982). In these studies, subjects learned to produce cortical positivities and negativities. Interestingly, EEG neurofeedback is currently used as alternative treatment strategy for attention-deficit hyperactivity disorder (ADHD) in children (Heinrich *et al.*, 2004). While the setup for BOLD neurofeedback is considerably more complex, compared to EEG, it also offers a number of advantages, especially to the researcher. First of all, self-regulation using rtfMRI provides high spatial resolution and therefore allows precise localization of the neurofeedback target region. Secondly, BOLD neurofeedback, unlike EEG, is not limited to the cortex and would in principle allow self-regulation of subcortical structure. To my knowledge, this interesting question has not been pursued. Neurofeedback studies of the thalamus may be especially valuable since they would permit to causally interfere with its putative sensory gating function. Lastly, BOLD neurofeedback permits investigation of mechanisms underlying self-regulation as data are acquired from the whole brain.

Brain systems involved in self-regulation

Our results provide tentative evidence for a circumscribed network of cortical regions underlying neurofeedback success. Clusters in medial PFC and posterior cingulate cortex (PCC) responded significantly stronger during activation periods of the third training run compared to the first. Interestingly, both areas are commonly identified with the brain's resting state network (RSN), which comprises regions characterized by low frequency coherences (0.01 – 0.05 Hz) when subjects are at rest (Biswal *et al.*, 1995; Shulman *et al.*,

1997; Damoiseaux *et al.*, 2006). Based on a recent classification of RSNs (De Luca *et al.*, 2006), medial PFC as well as PCC are the major component of RSN 2, which is characterized by pronounced deactivation when subjects are engaged in a complex task (Shulman *et al.*, 1997). Both areas have been suggested to play a role in internal monitoring and modulation of states of consciousness (Gusnard and Raichle, 2001). Keeping the limited scope of this study in mind, we would therefore tentatively suggest that successful self-regulation of MFC activation is associated with an increased awareness of internal thought processes.

To summarize, the preliminary results obtained in this neurofeedback study are encouraging and suggest that the technique may soon emerge as a new tool for studying the relation between various brain regions and cognitive function. Furthermore, the investigation of neuronal mechanisms underlying self-control will in itself be an interesting topic for future research.

8. General Discussion

Towards a theory of MFC function

In the preceding chapters, two experiments have been presented that investigated the functional anatomy of MFC during cognitive tasks. Furthermore, in the final experiment, a novel neurofeedback approach based on fMRI has been presented that may prove useful for investigation of the causal role of brain regions such as ACC in the generation of behavior. It is clear that the scope of studies presented here is too limited to allow for a comprehensive assessment and evaluation of MFC function. In the final chapter, I will nevertheless attempt to provide a general framework for MFC function, based on current models, previous studies as well as our own experiments.

Although medial frontal cortex is still frequently used as an anatomical label, in the literature as well as this thesis, the evidence now strongly supports distinct functional roles for superior frontal and anterior cingulate gyri. The combination of both regions into the term MFC probably stems from the fact that they are hard to distinguish, using standard imaging protocols, due to their close spatial proximity as well as the highly variable sulcal architecture in the region (Crosson *et al.*, 1999). Most notably, unlike ACC, SFG seems to be strongly associated with actual response execution, especially the voluntary selection of actions (Lau *et al.*, 2006). Pre-SMA, which forms the largest functional area within SFG, is thought to mediate response selection by resolution of competing motor plans, such as the right and left hand responses in the Flanker paradigm. The neural representations of the incompatible responses compete in a 'winner-take-all' fashion for a unitary output channel (Nachev *et al.*, 2007; Sumner *et al.*, 2007). Selection of the appropriate response may be facilitated by top-down priming of the corresponding neural representation. A major advantage of such a mechanistic model of response selection is that specific actions emerge from the internal neuronal dynamics in the pre-SMA and no 'selector' module is required, avoiding the problem of an infinite regress in previous selection models.

Pinpointing the precise role of ACC in the generation of behavior seems to be substantially more difficult. It is in this region where the vast majority of activations discussed in the introduction cluster. Furthermore, ACC shows the most pronounced inter-subject variability along its dorsal – rostral axis, as demonstrated above. Although ACC has been designated previously as a high level motor area (Picard and Strick, 1996), current evidence suggests that the region is substantially less closely associated with response execution then, for example, pre-SMA. Furthermore, in light of the multitude of observed

activations, it seems plausible that ACC subserves a task general role which is implicated by many different paradigms.

Important insights as to what this role may be comes from a recent lesion study in rhesus monkeys (Kennerley *et al.*, 2006). In these experiments, monkeys were trained to respond in two possible ways, with only one action being rewarded. Crucially, the rewarded action changed occasionally and without warning, so that animals had to adapt their behavior accordingly. Interestingly, in the majority of cases, the monkeys did not switch immediately to the alternative response after a non-rewarded trial but became increasingly more likely to initiate the new action. This suggests that behavior was determined by the reward history rather than a single erroneous trials. ACC lesioned animals performed similar to controls after an error. Careful manipulation of reward probabilities as well as extensive data analysis revealed, however, that lesioned animals failed to take into account the outcome of previous trials in order to make their choice. According to the authors, these results suggest that ACC plays a crucial role in guiding decisions based on previous actions and their associated outcomes (Kennerley *et al.*, 2006). Based on their results, as well as recent neuroimaging (Behrens *et al.*, 2007) and electrophysiological (Amiez *et al.*, 2006) data, Rushworth and colleagues have proposed an integrated framework for ACC function (Rushworth *et al.*, 2007; Walton *et al.*, 2007). In this model, ACC activation may reflect the salience of a particular stimulus for guiding current behavior, in the light of the previous reinforcement history. In other words, ACC performs an informed evaluation of a particular stimulus and determines the value of responses afforded by it. Consequently, ACC may be a key region for initiating adaptive strategic and bodily changes in order to bring about the action judged to be most valuable. In this context, ACC probably recruits brain regions responsible for adjustment of autonomic arousal or allocation of top-down control.

Compared to the premotor areas of the medial wall, ACC has a substantially wider range of anatomical connections with other brain regions. These include prefrontal and subcortical limbic structures as well as direct projections to the spinal cord (Bates and Goldman-Rakic, 1993; He *et al.*, 1995). Importantly, ACC receives input from the dopaminergic centers in the midbrain which are thought to carry a reward-prediction error signal (Holroyd and Coles, 2002). Thus, ACC is located in a prime anatomical position to flexibly integrate the value of choices over time and determine which actions are worth making.

Previous authors have implicated ACC in either error or conflict monitoring, a controversy which has motivated parts of the research described in this thesis. Arguably,

however, both erroneous and high conflict trials are of substantial behavioral relevance for subjects. Consequently, they demand an internal evaluation of response strategies as well as the recruitment of attentional resources and, possibly, an adjustment of autonomic arousal. Equally, cue stimuli in the anticipation paradigm possess a high salience as they signal an upcoming decision process. Intriguingly, the shared ACC activation observed in our experiments for three different cognitive processes (error and conflict monitoring as well as response anticipation) may thus reflect the extensive internal behavioral evaluation by subjects in these three conditions. Subsequently, ACC may be involved in the recruitment of the inferior frontal control system in the frontopolar cortex to allocate task-specific attentional resources. In the case of response competition between two alternative actions in the Flanker task, top-down modulation may subsequently prime the neural representation of the correct response in pre-SMA, as has been described above. Alternatively, top-down control may be directed to subcortical nuclei via the mediothalamic frontocortical system (MTFCS), as has been hypothesized for response anticipation (see above). Additionally, modulation of autonomic arousal may be initiated by ACC via anterior thalamic nuclei and insular cortex, as has been observed during response conflict and anticipation.

Adaptive selection of actions based on past experiences may be particularly important in social contexts (Rushworth *et al.*, 2007) where acquisition of information about conspecifics as well as their relation to oneself are prerequisites for successful interactions. From this point of view, ACC activation in social paradigms (see Amodio and Frith, 2006) reflects task-general behavioral integration and evaluation in a particularly challenging cognitive situation. Indeed, ACC lesions in macaques selectively impair valuation of social information which leads to a reduced interaction with conspecifics (Rudebeck *et al.*, 2006).

As discussed above, ACC has been implicated in emotional as well as pain processing. While these paradigms have so far not been explicitly integrated into the presented account of ACC function, painful stimuli in particular are highly salient for any organism. Consequently, they demand an evaluation of past response patterns as well as a decision for the future course of action, for example to minimize tissue damage. ACC may be involved in these aspects of pain processing which ultimately lead to the mobilization of cognitive resources as well as the modulation of autonomic functions in order to cope successfully with the situation.

The framework of MFC proposed by Rushworth and colleagues (Rushworth *et al.*, 2007) presents a powerful integration of diverse experimental findings obtained by a range of techniques. Nevertheless, several open questions remain. Most obviously, one would like to know just how ACC manages to integrate information over an extended period of time in

order to determine a suitable action. Furthermore, the precise relation between valuation of behavior over time and working memory, which is mediated by lateral prefrontal cortex, has thus far not been addressed. Finally, the interaction of ACC with other brain regions, such as frontopolar cortex, remains poorly understood largely due to the current limitations of neuroimaging techniques. Future studies will therefore have to rely on 'loss-of-function' experiments just as much as traditional brain imaging in order to establish causal relations between regions and their functions as well as between distinct areas. In this context, we hope that the BOLD neurofeedback approach presented in the third experiment will prove to be a useful tool for targeted interference with known brain areas in humans.

MFC function at multiple spatial scales

Even if a common, though high level, function underlies the plethora of observed activations in ACC, it remains puzzling why there should be such a huge variability in the activation foci. As shown in experiment 2, locations of activated clusters vary widely for different subjects and, even more surprising, for the same subject in different tasks. On the other hand, some tasks elicit a more robust BOLD response pattern, as shown by a greater similarity of the raw activation maps. Based on our high-resolution fMRI results, it seems that for the same task and subject, at least, activations are very reproducible. Thus, for a given subject and task, only a small part of ACC seems to be involved. Naturally, the question then arises what the remainder of ACC is doing. One possible solution to this problem may be the existence of degenerate neural systems within ACC that, though structurally distinct, may perform the same function (this concept of degeneracy in cognitive architecture has been introduced by Price and Friston, 2002). While an attractive hypothesis, it may prove extremely hard to test with currently available techniques.

Alternatively, it seems likely that at least some functional specialization exists within ACC. This view is supported by the differential activation patterns for error and conflict processing observed at high spatial resolution. Future studies should employ high-resolution fMRI, together with a wider range of tasks to investigate the fine scale functional organization of ACC in individual volunteers.

In conclusion, current evidence suggests that the question of functional specialization within MFC may be addressed at multiple spatial scales. At the highest level, interacting brain regions, such as ACC, frontopolar cortex and subcortical centers, are involved in the organization of behavior. The conception that ACC integrates across the outcomes of previous actions in order to decide what is worth doing now may be valid at this level and

merits further investigation. When zooming into ACC with high resolution techniques, however, the assumption that a unitary function is homogenously distributed throughout the area seems no longer valid. Instead, subregions of ACC seem to be functionally specialized for specific processes. A more extensive characterization of these specializations, with respect to the observed activations in ACC at the whole brain level, is now required.

9. Summary and concluding remarks

Here we have used fMRI to investigate the functional anatomy of human medial frontal cortex, and especially its anterior cingulate part, during performance of three different cognitive tasks. In the first experiment, we imaged ACC activation to correct and erroneous response inhibitions in a GoNogo task using a novel fMRI approach which allows for substantially enhanced spatial resolution. Our results suggest a bilateral distribution of error-related processes in ACC, whereas correct inhibitions only activated ACC in the right hemisphere. The experiment contributes towards a better understanding of the microanatomy of ACC and demonstrates the potential of fMRI for mapping the functional architecture of brain regions involved in cognitive tasks at a previously unaccomplished spatial scale.

In a second experiment, we investigated the neural basis of response conflict and anticipation, with special focus on MFC. At standard resolution, both processes were associated with overlapping activation in ACC. On the other hand, superior frontal gyrus was differentially activated for anticipation and conflict. These results support a functional heterogeneity within MFC. Superior frontal gyrus seems to be involved in task specific processes such as inhibition of competing responses. On the other hand, ACC plays a role in more abstract, task general aspects of behavior, as has been suggested recently. However, the substantial between-subject variability in activation centers observed in MFC cautions against an over-interpretation of group results.

In the final experiment, we used recent advances in the real-time analysis of fMRI data to develop a BOLD neurofeedback approach. We show that subjects are able to modulate the activity in a small functionally defined region of MFC. These results provide the basis for future experiments in which intentional regulation of activity in a circumscribed brain region may allow causal inference about the area's function as well as its interaction with other parts of the brain.

Ten years of neuroimaging research on MFC have highlighted the vital role of this brain region in the generation of purposeful and adaptive behavior. Nevertheless, to date no theory accounts for the whole range of paradigms associated with MFC activation. Promisingly, as the field starts to focus on previously neglected issues, such as between-subject variability, it may be hoped that a number of existing controversies will be resolved over the next decade, paving the way for a mechanistic model of MFC as a structure at the crossroads between cognition, emotion and autonomic control.

References

Amiez C, Joseph JP, Procyk E (2006) Reward encoding in the monkey anterior cingulate cortex. Cereb Cortex 16:1040-1055.

Amodio DM, Frith CD (2006) Meeting of minds: the medial frontal cortex and social cognition. Nat Rev Neurosci 7:268-277.

Aron AR, Robbins TW, Poldrack RA (2004) Inhibition and the right inferior frontal cortex. Trends Cogn Sci 8:170-177.

Barch DM, Braver TS, Akbudak E, Conturo T, Ollinger J, Snyder A (2001) Anterior cingulate cortex and response conflict: effects of response modality and processing domain. Cereb Cortex 11:837-848.

Bates JF, Goldman-Rakic PS (1993) Prefrontal connections of medial motor areas in the rhesus monkey. J Comp Neurol 336:211-228.

Baudewig J, Dechent P, Merboldt KD, Frahm J (2003) Thresholding in correlation analyses of magnetic resonance functional neuroimaging. Magn Reson Imaging 21:1121-1130.

Beckmann CF, Jenkinson M, Smith SM (2003) General multilevel linear modeling for group analysis in FMRI. Neuroimage 20:1052-1063.

Behrens TE, Woolrich MW, Walton ME, Rushworth MF (2007) Learning the value of information in an uncertain world. Nat Neurosci 10:1214-1221.

Bestmann S, Baudewig J, Frahm J (2003) On the synchronization of transcranial magnetic stimulation and functional echo-planar imaging. J Magn Reson Imaging 17:309-316.

Birbaumer N, Elbert T, Canavan AG, Rockstroh B (1990) Slow potentials of the cerebral cortex and behavior. Physiol Rev 70:1-41.

Biswal B, Yetkin FZ, Haughton VM, Hyde JS (1995) Functional connectivity in the motor cortex of resting human brain using echo-planar MRI. Magn Reson Med 34:537-541.

Botvinick M, Nystrom LE, Fissell K, Carter CS, Cohen JD (1999) Conflict monitoring versus selection-for-action in anterior cingulate cortex. Nature 402:179-181.

Botvinick MM, Braver TS, Barch DM, Carter CS, Cohen JD (2001) Conflict monitoring and cognitive control. Psychol Rev 108:624-652.

Botvinick MM, Cohen JD, Carter CS (2004) Conflict monitoring and anterior cingulate cortex: an update. Trends Cogn Sci 8:539-546.

Bray S, Shimojo S, O'Doherty JP (2007) Direct instrumental conditioning of neural activity using functional magnetic resonance imaging-derived reward feedback. J Neurosci 27:7498-7507.

Brown VJ, Bowman EM (2002) Rodent models of prefrontal cortical function. Trends Neurosci 25:340-343.

Brunia CH, Damen EJ (1988) Distribution of slow brain potentials related to motor preparation and stimulus anticipation in a time estimation task. Electroencephalogr Clin Neurophysiol 69:234-243.

Bush G, Luu P, Posner MI (2000) Cognitive and emotional influences in anterior cingulate cortex. Trends Cogn Sci 4:215-222.

Caria A, Veit R, Sitaram R, Lotze M, Weiskopf N, Grodd W, Birbaumer N (2007) Regulation of anterior insular cortex activity using real-time fMRI. Neuroimage 35:1238-1246.

Carlson S, Martinkauppi S, Rama P, Salli E, Korvenoja A, Aronen HJ (1998) Distribution of cortical activation during visuospatial n-back tasks as revealed by functional magnetic resonance imaging. Cereb Cortex 8:743-752.

Carter CS, Braver TS, Barch DM, Botvinick MM, Noll D, Cohen JD (1998) Anterior cingulate cortex, error detection, and the online monitoring of performance. Science 280:747-749.

Corbetta M, Shulman GL (2002) Control of goal-directed and stimulus-driven attention in the brain. Nat Rev Neurosci 3:201-215.

Cox RW, Jesmanowicz A, Hyde JS (1995) Real-time functional magnetic resonance imaging. Magn Reson Med 33:230-236.

Critchley HD, Mathias CJ, Josephs O, O'Doherty J, Zanini S, Dewar BK, Cipolotti L, Shallice T, Dolan RJ (2003) Human cingulate cortex and autonomic control: converging neuroimaging and clinical evidence. Brain 126:2139-2152.

Critchley HD, Tang J, Glaser D, Butterworth B, Dolan RJ (2005) Anterior cingulate activity during error and autonomic response. Neuroimage 27:885-895.

Crosson B, Sadek JR, Bobholz JA, Gokcay D, Mohr CM, Leonard CM, Maron L, Auerbach EJ, Browd SR, Freeman AJ, Briggs RW (1999) Activity in the paracingulate and cingulate sulci during word generation: an fMRI study of functional anatomy. Cereb Cortex 9:307-316.

Dale AM, Liu AK, Fischl BR, Buckner RL, Belliveau JW, Lewine JD, Halgren E (2000) Dynamic statistical parametric mapping: combining fMRI and MEG for high-resolution imaging of cortical activity. Neuron 26:55-67.

Damasio AR, Grabowski TJ, Bechara A, Damasio H, Ponto LL, Parvizi J, Hichwa RD (2000) Subcortical and cortical brain activity during the feeling of self-generated emotions. Nat Neurosci 3:1049-1056.

Damoiseaux JS, Rombouts SA, Barkhof F, Scheltens P, Stam CJ, Smith SM, Beckmann CF (2006) Consistent resting-state networks across healthy subjects. Proc Natl Acad Sci U S A 103:13848-13853.

De Luca M, Beckmann CF, De Stefano N, Matthews PM, Smith SM (2006) fMRI resting state networks define distinct modes of long-distance interactions in the human brain. Neuroimage 29:1359-1367.

deCharms RC, Christoff K, Glover GH, Pauly JM, Whitfield S, Gabrieli JD (2004) Learned regulation of spatially localized brain activation using real-time fMRI. Neuroimage 21:436-443.

deCharms RC, Maeda F, Glover GH, Ludlow D, Pauly JM, Soneji D, Gabrieli JD, Mackey SC (2005) Control over brain activation and pain learned by using real-time functional MRI. Proc Natl Acad Sci U S A 102:18626-18631.

Devinsky O, Morrell MJ, Vogt BA (1995) Contributions of anterior cingulate cortex to behaviour. Brain 118 (Pt 1):279-306.

Duncan J, Owen AM (2000) Common regions of the human frontal lobe recruited by diverse cognitive demands. Trends Neurosci 23:475-483.

Eichler M (2005) A graphical approach for evaluating effective connectivity in neural systems. Philos Trans R Soc Lond B Biol Sci 360:953-967.

Eriksen BA, Eriksen CW (1974) Effects of Noise Letters Upon Identification of a Target Letter in a Nonsearch Task. Perception & Psychophysics 16:143-149.

Esposito F, Seifritz E, Formisano E, Morrone R, Scarabino T, Tedeschi G, Cirillo S, Goebel R, Di Salle F (2003) Real-time independent component analysis of fMRI time-series. Neuroimage 20:2209-2224.

Falkenstein M, Hohnsbein J, Hoormann J, Blanke L (1991) Effects of crossmodal divided attention on late ERP components. II. Error processing in choice reaction tasks. Electroencephalogr Clin Neurophysiol 78:447-455.

Fan J, Kolster R, Ghajar J, Suh M, Knight RT, Sarkar R, McCandliss BD (2007) Response anticipation and response conflict: an event-related potential and functional magnetic resonance imaging study. J Neurosci 27:2272-2282.

Fassbender C, Foxe JJ, Garavan H (2006) Mapping the functional anatomy of task preparation: priming task-appropriate brain networks. Hum Brain Mapp 27:819-827.

Fletcher PC, Happe F, Frith U, Baker SC, Dolan RJ, Frackowiak RS, Frith CD (1995) Other minds in the brain: a functional imaging study of "theory of mind" in story comprehension. Cognition 57:109-128.

Floel A, Cohen LG (2007) Contribution of noninvasive cortical stimulation to the study of memory functions. Brain Res Rev 53:250-259.

Fransson P, Krüger G, Merboldt KD, Frahm J (1998) Temporal characteristics of oxygenation-sensitive MRI responses to visual activation in humans. Magn Reson Med 39:912-919.

Freeman A, Ciliax B, Bakay R, Daley J, Miller RD, Keating G, Levey A, Rye D (2001) Nigrostriatal collaterals to thalamus degenerate in parkinsonian animal models. Ann Neurol 50:321-329.

Freyschuss U, Hjemdahl P, Juhlin-Dannfelt A, Linde B (1988) Cardiovascular and sympathoadrenal responses to mental stress: influence of beta-blockade. Am J Physiol 255:H1443-1451.

Friston K (2002) Beyond phrenology: what can neuroimaging tell us about distributed circuitry? Annu Rev Neurosci 25:221-250.

Funahashi S, Bruce CJ, Goldman-Rakic PS (1989) Mnemonic coding of visual space in the monkey's dorsolateral prefrontal cortex. J Neurophysiol 61:331-349.
Fuster JM (2002) Frontal lobe and cognitive development. J Neurocytol 31:373-385.
Garavan H, Ross TJ, Stein EA (1999) Right hemispheric dominance of inhibitory control: an event-related functional MRI study. Proc Natl Acad Sci U S A 96:8301-8306.
Garavan H, Ross TJ, Kaufman J, Stein EA (2003) A midline dissociation between error-processing and response-conflict monitoring. Neuroimage 20:1132-1139.
Gehring WJ, Goss B, Coles MGH, Meyer DE, Donchin E (1993) A Neural System for Error-Detection and Compensation. Psychol Sci 4:385-390.
Gehring WJ, Fencsik DE (2001) Functions of the medial frontal cortex in the processing of conflict and errors. J Neurosci 21:9430-9437.
Gemba H, Sasaki K, Brooks VB (1986) 'Error' potentials in limbic cortex (anterior cingulate area 24) of monkeys during motor learning. Neurosci Lett 70:223-227.
Gembris D, Taylor JG, Schor S, Frings W, Suter D, Posse S (2000) Functional magnetic resonance imaging in real time (FIRE): sliding-window correlation analysis and reference-vector optimization. Magn Reson Med 43:259-268.
Genovese CR, Lazar NA, Nichols T (2002) Thresholding of statistical maps in functional neuroimaging using the false discovery rate. Neuroimage 15:870-878.
Grill-Spector K, Sayres R, Ress D (2006) High-resolution imaging reveals highly selective nonface clusters in the fusiform face area. Nat Neurosci 9:1177-1185.
Gusnard DA, Raichle ME (2001) Searching for a baseline: functional imaging and the resting human brain. Nat Rev Neurosci 2:685-694.
Hallett M (2007) Transcranial Magnetic Stimulation: A Primer. Neuron 55:187-199.
He SQ, Dum RP, Strick PL (1995) Topographic organization of corticospinal projections from the frontal lobe: motor areas on the medial surface of the hemisphere. J Neurosci 15:3284-3306.
Heinrich H, Gevensleben H, Freisleder FJ, Moll GH, Rothenberger A (2004) Training of slow cortical potentials in attention-deficit/hyperactivity disorder: evidence for positive behavioral and neurophysiological effects. Biol Psychiatry 55:772-775.
Hellier P, Barillot C, Corouge I, Gibaud B, Le Goualher G, Collins DL, Evans A, Malandain G, Ayache N, Christensen GE, Johnson HJ (2003) Retrospective evaluation of intersubject brain registration. IEEE Trans Med Imaging 22:1120-1130.
Holroyd CB, Coles MG (2002) The neural basis of human error processing: reinforcement learning, dopamine, and the error-related negativity. Psychol Rev 109:679-709.
Holroyd CB, Nieuwenhuis S, Yeung N, Nystrom L, Mars RB, Coles MG, Cohen JD (2004) Dorsal anterior cingulate cortex shows fMRI response to internal and external error signals. Nat Neurosci 7:497-498.
Jenkinson M, Smith S (2001) A global optimisation method for robust affine registration of brain images. Medical Image Analysis 5:143-156.
Jenkinson M, Bannister P, Brady M, Smith S (2002) Improved optimization for the robust and accurate linear registration and motion correction of brain images. Neuroimage 17:825-841.
Jezzard P, Matthews PM, Smith SM (2001) Functional MRI: an introduction to methods. Oxford: Oxford University Press.
Jones AK, Brown WD, Friston KJ, Qi LY, Frackowiak RS (1991) Cortical and subcortical localization of response to pain in man using positron emission tomography. Proc Biol Sci 244:39-44.
Kandel ER, Schwartz JH, Jessell TM (2000) Principles of neural science, 4th Edition. New York: McGraw-Hill, Health Professions Division.
Kennerley SW, Walton ME, Behrens TE, Buckley MJ, Rushworth MF (2006) Optimal decision making and the anterior cingulate cortex. Nat Neurosci 9:940-947.
Kobayashi N, Yoshino A, Takahashi Y, Nomura S (2007) Autonomic arousal in cognitive conflict resolution. Auton Neurosci 132:70-75.
Konishi S, Nakajima K, Uchida I, Sekihara K, Miyashita Y (1998) No-go dominant brain activity in human inferior prefrontal cortex revealed by functional magnetic resonance imaging. Eur J Neurosci 10:1209-1213.
Kotchoubey B (2006) Event-related potentials, cognition, and behavior: a biological approach. Neurosci Biobehav Rev 30:42-65.

Koyama T, McHaffie JG, Laurienti PJ, Coghill RC (2005) The subjective experience of pain: where expectations become reality. Proc Natl Acad Sci U S A 102:12950-12955.

Kretschmann H-J, Weinrich W (2003) Klinische Neuroanatomie und kranielle Bilddiagnostik, 3rd Edition. Stuttgart: Georg Thieme Verlag.

Lau H, Rogers RD, Passingham RE (2006) Dissociating response selection and conflict in the medial frontal surface. Neuroimage 29:446-451.

Loveless NE, Sanford AJ (1974) Effects of age on the contingent negative variation and preparatory set in a reaction-time task. J Gerontol 29:52-63.

Luria AR (1980) Higher cortical functions in man, 2d Edition. New York: Basic Books.

Lütcke H (2006) Parcellating the medial frontal cortex: evaluative and cognitive components of performance monitoring. J Neurosci 26:7129-7130.

Lütcke H, Frahm J (in press) Lateralized Anterior Cingulate Function during Error Processing and Conflict Monitoring as Revealed by High-Resolution fMRI. Cereb Cortex.

Lutzenberger W, Elbert T, Rockstroh B, Birbaumer N (1982) Biofeedback produced slow brain potentials and task performance. Biol Psychol 14:99-111.

McCarthy G, Blamire AM, Puce A, Nobre AC, Bloch G, Hyder F, Goldman-Rakic P, Shulman RG (1994) Functional magnetic resonance imaging of human prefrontal cortex activation during a spatial working memory task. Proc Natl Acad Sci U S A 91:8690-8694.

Menon V, Adleman NE, White CD, Glover GH, Reiss AL (2001) Error-related brain activation during a Go/NoGo response inhibition task. Hum Brain Mapp 12:131-143.

Mitchell JP, Neil Macrae C, Banaji MR (2005) Forming impressions of people versus inanimate objects: social-cognitive processing in the medial prefrontal cortex. Neuroimage 26:251-257.

Morgane PJ, Galler JR, Mokler DJ (2005) A review of systems and networks of the limbic forebrain/limbic midbrain. Prog Neurobiol 75:143-160.

Moses P, Stiles J (2002) The lesion methodology: contrasting views from adult and child studies. Dev Psychobiol 40:266-277.

Nachev P, Wydell H, O'Neill K, Husain M, Kennard C (2007) The role of the pre-supplementary motor area in the control of action. Neuroimage 36 Suppl 2:T155-163.

Nagai Y, Critchley HD, Featherstone E, Fenwick PB, Trimble MR, Dolan RJ (2004) Brain activity relating to the contingent negative variation: an fMRI investigation. Neuroimage 21:1232-1241.

Nakai T, Bagarinao E, Matsuo K, Ohgami Y, Kato C (2006) Dynamic monitoring of brain activation under visual stimulation using fMRI--the advantage of real-time fMRI with sliding window GLM analysis. J Neurosci Methods 157:158-167.

Nitsche MA, Liebetanz D, Tergau F, Paulus W (2002) Modulation of cortical excitability by transcranial direct current stimulation. Nervenarzt 73:332-335.

Ogawa S, Tank DW, Menon R, Ellermann JM, Kim SG, Merkle H, Ugurbil K (1992) Intrinsic signal changes accompanying sensory stimulation: functional brain mapping with magnetic resonance imaging. Proc Natl Acad Sci U S A 89:5951-5955.

Papez JW (1995) A proposed mechanism of emotion. 1937. J Neuropsychiatry Clin Neurosci 7:103-112.

Paus T, Tomaiuolo F, Otaky N, MacDonald D, Petrides M, Atlas J, Morris R, Evans AC (1996) Human cingulate and paracingulate sulci: pattern, variability, asymmetry, and probabilistic map. Cereb Cortex 6:207-214.

Paus T (2005) Inferring causality in brain images: a perturbation approach. Philos Trans R Soc Lond B Biol Sci 360:1109-1114.

Phan KL, Wager T, Taylor SF, Liberzon I (2002) Functional neuroanatomy of emotion: a meta-analysis of emotion activation studies in PET and fMRI. Neuroimage 16:331-348.

Picard N, Strick PL (1996) Motor areas of the medial wall: a review of their location and functional activation. Cereb Cortex 6:342-353.

Ploghaus A, Tracey I, Gati JS, Clare S, Menon RS, Matthews PM, Rawlins JN (1999) Dissociating pain from its anticipation in the human brain. Science 284:1979-1981.

Polli FE, Barton JJ, Cain MS, Thakkar KN, Rauch SL, Manoach DS (2005) Rostral and dorsal anterior cingulate cortex make dissociable contributions during antisaccade error commission. Proc Natl Acad Sci U S A 102:15700-15705.

Price CJ, Mummery CJ, Moore CJ, Frakowiak RS, Friston KJ (1999) Delineating necessary and sufficient neural systems with functional imaging studies of neuropsychological patients. J Cogn Neurosci 11:371-382.

Price CJ, Friston KJ (2002) Degeneracy and cognitive anatomy. Trends Cogn Sci 6:416-421.

Pulvermüller F, Lutzenberger W, Müller V, Mohr B, Dichgans J, Birbaumer N (1996) P3 and contingent negative variation in Parkinson's disease. Electroencephalogr Clin Neurophysiol 98:456-467.

Rabbitt PM (1966) Errors and error correction in choice-response tasks. J Exp Psychol 71:264-272.

Rainville P, Duncan GH, Price DD, Carrier B, Bushnell MC (1997) Pain affect encoded in human anterior cingulate but not somatosensory cortex. Science 277:968-971.

Rainville P (2002) Brain mechanisms of pain affect and pain modulation. Curr Opin Neurobiol 12:195-204.

Ridderinkhof KR, van den Wildenberg WP, Segalowitz SJ, Carter CS (2004) Neurocognitive mechanisms of cognitive control: the role of prefrontal cortex in action selection, response inhibition, performance monitoring, and reward-based learning. Brain Cogn 56:129-140.

Roebroeck A, Formisano E, Goebel R (2005) Mapping directed influence over the brain using Granger causality and fMRI. Neuroimage 25:230-242.

Rosen BR, Buckner RL, Dale AM (1998) Event-related functional MRI: past, present, and future. Proc Natl Acad Sci U S A 95:773-780.

Rubia K, Russell T, Overmeyer S, Brammer MJ, Bullmore ET, Sharma T, Simmons A, Williams SC, Giampietro V, Andrew CM, Taylor E (2001) Mapping motor inhibition: conjunctive brain activations across different versions of go/no-go and stop tasks. Neuroimage 13:250-261.

Rudebeck PH, Buckley MJ, Walton ME, Rushworth MF (2006) A role for the macaque anterior cingulate gyrus in social valuation. Science 313:1310-1312.

Rushworth MF, Walton ME, Kennerley SW, Bannerman DM (2004) Action sets and decisions in the medial frontal cortex. Trends Cogn Sci 8:410-417.

Rushworth MF, Buckley MJ, Behrens TE, Walton ME, Bannerman DM (2007) Functional organization of the medial frontal cortex. Curr Opin Neurobiol 17:220-227.

Sarter M, Berntson GG, Cacioppo JT (1996) Brain imaging and cognitive neuroscience. Toward strong inference in attributing function to structure. Am Psychol 51:13-21.

Schneider KA, Richter MC, Kastner S (2004) Retinotopic organization and functional subdivisions of the human lateral geniculate nucleus: a high-resolution functional magnetic resonance imaging study. J Neurosci 24:8975-8985.

Schwarzlose RF, Baker CI, Kanwisher N (2005) Separate face and body selectivity on the fusiform gyrus. J Neurosci 25:11055-11059.

Scouten A, Papademetris X, Constable RT (2006) Spatial resolution, signal-to-noise ratio, and smoothing in multi-subject functional MRI studies. Neuroimage 30:787-793.

Shallice T (1982) Specific impairments of planning. Philos Trans R Soc Lond B Biol Sci 298:199-209.

Shulman GL, Corbetta M, Buckner RL, Raichle ME, Fiez JA, Miezin FM, Petersen SE (1997) Top-down modulation of early sensory cortex. Cereb Cortex 7:193-206.

Smith SM, Brady JM (1997) Susan - a New Approach to Low Level Image Processing. Int J Comput Vis 23:45-78.

Smith SM (2002) Fast robust automated brain extraction. Hum Brain Mapp 17:143-155.

Smith SM, Jenkinson M, Woolrich MW, Beckmann CF, Behrens TE, Johansen-Berg H, Bannister PR, De Luca M, Drobnjak I, Flitney DE, Niazy RK, Saunders J, Vickers J, Zhang Y, De Stefano N, Brady JM, Matthews PM (2004) Advances in functional and structural MR image analysis and implementation as FSL. Neuroimage 23 Suppl 1:S208-219.

Stephan KE, Marshall JC, Friston KJ, Rowe JB, Ritzl A, Zilles K, Fink GR (2003) Lateralized cognitive processes and lateralized task control in the human brain. Science 301:384-386.

Stroop JR (1935) Studies of interference in serial verbal reactions. J Exp Psychol 18:643-662.

Sumner P, Nachev P, Morris P, Peters AM, Jackson SR, Kennard C, Husain M (2007) Human medial frontal cortex mediates unconscious inhibition of voluntary action. Neuron 54:697-711.

Tamas LB, Shibasaki H (1985) Cortical potentials associated with movement: a review. J Clin Neurophysiol 2:157-171.

Taylor SF, Martis B, Fitzgerald KD, Welsh RC, Abelson JL, Liberzon I, Himle JA, Gehring WJ (2006) Medial frontal cortex activity and loss-related responses to errors. J Neurosci 26:4063-4070.

Tecce JJ (1972) Contingent negative variation (CNV) and psychological processes in man. Psychol Bull 77:73-108.

Ullsperger M, von Cramon DY (2003) Error monitoring using external feedback: specific roles of the habenular complex, the reward system, and the cingulate motor area revealed by functional magnetic resonance imaging. J Neurosci 23:4308-4314.

van Boxtel GJ, Brunia CH (1994) Motor and non-motor aspects of slow brain potentials. Biol Psychol 38:37-51.

Voit D, Frahm J (2005) Echo train shifted multi-echo FLASH for functional MRI of the human brain at ultra-high spatial resolution. NMR Biomed 18:481-488.

Walter WG, Cooper R, Aldridge VJ, McCallum WC, Winter AL (1964) Contingent Negative Variation: an Electric Sign of Sensorimotor Association and Expectancy in the Human Brain. Nature 203:380-384.

Walton ME, Croxson PL, Behrens TE, Kennerley SW, Rushworth MF (2007) Adaptive decision making and value in the anterior cingulate cortex. Neuroimage 36 Suppl 2:T142-154.

Weiskopf N, Veit R, Erb M, Mathiak K, Grodd W, Goebel R, Birbaumer N (2003) Physiological self-regulation of regional brain activity using real-time functional magnetic resonance imaging (fMRI): methodology and exemplary data. Neuroimage 19:577-586.

Weiskopf N, Mathiak K, Bock SW, Scharnowski F, Veit R, Grodd W, Goebel R, Birbaumer N (2004) Principles of a brain-computer interface (BCI) based on real-time functional magnetic resonance imaging (fMRI). IEEE Trans Biomed Eng 51:966-970.

Weiskopf N, Sitaram R, Josephs O, Veit R, Scharnowski F, Goebel R, Birbaumer N, Deichmann R, Mathiak K (2007) Real-time functional magnetic resonance imaging: methods and applications. Magn Reson Imaging 25:989-1003.

Whalen PJ, Bush G, McNally RJ, Wilhelm S, McInerney SC, Jenike MA, Rauch SL (1998) The emotional counting Stroop paradigm: a functional magnetic resonance imaging probe of the anterior cingulate affective division. Biol Psychiatry 44:1219-1228.

Woolrich MW, Ripley BD, Brady M, Smith SM (2001) Temporal autocorrelation in univariate linear modeling of FMRI data. Neuroimage 14:1370-1386.

Woolrich MW, Behrens TEJ, Beckmann CF, Jenkinson M, Smith SM (2004) Multilevel linear modelling for FMRI group analysis using Bayesian inference. Neuroimage 21:1732-1747.

Worsley KJ, Evans AC, Marrett S, Neelin P (1992) A three-dimensional statistical analysis for CBF activation studies in human brain. J Cereb Blood Flow Metab 12:900-918.

Yeung N, Cohen JD, Botvinick MM (2004) The neural basis of error detection: conflict monitoring and the error-related negativity. Psychol Rev 111:931-959.

Yoo SS, O'Leary HM, Fairneny T, Chen NK, Panych LP, Park H, Jolesz FA (2006) Increasing cortical activity in auditory areas through neurofeedback functional magnetic resonance imaging. Neuroreport 17:1273-1278.

Zeki S (1990) The motion pathways of the visual cortex. In: Vision: Coding and Efficiency (Blakemore C, ed), pp 321-345. Cambridge: Cambridge Univ. Press.

Zumsteg D, Lozano AM, Wieser HG, Wennberg RA (2006) Cortical activation with deep brain stimulation of the anterior thalamus for epilepsy. Clin Neurophysiol 117:192-207.

Zysset S, Müller K, Lohmann G, von Cramon DY (2001) Color-word matching stroop task: separating interference and response conflict. Neuroimage 13:29-36.

Abbreviations

3D	3-dimensional
4D	4-dimensional
ACC	anterior cingulate cortex
ADHD	attention deficit hyperactivity disorder
Ag / AgCl	silver / silver chloride
ANOVA	analysis of variance
b	beta-weight
BA	Brodmann's area
BOLD	blood oxygen level dependent
CBF	cerebral blood flow
CNV	contingent negative variation
COG	center of gravity
CPT	continuous performance test
CR	correct rejection
Cz	EEG electrode at vertex
dACC	dorsal anterior cingulate cortex
DLPFC	dorsolateral prefrontal cortex
EEG	electroencephalogram
EOG	electrooculogram
EPI	echoplanar imaging
ERN	error-related negativity
FA	false alarm
FCz	frontocentral electrode
FDR	false discovery rate
FLASH	fast low angle shot
fMRI	functional magnetic resonance imaging
FMRIB	functional magnetic resonance imaging of the brain
FOV	field of view
FPC	frontopolar cortex
FSL	FMRIB software library
FTP	file transfer protocol
FWHM	full width at half maximum

GABA	γ-aminobutyric acid
GLM	general linear model
GRF	Gaussian random field
Hz	hertz
iCNV	initial contingent negative variation
IPS	intra-parietal sulcus
ISI	interstimulus interval
kΩ	kilo Ohm
LAN	local area network
MEG	magnetoencephalography
MFC	medial frontal cortex
MHz	megahertz
MNI	Montreal Neurological Institute
MPFC	medial prefrontal cortex
MPRAGE	magnetization prepared rapid gradient echo
MR	magnetic resonance
MRI	magnetic resonance imaging
MTFCS	mediothalamic frontocortical system
NMR	nuclear magnetic resonance
p	probability
PCC	posterior cingulate cortex
PCE	positive compatibility effect
PET	positron emission tomography
PFC	prefrontal cortex
pre-SMA	pre-supplementary motor area
RA	response anticipation
rACC	rostral anterior cingulate cortex
RC	response conflict
rHb	deoxygenated hemoglobin
ROI	region of interest
RSN	resting state network
RT	reaction time
rtfMRI	real-time functional magnetic resonance imaging

S_1-S_2	stimulus 1 - stimulus 2 paradigm
SCP	slow cortical potential
SEF	supplementary eye field
SEM	standard error of the mean
SFG	superior frontal gyrus
SMA	supplementary motor area
SN	substantia nigra
SNR	signal to noise ratio
SUSAN	smallest univalue segment assimilating nucleus
T	tesla
T_1	spin-lattice relaxation time
T_2	spin-spin relaxation time
T_2^*	effective spin-spin relaxation time
tCNV	terminal contingent negative variation
TDCS	transcranial direct current stimulation
TE	echo time
TMS	transcranial magnetic stimulation
TR	repetition time
Var	variance
Vox	voxel

Acknowledgments

I wish to express my sincere gratefulness to:

My supervisor, Prof. Jens Frahm, for giving me the opportunity to carry out the project in his laboratory and for providing a well-equipped and professional working environment.

My supervisor, Prof. Stefan Treue, for guiding my first steps in the world of neuroscience and fueling my passion for the subject.

All members of my thesis committee for valuable and insightful comments and suggestions during the meetings.

Dr. Klaus-Dietmar Merboldt for introducing me to the technical aspects of MRI and for providing valuable advice throughout the project.

Dr. Renate Schweizer for her never ending patience and support in discussing my work, for critical reading of all the manuscripts as well as general encouragement in the daily routine. It's been fun working with you, Renate, thank you so much!

Dr. Susan Boretius for helpful advice, good humor as well as for sharing her vision of science with me.

Dr. Dirk Voit and Kurt Böhm for providing the necessary technical know-how whenever it was needed most.

Prof. Aribert Rothenberger, Björn Albrecht and Holger Gevensleben for valuable advice and for performing EEG measurements as well as subject recruitment in the second experiment.

Dr. Nikolaus Weiskopf for developing and kindly sharing the real-time fMRI data export software. He, together with Dr. Ralf Veit, also provided valuable insights into the design of neurofeedback experiments.

All my students, in two lab rotations and two courses at DeutscheSchülerakademie, for never stopping to ask questions and for being so passionate about science.

My friends in Göttingen, especially the Neuroscience 2003 / 2004 'batch', but also outside 'The Program', for an enjoyable and memorable time.

My friends allover the world, Christian, Jörg, Annemarie, Anne, Cat, Tabea. I apologize for being so bad at keeping in touch but I nevertheless think of you a lot.

My brother, grandparents and parents, whose unquestioning love and support forms the base on which I can build. *Habt vielen Dank!*

Lastly, but most of all, Véronique, for going the hardest part of the journey together with me and for putting up with so much. *Merci!*

Curriculum Vitae

Name	Henry Harry Lütcke
Date of birth	October 19, 1979
Place of birth	Eberswalde-Finow, Germany
Current address	Papendiek 6-7, App. 4 37073 Göttingen Germany
Phone	+49-551-2011072 +49-176-20808069
Email	hluetck@gwdg.de, hluetck@gmail.com

Education

Since September 2004	PhD in the laboratory of Prof. Frahm, Biomedizinische NMR Forschungs GmbH am Max Planck Institut für biophysikalische Chemie
Since September 2003	International MSc / PhD Program in Neurosciences, Göttingen, Germany
October 1999 – July 2003	BSc Biological Sciences, The University of Edinburgh, Edinburgh, UK
October 2001 – July 2002	ERASMUS exchange, Université Pierre Mendès-France, Grenoble, France
November 1998 – August 1999	Military Service, Rendsburg, Germany
October 1996 – June 1998	A-Levels, Sedbergh School, Sedbergh, UK

List of publications

1. **Lütcke H**, Merbold K-D, Frahm J (2006) The cost of parallel imaging in functional MRI of the human brain. Magn Reson Imaging 24:1-5.
2. **Lütcke H**, Frahm J (in press) Lateralized Anterior Cingulate Function during Error Processing and Conflict Monitoring as Revealed by High-Resolution fMRI. Cereb Cortex.
3. **Lütcke H** (2006) Parcellating the medial frontal cortex: evaluative and cognitive components of performance monitoring. J Neurosci 26:7129-7130.

Poster abstracts

1. **Lütcke H**, Merbold K-D, Frahm J (2006) High-resolution fMRI of anterior cingulate function during error processing and conflict monitoring. *Program No. 367.8. 2006 Abstract Viewer / Itinery Planner.* Washington, DC: Society for Neuroscience. Presented at: **SfN 36th Annual Meeting**, Oct 14-18, 2006, Atlanta, Georgia, USA

Appendix 1

Available online at www.sciencedirect.com

SCIENCE DIRECT®

Magnetic Resonance Imaging 24 (2006) 1–5

MAGNETIC RESONANCE IMAGING

Original contributions

The cost of parallel imaging in functional MRI of the human brain

Henry Lütcke*, Klaus-Dietmar Merboldt, Jens Frahm

Biomedizinische NMR Forschungs GmbH am Max-Planck-Institut für Biophysikalische Chemie, 37070 Göttingen, Germany

Received 30 June 2005; revised 31 October 2005; accepted 31 October 2005

Abstract

While the advantages of parallel acquisition techniques for echo-planar imaging (EPI) are well documented for studies affected by magnetic field inhomogeneities, this work focuses on the costs in functional MRI of brain regions without artifacts due to susceptibility effects. For a visual stimulation paradigm and relative to conventional EPI (2.9 T; TR/TE=2000/36 ms), the use of parallel acquisition at a reduction factor of 2 decreased the mean number of activated voxels by 21% at 2×2×2-mm^3 resolution (n=6) and by 15% at 3×3×3-mm^3 resolution (n=6). The loss of sensitivity reflects both a decreased signal-to-noise ratio of the native images due to a lower number of contributing gradient echoes and a decreased BOLD MRI sensitivity due to the coverage of a smaller range of TEs.

Keywords: Magnetic resonance imaging; Parallel acquisitions; Echo-planar imaging; Functional brain mapping

1. Introduction

One of the most promising innovations in the field of magnetic resonance imaging (MRI) is the recent introduction of parallel acquisition techniques [1,2]. At the cost of a somewhat lower signal-to-noise ratio (SNR), pertinent approaches enable substantially faster image acquisition and, for echo-planar imaging (EPI), a reduced sensitivity to magnetic field inhomogeneities and related image artifacts. Parallel acquisition techniques use the distinct spatial sensitivity profiles of individual coils in an array of receive coils to reconstruct undistorted images from individually undersampled data. In practice, two approaches have been developed to achieve this goal. Techniques based on k space derive the missing Fourier lines by combining the weighted sum of the signal from each coil based on individual sensitivity profiles [1]. A few additional lines are usually acquired at the center of k space to improve the reliability of the reconstruction algorithm. In a recent modification of the k space technique [3], these reference lines are acquired before each scan, hence giving rise to the term "generalized autocalibrating partially parallel acquisition" (GRAPPA). Alternatively, image-based methods such as sensitivity encoding (SENSE) attempt to unfold individual aliased images by solving a system of linear equations based on the known sensitivity profiles of the coils [2]. For both k space- and image-based parallel techniques, the ratio of total k-space lines to the sampled k-space lines provides a rough estimate of the acceleration of the acquisition process.

Apart from being faster, single-shot gradient-echo sequences such as EPI and spiral imaging may benefit from the fact that the parallel acquisition-related reduction of the echo train length decreases the signal loss and geometric distortions caused by susceptibility differences. This is particularly well documented in diffusion-weighted EPI where no T_2* effect is desired [4,5]. For functional MRI (fMRI) of the human brain, the use of parallel acquisition has been reported to increase performance similar to the improvements observed with diffusion-weighted sequences in regions where conventional gradient-echo images suffer from profound susceptibility problems. For example, at 1.5 T, a spiral SENSE technique with an acceleration factor of 2 significantly better recovered orbitofrontal activations associated with a taste paradigm in comparison with spiral imaging without parallel acquisition [6]. In a recent memory study at 3 T, medial temporal lobe activations were observed more reliably when acquired with SENSE-EPI than with EPI as susceptibility-related image distortions were found to be reduced with increasing SENSE acceleration [7].

While there is minimal doubt that parallel fMRI can improve image quality in brain regions affected by magnetic field inhomogeneities, the putative cost of these

* Corresponding author. Tel.: +49 551 201 1735; fax: +49 551 201 1307.

E-mail address: hluetck@gwdg.de (H. Lütcke).

0730-725X/$ – see front matter © 2006 Elsevier Inc. All rights reserved.
doi:10.1016/j.mri.2005.10.028

techniques in terms of functional activation has been more controversial. Because of the inherent decrease in SNR associated with GRAPPA or SENSE, any potential decrease of extent or magnitude of the BOLD MRI response to human brain activation needs to be evaluated in areas that are not directly affected by magnetic field inhomogeneities. In contrast to reports of no reduction in activation volume in visual and motor areas [6], two other studies showed consistent t score decreases of 18% [8] and 7% [9] in the motor cortex as well as a 20% decrease of the activation volume due to SENSE-EPI with an acceleration factor of 2 [9].

In view of the increasing number of parallel acquisition applications in functional neuroimaging (see, for example, References [10,11]), it seems mandatory to assess their overall performance in a slightly more comprehensive manner; that is, in areas of the brain that show limited or no susceptibility effect at all. Thus, the purpose of this work was to address the consequences of GRAPPA in terms of visual functional activation in large parts of the brain not suffering from gradient-echo artifacts. In more detail, the study comprised EPI acquisitions at high ($2\times2\times2$ mm^3) and low ($3\times3\times3$ mm^3) spatial resolutions as commonly used in cognitive neuroimaging studies. EPI acquisitions with GRAPPA at an acceleration factor of 2 and at two TEs (36 and 25 ms) were compared with conventional EPI at TE=36 ms. Functional activation was evaluated with a correlation analysis approach [12] and quantified as the number of activated voxels.

2. Materials and methods

Twelve healthy volunteers (7 females and 5 males; age range, 18–42 years; mean age, 27±6 years) participated in the study. Informed written consent was obtained from each subject before all examinations were carried out in accordance with institutional guidelines. Three subjects had to be excluded from the analysis because of changes in vigilance during the acquisition of the six protocols (see below) as evidenced by marked reductions or even a complete loss of activations.

2.1. MRI

All studies were conducted at 2.9 T (Siemens Magnetom Trio, Erlangen, Germany) using an eight-channel receive-only phased array head coil in combination with a body coil for radio frequency transmission. Each session comprised T_1-weighted MRI (RF spoiled 3D FLASH; TR/TE=11/4.9 ms; flip angle, 15°) at $1\times1\times1$-mm^3 resolution for anatomic referencing.

fMRI was based on a single-shot gradient-echo EPI sequence with frequency-selective fat suppression (TR=2000 ms; mean TE=36 or 25 ms; flip angle, 70°). For high-resolution scans with a voxel size of $2\times2\times2$ mm^3, 16 sections were acquired (no slice gap) using an 84×128 acquisition matrix (75% rectangular FOV of 256 mm; 7/8 partial Fourier encoding in A–P direction). Low-resolution scans with a voxel size of $3\times3\times3$ mm^3 were based on a 64×64 matrix (FOV of 192 mm; conventional phase encoding) and comprised 26 sections (no slice gap). In either case, the volume was positioned in an oblique transverse-to-coronal orientation along the calcarine fissure. To approximately match the volume coverage for high- and low-resolution scans, we included only the 11 central sections of the low-resolution scan in the analysis. Motion correction was applied for all BOLD MRI recordings (Siemens Magnetom Trio). EPI acquisitions were performed using GRAPPA, as implemented by the vendor, and a reduction factor of 2. Twenty-four reference lines were obtained in a single acquisition (external calibration) prior to each functional series. The order of functional recordings with the three sequences studied (conventional EPI as well as EPI with GRAPPA at TEs of 36 and 25 ms) was pseudorandomized for each subject as previously described [13].

Functional activation was elicited using a passive visual stimulation task, which compared a flickering (1 Hz) black-and-white checkerboard with a gray screen. The paradigm was presented as a simple block design where 12 s of visual stimulation alternated with 18 s of control. Each experiment started with an 18-s control condition followed by eight experimental cycles. Subjects were instructed to fixate toward a red cross in the center of the screen throughout the experiment. MRI-compatible liquid crystal display goggles (Resonance Technology, Northridge, CA, USA) were used to present visual stimuli (60-Hz refresh rate; 1024×768-pixel resolution; visual field, $22.5\times30°$; virtual eye-to-screen distance, ~120 cm). Corrective lenses were applied if necessary.

2.2. Data analysis

A correlation analysis of cross-sectional BOLD MRI data was accomplished using in-house software. Activation maps were calculated for a boxcar reference function derived from the task protocol and shifted by 6 s to account for the delayed hemodynamic response. Significant activations were identified by a statistical evaluation of correlation coefficients following a procedure described previously [12]. First, a histogram of correlation coefficients originating from brain voxels within individual sections is determined. Second, a gaussian curve is fitted to the central portion of the histogram, covering a 50% range of the observed peak heights extending from the 30% level to the 80% level, to estimate the noise distribution of the correlation coefficients. Finally, the distribution of correlation coefficients is rescaled into percentile ranks of the individual noise distribution. Subsequently, pixels are accepted as activated if their correlation coefficients exceed the 99.99% percentile rank of the noise distribution estimated on an individual basis from the actual measurement. In a second step, neighboring pixels of such activation centers are iteratively added as long as their correlation

coefficients exceed the 95% percentile rank of the noise distribution. Importantly, identical thresholds were used for determining significantly activated voxels without and with GRAPPA, thus validating the extent of activation as a true measure of functional contrast. The resulting activation maps were superimposed onto T_2*-weighted echo-planar images.

The mean number of activated voxels for each of the three sequences was calculated by averaging across subjects. In addition, relative measures of activated voxels for EPI with GRAPPA were calculated by first normalizing individual results to conventional EPI and then averaging across subjects.

Regions of interest (ROIs) were defined in the primary visual cortex to estimate the amount of BOLD MRI signal change associated with stimulus presentation (i.e., the functional contrast). For each of three sections that best covered the sulcus calcarinus, an ROI was placed centrally in the occipital part of the brain comprising 100–150 voxels (800–1200 mm^3) for 2×2×2-mm^3 resolution and 30–45 voxels (810–1215 mm^3) for 3×3×3-mm^3 resolution. For individual subjects, the signal intensity time courses were averaged across ROIs and stimulation cycles and normalized to the mean signal strength of the entire time course. Finally, the mean stimulus-induced BOLD MRI signal changes for the six experimental conditions were estimated as the differences between the minimum and the maximum signal intensity of the time courses and averaged across subjects.

3. Results

Fig. 1 shows the representative activation maps of two subjects obtained for EPI acquisitions without and with GRAPPA at a reduction factor of 2 for two voxel sizes and TEs. Visual inspection suggests that, relative to conventional EPI, the extent of activation is reduced for GRAPPA versions under all circumstances (i.e., for both voxel sizes and TEs).

The quantitative data summarized in Table 1 confirm a reduction in the mean number of activated voxels for EPI with GRAPPA at identical TEs. If the shorter acquisition period is exploited for a shorter TE of 25 ms, then the extent of activation is decreased even further. When normalized to the number of activated voxels obtained without parallel acquisition, the analysis of the high-resolution data revealed a decrease in activation by 21% and 29% for GRAPPA at TE=36 ms and TE=25 ms, respectively. With paired t tests, significantly less activation was obtained with GRAPPA at TE=25 ms as compared with conventional EPI at TE=36 ms [$t_{(5)}$=2.7; P<.05], whereas the comparison failed to reach significance for GRAPPA at TE=36 ms [$t_{(5)}$=2.2; P=.08]. At a lower resolution, the amount of activation was again clearly reduced by 15% and by 23% at TE=36 ms and TE=25 ms, respectively, without reaching statistical significance [$t_{(5)}$=2.1 and P=.09 for TE=36 ms; $t_{(5)}$=2.3 and P=.07 for TE=25 ms].

To characterize the extent of activation further, as well as to optimize the statistical power of the comparison, we

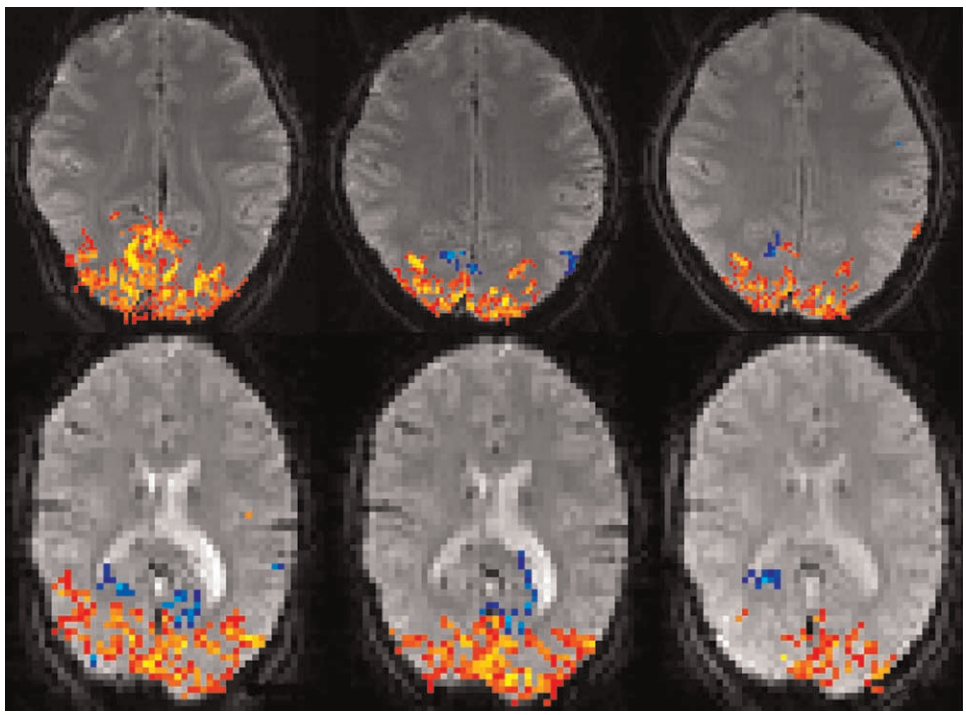

Fig. 1. Representative activation maps obtained for (top) 2×2×2-mm^3 resolution and (bottom) 3×3×3-mm^3 resolution (two subjects). The maps represent acquisitions with (left) conventional EPI at TE=36 ms, (middle) EPI with GRAPPA at a reduction factor of 2 and TE=36 ms and (right) EPI with GRAPPA at a reduction factor of 2 and TE=25 ms. Red–yellow=positive correlations; blue=negative correlations.

Table 1
Number of activated pixels and BOLD MRI signal change without and with GRAPPA at a reduction factor of 2

EPI	Normal (36 ms)	GRAPPA (36 ms)	GRAPPA (25 ms)
2×2×2 mm³			
TE range (ms)	8–74	22–55	11–44
Activated pixels	4482±1405	3313±392	3052±594
Normalized	1.00	0.79±0.21*	0.71±0.15**
Signal change (%)	2.56±0.83	2.48±0.86	1.77±0.56**
3×3×3 mm³			
TE range (ms)	10–61	23.5–48.5	12.5–37.5
Activated pixels	1599±336	1385±444	1208±331
Normalized	1.00	0.85±0.18*	0.77±0.21*
Signal change (%)	2.77±1.07	2.69±1.03	1.96±0.80**

Values are given as mean±S.D. (n=6 for 8-mm³ voxels and n=6 for 27-mm³ voxels). Normalized values are relative to the number of activated pixels obtained for EPI without PPA. Mean BOLD MRI signal change is given in percentage of mean signal strength in standardized ROIs of the primary visual cortex.

* P<.1 (paired t test).

** P<.05 (paired t test).

combined low- and high-resolution data in a 3×2 (Sequence×Resolution) mixed analysis of variance. This procedure demonstrated a highly significant decrease in the extent of activation for GRAPPA-supported acquisitions [$F_{(2,20)}$=7.5; P<.01]. The interaction between the factors Sequence and Resolution was nonsignificant [$F_{(2,20)}$=2.8; P=NS], which demonstrates that the reduction in activation volume due to parallel imaging is similar for high- and low-resolution acquisitions. Planned comparisons of activation volume revealed a significantly reduced number of activated voxels both for GRAPPA at TE=36 ms [$t_{(11)}$=2.3; P<.05] and for that at TE=25 ms [$t_{(11)}$=3.0; P<.05] as compared with conventional acquisition (corrected for multiple comparisons using the procedure set forth by Holm [14]).

With a standardized set of ROIs in the primary visual cortex, the BOLD MRI signal change was significantly reduced for EPI with GRAPPA at TE=25 ms as compared with both conventional EPI and EPI with GRAPPA at TE=36 ms for high resolution [$t_{(5)}$=4.4, P<.05, and $t_{(5)}$=3.9, P<.05, respectively] and low resolution [$t_{(5)}$=6.1, P<.05, and $t_{(5)}$=4.6, P<.05, respectively].

4. Discussion

The present study revealed a substantial reduction in functional activation (as assessed by the number of activated voxels) when using EPI in conjunction with GRAPPA at a reduction factor of 2. The finding applies to large parts of the occipital and parietal cortices (i.e., regions that are only mildly or not at all affected by susceptibility problems and related EPI distortions). Reduction of the activation volume due to GRAPPA alone amounted to 15% and 21% for low- and high-resolution sequences, respectively, whereas a concurrent decrease of the TE diminished the extent of activation even more.

The proportion of the total variance in the extent of activation explained by parallel imaging may be calculated by dividing the sum of squares of the effect by the total sum of squares (Effect+Interaction+Error Term):

$$\eta^2 = \frac{SS_{effect}}{SS_{total}}$$

With η^2 as a measure of the effect size, parallel imaging accounted for 37% of the total variability in the extent of activation. Considering the large between-subject variability typical for fMRI studies, the effect of GRAPPA on the activation volume must be considered as substantial.

The observed loss of overall BOLD sensitivity with GRAPPA may be attributed to at least two independent factors. First, because the number of sampled k-space lines is reduced for GRAPPA, the SNR is also reduced. Second, an independent source of BOLD contrast attenuation becomes evident when considering the range of TEs covered by EPI while scanning k space (compare Table 1). GRAPPA alone caused a reduction of the TE range by approximately 50%, whereas a mean TE of only 25 ms further decreased the range of absolute TE values. The mean TE should be approximately equal to tissue T_2*, which at 3 T is approximately 40–50 ms, to achieve optimal BOLD MRI sensitivity. Table 1 shows that this range is covered sufficiently well by EPI without and even with parallel acquisition as long as the mean TE is kept at 36 ms. Accordingly, the achievable BOLD MRI signal change was very similar for both conditions. In contrast, a combination of GRAPPA with a TE of only 25 ms moves the upper limit of the acquired TE range near the TE value for optimal T_2* weighting. Consequently, a large part of k space, and particularly its center, is acquired with TEs that are far too low to result in effective T_2* weighting and corresponding BOLD MRI sensitivity. This observation is supported by the approximately 30% decrease of the BOLD MRI signal change at TE=25 ms for both high and low spatial resolutions.

Our results were obtained using a k space-based parallel acquisition technique and correlation analysis of functional time series, yet they are in broad agreement with previous results by others, one of which, for example, reported a 20% reduction in the extent of motor cortex activation for SENSE-EPI [9]. Moreover, a recent comparison of EPI with SENSE-EPI obtained larger activation clusters in the inferior frontal gyrus, which hardly suffers from susceptibility artifacts, when the acquisition was performed without parallel acquisition, whereas improvements with SENSE were seen in critical regions such as the anterior hippocampus, amygdala and fusiform gyrus [7].

5. Conclusions

The present study demonstrates that fMRI of human brain activation may suffer from the use of parallel acquisition techniques. In comparison with conventional

EPI, the combination of EPI with GRAPPA at a reduction factor of 2 incurs a substantial cost on BOLD MRI sensitivity in brain areas not or only mildly affected by magnetic field inhomogeneities. The 20% reduction of the extent of activation observed here must be considered as a substantial loss, especially in view of cognitive neuroimaging studies where activated areas tend to be small. Investigators planning GRAPPA-supported fMRI studies certainly are knowledgeable about the benefits in terms of reduced susceptibility artifacts and scan time, but they should also be aware of the associated cost due to a lower SNR and partial loss of T_2* weighting. It may be advisable to invest the saved time into signal averaging for improved SNR while retaining the parallel acquisition advantages with respect to susceptibility artifacts to achieve a reasonable compromise between enhanced speed, improved image quality and reduced BOLD MRI sensitivity.

References

[1] Sodickson DK, Manning WJ. Simultaneous acquisition of spatial harmonics (SMASH): fast imaging with radiofrequency coil arrays. Magn Reson Med 1997;38:591–603.

[2] Pruessmann KP, Weiger M, Scheidegger MB, Boesiger P. SENSE: sensitivity encoding for fast MRI. Magn Reson Med 1999;42: 952–62.

[3] Griswold MA, Jakob PM, Heidemann RM, Nittka M, Jellus V, Wang J, et al. Generalized autocalibrating partially parallel acquisitions (GRAPPA). Magn Reson Med 2002;47:1202–10.

[4] Bammer R, Keeling SL, Augustin M, Pruessmann KP, Wolf R, Stollberger R, et al. Improved diffusion-weighted single-shot echo-planar imaging (EPI) in stroke using sensitivity encoding (SENSE). Magn Reson Med 2001;46:548–54.

[5] Jaermann T, Crelier G, Pruessmann KP, Golay X, Netsch T, van Muiswinkel AM, et al. SENSE-DTI at 3 T. Magn Reson Med 2004; 51:230–6.

[6] Weiger M, Pruessmann KP, Osterbauer R, Bornert P, Boesiger P, Jezzard P. Sensitivity-encoded single-shot spiral imaging for reduced susceptibility artifacts in BOLD fMRI. Magn Reson Med 2002; 48:860–6.

[7] Schmidt CF, Degonda N, Luechinger R, Henke K, Boesiger P. Sensitivity-encoded (SENSE) echo planar fMRI at 3 T in the medial temporal lobe. Neuroimage 2005;25:625–41.

[8] de Zwart JA, van Gelderen P, Kellman P, Duyn JH. Application of sensitivity-encoded echo-planar imaging for blood oxygen level-dependent functional brain imaging. Magn Reson Med 2002;48: 1011–20.

[9] Preibisch C, Pilatus U, Bunke J, Hoogenraad F, Zanella F, Lanfermann H. Functional MRI using sensitivity-encoded echo planar imaging (SENSE-EPI). Neuroimage 2003;19:412–21.

[10] Kirwan CB, Stark CE. Medial temporal lobe activation during encoding and retrieval of novel face–name pairs. Hippocampus 2004;14:919–30.

[11] Okado Y, Stark CE. Neural activity during encoding predicts false memories created by misinformation. Learn Mem 2005;12:3–11.

[12] Baudewig J, Dechent P, Merboldt KD, Frahm J. Thresholding in correlation analyses of magnetic resonance functional neuroimaging. Magn Reson Imaging 2003;21:1121–30.

[13] Williams EJ. Experimental designs balanced for the estimation of residual effects of treatments. Aust J Sci Res Ser A 1949;2:149–68.

[14] Holm S. A simple sequentially rejective multiple test procedure. Scand J Stat 1979;6:65–70.

Appendix 2

Cerebral Cortex Advance Access published June 18, 2007

Cerebral Cortex
doi:10.1093/cercor/bhm090

Lateralized Anterior Cingulate Function during Error Processing and Conflict Monitoring as Revealed by High-Resolution fMRI

Henry Lütcke and Jens Frahm

Biomedizinische NMR Forschungs GmbH am Max-Planck-Institut für biophysikalische Chemie, 37070 Göttingen, Germany

Recent studies have reported that functional subdivisions of anterior cingulate cortex (ACC) may be selectively responsible for conflict and error-related processing. We examined this claim by imaging ACC activation to correct and erroneous response inhibitions in a GoNogo task. After localizing the ACC cluster in individual subjects using functional magnetic resonance imaging (fMRI) at standard resolution ($2 \times 2 \times 4$ mm^3), high-resolution fMRI ($1.5 \times 1.5 \times 1.5$ mm^3) of the ACC was performed in a second session to investigate its precise functional anatomy. At standard resolution, and in agreement with previous studies, ACC was activated for correct and incorrect responses, albeit more so for errors. High-resolution maps of activated ACC clusters revealed localized and reproducible foci in 9 out of 10 volunteers. Multi-subject analysis suggested a bilateral distribution of error-related processes in ACC, whereas correct inhibitions only seemed to activate ACC in the right hemisphere. Subsequent region of interest analysis largely confirmed the activation maps. Our results contribute toward a better understanding of the microanatomy of ACC and demonstrate the potential of fMRI for mapping the functional architecture of brain regions involved in cognitive tasks at a previously unaccomplished spatial scale.

Keywords: ACC, fMRI, high resolution, lateralization

Introduction

In a permanently changing environment, only few things seem to be more important for the pursuit of stable, long-term goals than the ability to constantly monitor one's own actions, initiate changes in the face of new external demands, or abandon unsuccessful strategies altogether. Such a capacity for cognitive control may well be one of the hallmarks of human behavior.

Numerous studies have identified the medial frontal cortex (MFC), and especially its anterior cingulate part (ACC), as one of the most reliable neural correlates of cognitive control in the human brain (Carter et al. 1998; Botvinick et al. 1999, 2004; Ridderinkhof, Ullsperger, et al. 2004; Ridderinkhof, van den Wildenberg, et al. 2004; Ullsperger and von Cramon 2004). Nevertheless, the precise mechanisms underlying this function are still a matter of debate. Whereas initial EEG experiments suggested that ACC might play a role in the detection of errors (Falkenstein et al. 1991; Gehring et al. 1993), subsequent functional magnetic resonance imaging (fMRI) studies argued for a more global role in monitoring of conflicting action sequences (Carter et al. 1998; Kiehl et al. 2000; Menon et al. 2001). Error detection, in this framework, is thought to occur once conflict rises above a certain threshold (Yeung et al. 2004).

More recently, a functional subdivision of ACC has been proposed (Polli et al. 2005; Taylor et al. 2006). Based on fMRI evidence, Taylor et al. (2006) suggested that the dorsal part of ACC plays a role in conflict monitoring, whereas its rostral component may be more involved in error-specific processing such as performance evaluation. Furthermore, these authors demonstrated a surprising degree of intersubject variability for activation foci along the mesial wall, suggesting that discrepancies in the localization of conflict or error-related processing between previous studies may be due to differential clustering of the subjects' activation in the different samples. Moreover, because the spatial resolution of respective experiments has been limited, important differences at an even finer scale may have been missed. In fact, most standard fMRI studies employ voxel sizes in the order of $3 \times 3 \times 3$ mm^3, whereas the technique itself allows for acquisitions with at least an 8 times smaller voxel size of $1.5 \times 1.5 \times 1.5$ mm^3.

Here, we used high-resolution fMRI in combination with a conflict eliciting GoNogo task to investigate the functional anatomy of the ACC at a previously unaccomplished spatial scale. The task, which was designed to generate high proportions of errors on Nogo trials, allowed us to compare putative neural correlates of conflict as well as of error-monitoring processes. Whereas successful conflict resolution implicates only conflict monitoring, error trials involve both conflict and error-related mechanisms.

fMRI at high spatial resolution has previously been used to study early sensory processes, mainly in the visual system, (Schneider et al. 2004; Schwarzlose et al. 2005; Grill-Spector et al. 2006). These studies benefited from the good functional contrast-to-noise ratio (CNR) as well as limited intersubject variability in sensory areas. Cognitive neuroimaging, on the other hand, suffers from low CNR and high variability, making it apparently unsuitable for high-resolution fMRI. Thus, a more general aim of the current study was to investigate the feasibility of a new strategy for cognitive neuroimaging combining low and high spatial resolution.

Materials and Methods

Subjects

Eleven right-handed volunteers (3 males and 8 females; mean age 27 ± 6 years) participated in 2 experimental sessions (separated by more than 1 day). One data set was excluded due to excessive motion (relative displacement in any direction of more than 1 mm). In each experimental session, subjects performed between 4 and 6 repetitions of the experiment, leaving us with a total of 50 standard and 64 high-resolution runs for analysis. Given the substantial variability in activation between subsequent runs, partly attributable to factors such as fatigue, motivation, or hardware changes, each experiment was treated independently for the purpose of statistical analysis. To investigate reproducibility of high-resolution activation maps, one male subject took part in 2 high-resolution sessions (separated by 6 months). All participants were informed about the purpose of the study as well as possible risks

associated with magnetic resonance imaging (MRI). Written consent was obtained prior to each experimental session. After the end of the second session, subjects were debriefed about the staircase procedure (see below). Participants earned 10 Euros per hour plus a bonus depending on their performance (see below). All experimental procedures conformed fully to institutional guidelines.

Task

We used a visual letter-based GoNogo task where subjects had to press a button with their right thumb or index finger whenever a Go (target) stimulus (A, J, S, O) appeared in the center of the screen. Subjects were instructed to refrain from pressing the button upon presentation of a Nogo (nontarget) stimulus (X).

All stimuli were presented in black color on a gray background. Two yellow vertical bars were continuously presented above and below the stimulus location, in order to direct subjects' attention to the center of the screen and to provide feedback (see below).

A total of 120 stimuli were presented per run (20% Nogo) with jittered stimulus onset asynchrony (2, 4, 6 s; mean 4 s) using a dedicated projection setup (Schäfter & Kirchhoff, Hamburg, Germany) or MRI-compatible liquid crystal display goggles (Resonance Technology Inc., Northridge, CA). Corrective lenses were applied if necessary.

The initial presentation duration for all stimuli was 500 ms, and subjects were instructed to respond within this time frame. Subjects were informed about an error (late response to target or response to nontarget) immediately after a trial by briefly changing the color of the vertical bars to red. Usually subjects achieve high performance accuracy on this task (less than 10% false alarms [FAs]), which makes the analysis of errors virtually impossible. Therefore, we modified the presentation time of targets over the course of each run depending on subjects performance on Nogo trials. More precisely, 2 consecutive successful inhibitions led to a reduction of the Go stimulus duration by 50 ms (minimum presentation time 250 ms), whereas 2 consecutive responses to Nogo stimuli increased target duration by 50 ms (maximum presentation time 750 ms). These values were found to yield approximately 50% errors during pretesting. Importantly, the presentation duration of Nogo stimuli was always 500 ms. Participants received a small bonus for correct trials, whereas errors incurred a financial penalty.

Magnetic Resonance Imaging

All studies were conducted at 2.9 T (Siemens Tim Trio, Erlangen, Germany) using a 12-channel receive-only head coil. Each session comprised T_1-weighted MRI (3D FLASH) at 1 × 1 × 1 mm^3 resolution for anatomic referencing. For fMRI, we employed a single-shot gradient-echo echo planar imaging sequence (repetition time/echo time = 2000/36 ms, flip angle 70°, 244 volumes per run). Scans with a voxel size of 2 × 2 × 4 mm^3 were based on a 84 × 96 acquisition matrix (192 mm field of view [FOV], 7/8 partial Fourier phase encoding, bandwidth 1336 Hz/pixel, echo spacing 0.81 ms) and comprised 22 transverse-to-coronal slices, covering the whole cerebrum. High-resolution fMRI with a voxel size of 1.5 × 1.5 × 1.5 mm^3 was achieved using a 90 × 128 matrix (180 × 192 mm rectangular FOV, 6/8 partial Fourier phase encoding, bandwidth 1396 Hz/pixel, echo spacing 0.86 ms) with 18 slices, positioned so as to achieve good coverage of the previously determined active region in ACC. All magnetic resonance images are presented in accordance with radiological convention throughout the manuscript (i.e., right and left sides are flipped).

Data Analysis

Evaluation of fMRI data was performed using tools from the FMRIB Software library (FSL, www.fmrib.ox.ac.uk) and MATLAB (The MathWorks, Natick, MA). After initial motion correction in *k*-space (Siemens), residual motion was accounted for by image-based registration (Jenkinson et al. 2002). Data at standard resolution were smoothed using a Gaussian kernel of full width half maximum (FWHM) 5 mm. Non-brain tissue was removed (Smith 2002), and all volumes were intensity normalized by the same factor and temporally high-pass filtered (Gaussian-weighted least-squares straight line fitting, with high-pass filter cutoff at 30 s). High-resolution data were preprocessed in a similar way, but, instead of Gaussian smoothing, the images were filtered with the smallest univalue segment assimilating nucleus noise reduction algorithm, also part of FSL (Smith and Brady 1997). Intensity thresholds for the definition of anatomical regions were set to one tenth of the maximum image intensity, separately for each volume, and smoothing was performed within regions of similar intensity using a 5-mm Gaussian kernel.

To compare brain responses associated with correctly resolved and erroneous Nogo trials, we created models for correct rejections (CRs) and FAs by convolving relevant events with a Gamma function that takes into account temporal properties of the hemodynamic response to neural activation. Model fit was determined by statistical time series analysis with local autocorrelation correction (Woolrich et al. 2001).

Standard resolution images were spatially normalized to the Montreal Neurological Institute 152 (MNI152) template brain, and mixed-effects group analysis was performed (Beckmann et al. 2003; Woolrich et al. 2004). Significant activations based on z statistic (Gaussianized T/F) images were obtained by first determining clusters of $z > 3.1$ and then applying a corrected cluster threshold of $P = 0.05$, as previously described (Worsley et al. 1992).

High-resolution images were spatially normalized to their respective anatomic scan as well as to the MNI152 template brain (Jenkinson and Smith 2001; Jenkinson et al. 2002) and summarized for each subject (fixed effects). Statistical inference was restricted to an anatomically defined region of interest (ROI) covering the entire MFC. We considered voxels active that surpassed an uncorrected threshold of $P < 0.01$ and had at least 5 activated neighbors. This rather liberal thresholding was motivated by the less severe multiple comparison problem due to spatial restrictions on statistical inference as well as the fact that maps of individual subjects were analyzed. A second higher level analysis examined effects across all subjects and over the whole volume covered. Thresholded activation maps were obtained by controlling the false discovery rate (FDR), which does not rely on spatial smoothness, at $q < 0.01$ (Genovese et al. 2002).

Subsequently, ROIs in dorsal ACC (dACC) and rostral ACC (rACC) were defined individually for each subject by drawing a line at the anterior boundary of the genu of the corpus callosum that was at right angles to the intercommisural plane (Devinsky et al. 1995; Polli et al. 2005). Rostral and dorsal parts were further subdivided according to hemisphere, yielding 4 ROIs. Normalized mean parameter estimates (beta values) from these regions as well as the number of activated voxels in each ROI were subjected to statistical analysis (all P values Bonferroni corrected for multiple comparisons).

Results

Psychophysics

There were no significant differences for any of the behavioral measures (reaction time and accuracy) between the standard and high-resolution sessions (see Table 1). The error rate on Nogo trials was high (57 ± 7% CRs), demonstrating validity of the staircase procedure.

Neuroimaging: Standard Resolution

Linear contrasts between CR and FA were calculated from their model parameter estimates. As expected, contrasting FA and CR (FA > CR) revealed a significant ($z > 3.1$ and corrected cluster $P < 0.05$) activation cluster in MFC as shown in Figure 1 (see

Table 1
Reaction time (RT) and accuracy (±standard deviation) during standard and high-resolution fMRI (sessions 1 and 2, respectively)

	Session 1	Session 2
	Standard resolution	High resolution
Target response (%)	86 ± 11	89 ± 10
Nontarget inhibition (%)	57 ± 7	57 ± 7
RT target response (ms)	360 ± 20	351 ± 19
RT FA (ms)	343 ± 23	333 ± 22

also Table 2). To explore the individual variability of this group activation cluster, we summarized individual runs for each subject and projected the center of gravity (COG) of the largest cluster in MFC into standard space. Although subjects' activation scattered around the cluster obtained from group analysis, there was also a considerable degree of variability, most notably along the dorsal–rostral axis of the MFC. In addition, error-related brain responses were detected in insular, extrastriate and motor cortices bilaterally, right postcentral gyrus, thalamus, as well as midbrain (see Table 2). Specific activation due to successful resolution of conflict (as measured by contrasting CR > FA, Fig. 1) was detected in a cluster in right inferior parietal lobule as well as right orbitofrontal cortex (see Table 2). No MFC activation was observed for this contrast.

Neuroimaging: High Resolution

To examine shared and distinct regions of error and conflict processing in MFC, we calculated linear contrasts between FA and rest (FA > Rest) as well as CR and rest (CR > Rest), respectively. Significant error-related brain responses at the preset criteria ($P < 0.01$, 5 connected voxels) were detected in 9/10 subjects. Activation maps of 2 representative volunteers, displayed on their respective anatomic scans, are shown in Figure 2. Although there appears to be "less activation" compared with conventional acquisitions at lower resolution, all significant voxels are located in the cortical gray matter and respect sulcal architecture. Interestingly, activation in response to impulse errors appears to be more pronounced in the ACC of the right hemisphere, although small foci are also present in left ACC. Note also that active clusters scatter along the whole length of ACC, even for single volunteers. To assess reliability of these maps, the high-resolution session was repeated in one subject. Individual foci colocalized to a surprising degree for these 2 sessions as demonstrated in Figure 3. Taken together, these findings suggest that the ACC foci obtained by high-resolution fMRI represent actual centers of neural activity that are blurred across anatomical borders by standard fMRI acquisition and analysis.

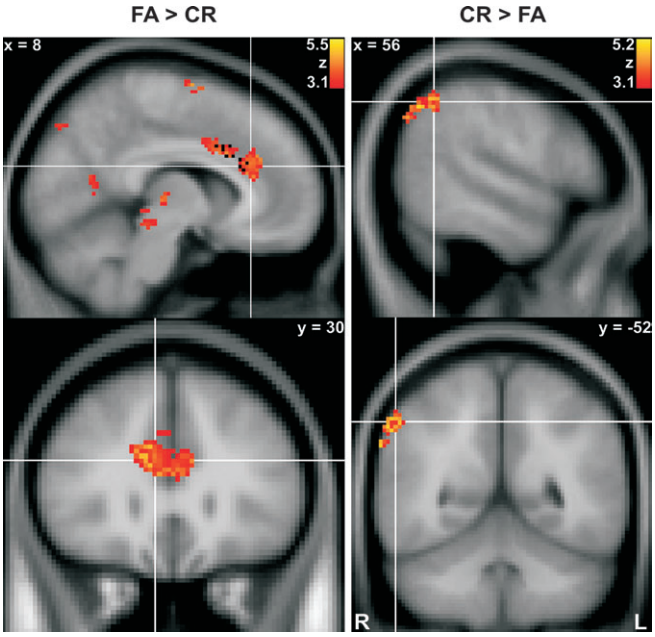

Figure 1. Low-resolution activation maps (averaged across 10 subjects) for responses to FAs and CRs. (Left) Contrasting FA with CR revealed significantly activated clusters ($z > 3.1$; $P < 0.05$) in ACC, thalamus, midbrain, and extrastriate visual areas. Black dots indicate the COGs of individual MFC activation clusters for 7 subjects (projected onto $x = 8$). (Right) The contrast between CR and FA revealed an activated cluster in right inferior parietal cortex.

Table 2

Atlas coordinates (in MNI space) and maximum *z* scores for the COGs of clusters significantly activated in contrasts between FAs and CRs at standard resolution

Contrast	Brain region	COG coordinates (*x*, *y*, *z*)	*z* Score
FA > CR	MFC	3, 19, 33	5.32
	Left insular cortex	−40, −4, −2	5.48
	Right insular cortex/postcentral gyrus	54, −17, 24	4.89
	Left/right extrastriate cortex	±34, −79, 22	5.23
	Right motor cortex	35, −34, 60	4.22
	Left motor cortex	−26, −41, 68	4.90
	Thalamus	−2, −24, 0	5.37
	Midbrain	6, −30, −12	4.22
CR > FA	Right inferior parietal lobule	53, −62, 43	4.96
	Right orbitofrontal cortex	42, 44, −20	5.16

Whereas ACC responded very strongly to FA, we could also detect a weak but significant activation for successful inhibitions in 8/10 subjects (as assessed by CR > Rest; see Fig. 2). CR foci were exclusively localized in the right ACC and largely overlapped with error-responsive activation clusters.

Results obtained from the evaluation of individual volunteers were confirmed and extended by a multisubject analysis. Significant ($q < 0.01$, FDR) and overlapping brain responses to FA > Rest and CR > Rest were detected in MFC (see Fig. 4). The error-related activation cluster was predominantly localized in the right ACC although activation was also seen in the left hemisphere (COG at $x = 2$, $y = 17$, $z = 34$; $z_{max} = 5.1$). In agreement with single subject results, activation for successful inhibitions was exclusively right lateralized (COG: 5, 21, 34; $z_{max} = 3.8$). Apart from activation in MFC, this analysis revealed a region in the right frontopolar cortex that responded significantly to both CR > Rest (COG: 36, 48, 20; $z_{max} = 4.6$) and FA > Rest (COG: 37, 43, 23; $z_{max} = 4.4$; see Fig. 4).

To exclude the possibility that error and conflict-related activations in MFC and prefrontal cortex are unspecific effects of stimulus presentation, we analyzed brain responses to correctly resolved target responses (compared with rest). As expected, an active cluster in left motor cortex (COG: –46, –17, 53; $z_{max} = 6.4$) could be detected in this case (data not shown). Furthermore, erroneous button presses on Nogo trials also elicited activation in left motor cortex (COG: –47, –14, 50; $z_{max} = 5.3$), whereas successful inhibitions failed to do so (data not shown).

A direct comparison of standard and high-resolution activation maps is impeded by the latter's low signal-to-noise ratio (SNR). To nevertheless illustrate the correspondence between standard and high-resolution fMRI, we calculated group activation maps for the FA > CR contrast (Supplementary Fig. 1) for both acquisitions. To account for the SNR difference, the standard resolution maps were required to pass a more stringent threshold ($q < 0.01$ vs. $q < 0.1$, FDR). An overlapping activation cluster in ACC was detected with standard and high-resolution acquisition, demonstrating the correspondence between the 2 approaches (Supplementary Fig. 1).

To quantify the high-resolution fMRI results, we determined the number of active voxels in response to FA, CR, and correct target responses for each experiment separately (thresholded at

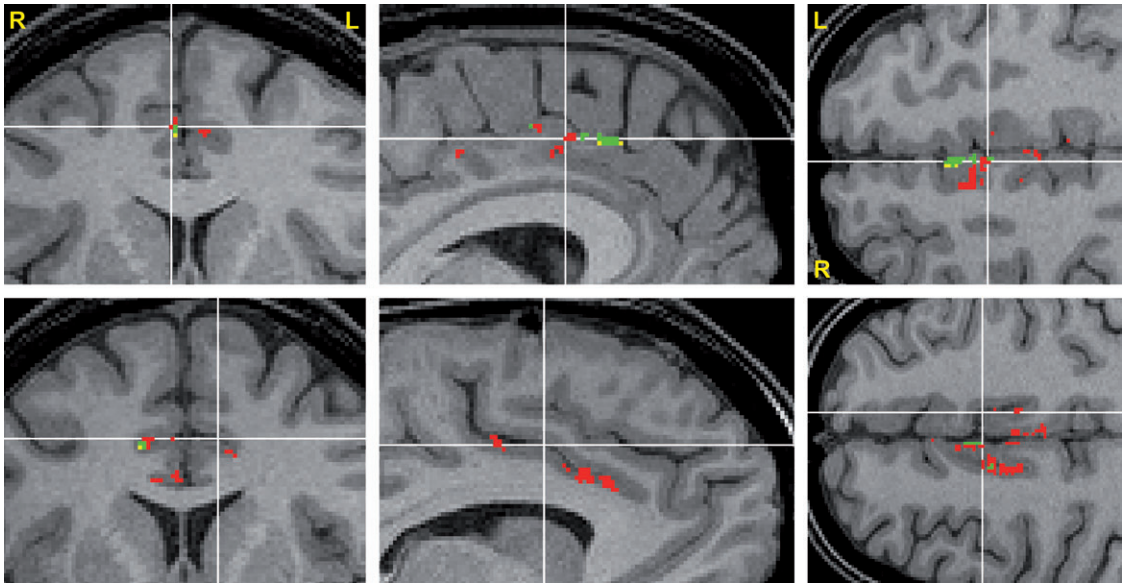

Figure 2. High-resolution activation maps (single subjects) for responses to FAs (FA > Rest) and CRs (CR > Rest). Maps were obtained by averaging across runs and projecting the results on the subjects' individual anatomy. Although active clusters scatter along the length of ACC, they are located in the cortical gray matter and respect sulcal architecture. Top and bottom rows show representative maps from 2 volunteers that demonstrate that active FA > Rest clusters (red) are located mainly, but not exclusively, in the right ACC. Significant responses to CR > Rest (yellow) occurred only in right ACC and overlapped (green) substantially with FA > Rest clusters.

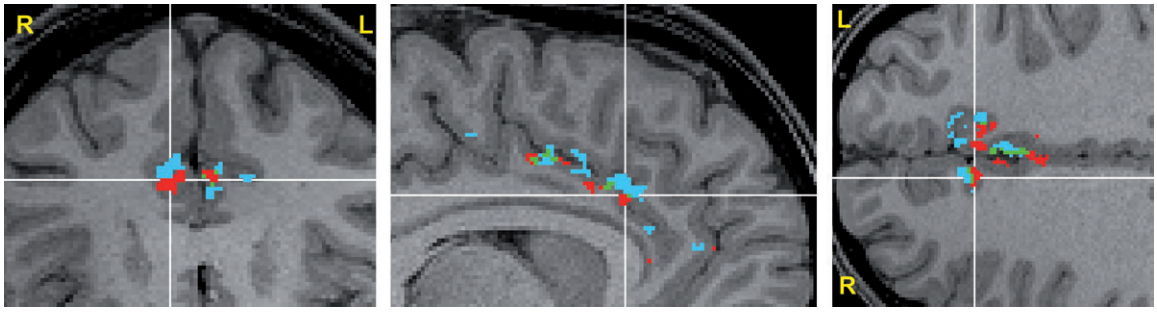

Figure 3. Activation maps for the contrast FA > Rest of a single subject obtained 6 months apart (time point 1: red; time point 2: blue) show a surprising colocalization as well as substantial overlap (green).

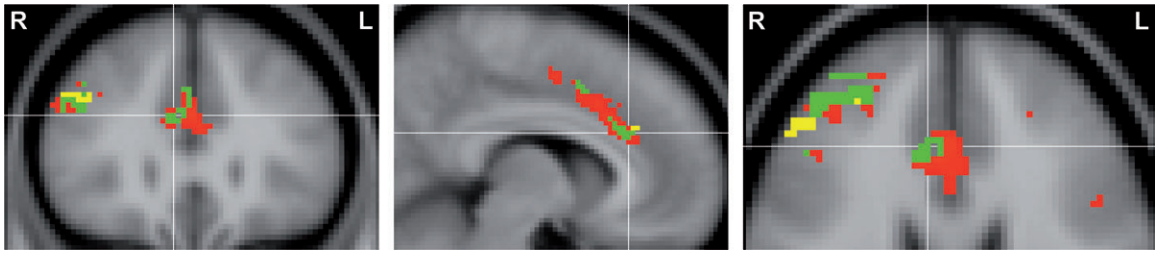

Figure 4. High-resolution activation maps (averaged across 10 subjects) for responses to FAs (FA > Rest, red) and CRs (CR > Rest, yellow). Largely bilateral activation of ACC was associated with impulse errors, whereas successful inhibitions only activated a smaller area in right ACC that overlapped (green) with the corresponding FA cluster. Further, partly overlapping, FA and CR activation was detected in the right frontopolar cortex (coronal and horizontal sections).

$P < 0.01$, 5 connected voxels) in 4 subregions of ACC (see Materials and Methods). A 2 × 3 (hemisphere: left – right; trial type: correct target response – CR – FA) analysis of variance (ANOVA) was carried out separately for dACC and rACC (see Fig. 5). Significant main effects for hemisphere and trial type were obtained in both dACC ($F_{1,63} = 5.6$, $P < 0.05$; $F_{1,78} = 19.7$, $P < 0.001$, respectively) and rACC ($F_{1,63} = 6.7$, $P < 0.05$; $F_{1,82} = 10.5$, $P < 0.01$, respectively). A significant interaction between both factors, indicating a differential modulation of the 2 hemispheres by CR and FA, was evident in rACC ($F_{2,114} = 3.6$, $P < 0.05$) but not dACC ($F_{2,107} = 0.2$, $P > 0.1$). As shown in Figure 5, FA activated significantly more voxel than correct target responses in all 4 ROIs (all $P < 0.05$, Bonferroni corrected for multiple comparisons). Furthermore, only rACC in the right hemisphere responded stronger to CR than to correct target responses ($t_{63} = 2.7$, $P = 0.05$, Bonferroni corrected for multiple

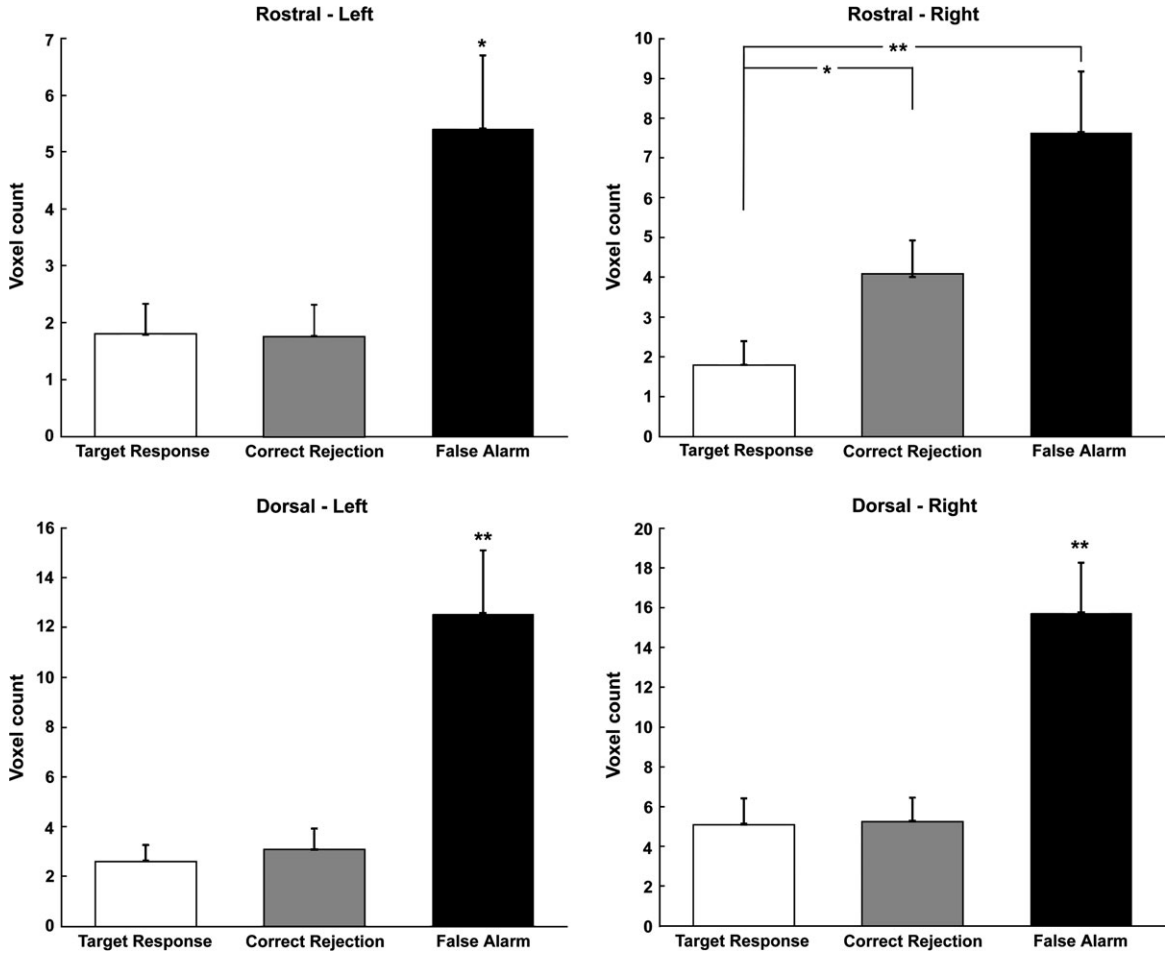

Figure 5. Mean number of activated voxels (single experiments) in dorsal and rostral as well as left and right ACCs. Whereas dACC as well as left rACC responded significantly stronger to FAs than to either correct target responses or CR, right dACC was activated by both CRs and FAs. $^{**}P \leq 0.01$, $^{*}P \leq 0.05$; Bonferroni corrected.

comparisons), whereas the number of voxels activated by FA did not differ from CR in this ROI ($t_{63} = 2.3$, $P = 0.1$). Such a pattern of activation would be expected if right rACC was to play a role in conflict monitoring, which is implicated by both CR and FA.

We obtained further evidence for a hemispheric specialization in ACC by calculating a "laterality index" for each subject from the number of activated voxels in right and left ACC (averaged across dorsal and rostral ROIs):

$$\text{laterality} = \frac{\text{Vox}_{\text{right}} - \text{Vox}_{\text{left}}}{\text{Vox}_{\text{right}} + \text{Vox}_{\text{left}}}$$

This index shows a strongly right-lateralized ACC response for CRs (0.73 ± 0.09), whereas FAs elicit a more bilateral response, though skewed to the right (0.27 ± 0.12).

Because the number of activated voxels only takes into account a very small fraction of the information that is available (and depends on the particular technique and cutoff used for thresholding), we additionally extracted and compared the normalized mean parameter estimates (beta values) of the fitted model for FA, CR, and correct target responses from the 4 ROIs (see Fig. 6). In accordance with the previous analysis, FA was associated with significantly stronger brain activation than correct button presses in all 4 ROIs (all $P < 0.01$, Bonferroni corrected for multiple comparisons). Furthermore, both left and right dACCs responded stronger to FA than to CR ($t_{63} = 5.1$, $P < 0.01$; $t_{63} = 4.6$, $P < 0.01$, respectively), whereas these comparisons failed to reach significance in rACC ($t_{63} = 2.1$, $P > 0.1$ and $t_{63} = 1.4$, $P > 0.1$, respectively). As before, right rACC responded significantly stronger to CR than to correct target responses ($t_{63} = 2.9$, $P < 0.05$), supporting a role for the region in conflict related processes.

Discussion

In this study, we used fMRI at high spatial resolution to uncover the functional microanatomy of human ACC during conflict monitoring and error processing. In line with previous studies, standard fMRI demonstrated a stronger ACC response for erroneous trials than for successful inhibitions. Based on these results, we imaged activated regions in MFC with higher spatial resolution and were able to obtain highly localized activation maps of neural foci both for conflict and error processing in the majority of subjects. Furthermore, these maps proved to be surprisingly reproducible. A multisubject analysis demonstrated bilateral error and right-lateralized conflict-associated processing in MFC as well as a cluster in right frontopolar cortex that responded significantly to Nogo trials. Subsequent ROI analysis largely agreed with the conclusions derived from high-resolution activation maps. Left rACC, as well as dACC, responded significantly to incorrect Nogo trials only and presumably play

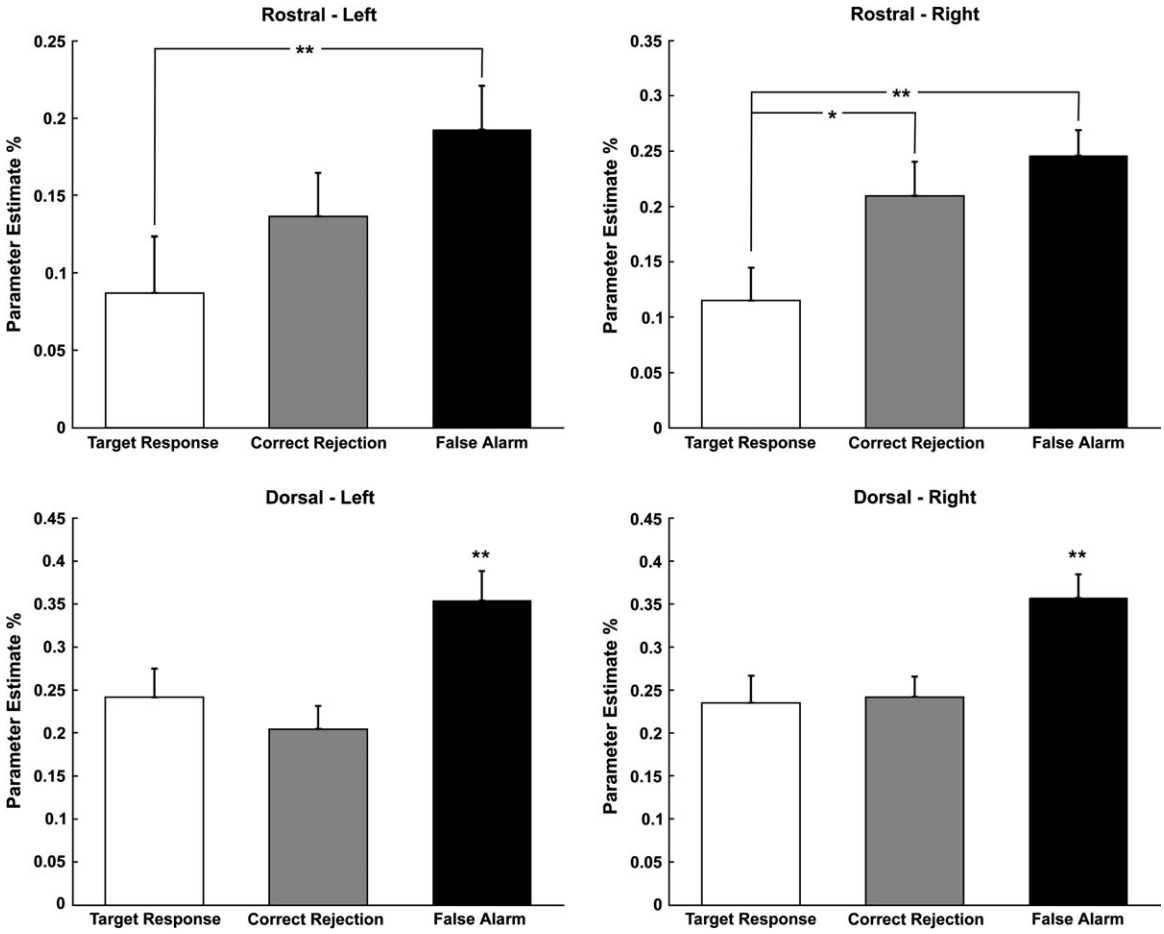

Figure 6. Mean parameter estimates of the fitted model in dorsal and rostral as well as left and right ACC. Whereas activation in dACC was associated with impulse errors, rACC in the right hemisphere responded significantly to errors as well as successful inhibitions. Left rACC responded significantly stronger to FAs than to target responses whereas responses to CRs did not differ from either FAs or target responses. $^{**}P \leq 0.01$, $^{*}P \leq 0.05$; Bonferroni corrected.

a role in error-related processes, such as error detection or evaluational aspects of error commission. Conversely, right rACC was activated both for successful and unsuccessful inhibition, albeit more strongly for the latter. This suggests that the region plays a role in monitoring and resolving cognitive conflict.

Although a number of previous GoNogo studies have reported conflict and error-related ACC activation (Konishi et al. 1998; Menon et al. 2001; Garavan et al. 2003), they remained inconclusive with respect to a differential involvement of the 2 hemispheres. Whereas lateralization was not mentioned in the majority of studies, some groups reported a specialization of either the left (Rubia et al. 2001) or the right hemisphere (Garavan et al. 1999) for conflict monitoring. In agreement with our results, Taylor et al. (2006) found that in a Flanker task, high conflict activation foci of individual subjects tended to cluster in the right MFC, whereas brain responses to errors were distributed more bilaterally. Stephan et al. (2003) showed, by analyzing effective connectivity, that ACC in the hemisphere that was occupied with the task at hand, also mediated the influence of cognitive control on the involved regions. Accordingly, for a visuospatial interference task that involved the right hemisphere, right ACC was also involved in monitoring for conflict, whereas left ACC mediated cognitive control when subjects processed verbal stimuli. These results seem to be at odds with the findings in our study because we used letter stimuli but nevertheless found conflict-related activation in the right ACC. It is, however, unclear to what extent subjects processed single letters verbally. Indeed, when we contrasted successful inhibition with FAs at standard resolution, the active cluster in inferior parietal cortex was close to the visuospatial activation reported by Stephan et al. (2003) yielding maximum voxel coordinates of 46, −76, 34 versus 54, −64, 42. This suggests that our subjects may have been relying more on configurational cues in solving the task than on verbal information about the letters. Further evidence for such a speculation derives from several subjects' introspective report that they did not verbalize the letters during the experiment.

Taken together, our results are in broad agreement with 2 previous studies that investigated the hemispheric lateralization of cognitive control in ACC. Using high-resolution fMRI, however, we were able to show for the first time directly that the right part of rACC mediated cognitive control in a letter-based GoNogo task, whereas left rACC as well as dACC were more concerned with error processing. It remains a question for future research whether dissociation between right and left ACC can be shown for tasks that are explicitly verbal or spatial (such as word or spatial GoNogo paradigms). Furthermore, it would be interesting to see if the opposite hemisphere always continues to process error-related information (as in our study).

Such a scenario would be in accordance with current models of conflict monitoring and error processing (Yeung et al. 2004). Thus, the ACC in the task-dominant hemisphere is implicated in cognitive control and monitors for conflict. Once conflict rises above a certain threshold, an error is assumed and the contralateral ACC is activated to initiate error-related processing. This interpretation would also explain why, in our study, right rACC was more strongly activated for errors than for CRs because errors simply are envisaged as situations of very high conflict.

Why did so many previous imaging studies detect no or inconsistent lateralization results in ACC? Considering the close proximity of both cortices as well as standard fMRI methodology, the failure to reliably identify lateralization is not very surprising. The average distance between left and right ACC, which are only separated by the interhemispheric fissure, is on the order of 1 cm. It can be shown that, with an image resolution of $3 \times 3 \times 3$ mm^3 and the use of substantial spatial smoothing (Scouten et al. 2006), such as a Gaussian kernel of 5 mm FWHM, focal neural activations in left and right ACCs may become at least partly indistinguishable. Inaccuracies introduced by imperfect spatial normalization (Hellier et al. 2003) as well as group averaging and the considerable variability of ACC anatomy (Paus et al. 1996; Huster et al. 2007) may have further contributed to the discrepancies in previous studies.

Although the primary aim of our study was to investigate the functional anatomy of ACC at high spatial resolution, we also detected a region in right frontopolar cortex that responded significantly to successful inhibitions as well as FAs and therefore presumably plays a role in conflict monitoring processes. Previously, Carlson et al. (1998) observed frontopolar activation when contrasting conditions of high and low memory load in a visuospatial *n*-back task. Furthermore, in a Stroop task, activation of right frontopolar brain areas was associated with the incongruent condition (Zysset et al. 2001). These experiments, together with results from the current study, provide support for the idea that lateral prefrontal cortex plays an important role in neural processes associated with cognitive conflict. Furthermore, the similar patterns of activation in right ACC and frontopolar cortex are in line with the conflict monitoring hypothesis of anterior cingulate function (Botvinick et al. 2001; Botvinick et al. 2004). In this model, ACC is thought to monitor for cognitive conflict and recruit other brain regions, such as lateral prefrontal cortex, which bring about behavioral readjustments to minimize subsequent conflict.

fMRI at an effective resolution (including postacquisition smoothing) comparable with that employed in the present study has previously been used solely to investigate the functional organization in subregions of the early visual system (Schneider et al. 2004; Schwarzlose et al. 2005; Grill-Spector et al. 2006). Here we demonstrate the feasibility of such an approach for brain regions involved in higher level processes, such as cognitive control. Improving the spatial resolution by a factor of 8 enabled us to explore the functional organization of ACC at a previously unaccomplished spatial scale and to reveal a dissociation between left and right ACC that has not been directly observed with standard techniques. Consequently, it may turn out fruitful to revisit a number of paradigms that have been reported to elicit ACC activation including pain stimulation (Jones et al. 1991; Talbot et al. 1991; Koyama et al. 2005) or emotional processing (Whalen et al. 1998; Bush et al. 2000). We predict that at high resolution a number of regional specializations will become apparent for stimuli and tasks that have so far been mapped to overlapping locations. Furthermore, given the high functional and anatomical variability in ACC, we would recommend extensive analysis of single-subject data in addition to traditional group approaches.

Importantly, high-resolution fMRI should be considered as a complementary technique to standard neuroimaging rather than as a replacement. Whereas standard approaches provide the benefits of whole-brain coverage in a reasonable time frame, good signal-to-noise ratio, and also offer the opportunity to estimate functional connectivity, high-resolution fMRI is limited in these respects. Indeed, the technique may be envisaged as "zooming into" a region that was previously identified as active by established imaging strategies. Although this approach has been used routinely to study early visual processing, we present the first successful attempt, to our knowledge, of mapping a higher level brain area in this way. We believe that the "zooming in" fMRI strategy will provide a powerful new tool for cognitive neuroscientists. It may help bridging the gap between neuroimaging and electrode recording and thereby contribute to our understanding of the neural basis of cognition.

In summary, our findings demonstrate a functional specialization in ACC: whereas the right rACC is involved in conflict monitoring, its left part as well as dACC activated solely for error-related processes. More generally, our study illustrates the usefulness of high-resolution fMRI to identify functional specializations in higher level, cognitively driven brain areas.

Supplementary Material

Supplementary material can be found at http://www.cercor.oxfordjournals.org/.

Notes

We would like to thank Klaus-Dietmar Merboldt and Dirk Voit for their help with the imaging protocols as well as Renate Schweizer for her comments on the manuscript. Parts of the work were presented at the 36th Annual Meeting of the Society for Neuroscience (Atlanta, GA) in October 2006. *Conflict of Interest*: None declared.

Address correspondence to email: hluetck@gwdg.de.

References

Beckmann CF, Jenkinson M, Smith SM. 2003. General multilevel linear modeling for group analysis in FMRI. Neuroimage. 20:1052–1063.

Botvinick M, Nystrom LE, Fissell K, Carter CS, Cohen JD. 1999. Conflict monitoring versus selection-for-action in anterior cingulate cortex. Nature. 402:179–181.

Botvinick MM, Braver TS, Barch DM, Carter CS, Cohen JD. 2001. Conflict monitoring and cognitive control. Psychol Rev. 108:624–652.

Botvinick MM, Cohen JD, Carter CS. 2004. Conflict monitoring and anterior cingulate cortex: an update. Trends Cogn Sci. 8:539–546.

Bush G, Luu P, Posner MI. 2000. Cognitive and emotional influences in anterior cingulate cortex. Trends Cogn Sci. 4:215–222.

Carlson S, Martinkauppi S, Rama P, Salli E, Korvenoja A, Aronen HJ. 1998. Distribution of cortical activation during visuospatial n-back tasks as revealed by functional magnetic resonance imaging. Cereb Cortex. 8:743–752.

Carter CS, Braver TS, Barch DM, Botvinick MM, Noll D, Cohen JD. 1998. Anterior cingulate cortex, error detection, and the online monitoring of performance. Science. 280:747–749.

Devinsky O, Morrell MJ, Vogt BA. 1995. Contributions of anterior cingulate cortex to behaviour. Brain. 118(Pt 1):279–306.

Falkenstein M, Hohnsbein J, Hoormann J, Blanke L. 1991. Effects of crossmodal divided attention on late ERP components. 2. Error processing in choice reaction tasks. Electroencephalogr Clin Neurophysiol. 78:447–455.

Garavan H, Ross TJ, Kaufman J, Stein EA. 2003. A midline dissociation between error-processing and response-conflict monitoring. Neuroimage. 20:1132–1139.

Garavan H, Ross TJ, Stein EA. 1999. Right hemispheric dominance of inhibitory control: an event-related functional MRI study. Proc Natl Acad Sci USA. 96:8301–8306.

Gehring WJ, Goss B, Coles MGH, Meyer DE, Donchin E. 1993. A Neural system for error-detection and compensation. Psychol Sci. 4:385–390.

Genovese CR, Lazar NA, Nichols T. 2002. Thresholding of statistical maps in functional neuroimaging using the false discovery rate. Neuroimage. 15:870–878.

Grill-Spector K, Sayres R, Ress D. 2006. High-resolution imaging reveals highly selective nonface clusters in the fusiform face area. Nat Neurosci. 9:1177–1185.

Hellier P, Barillot C, Corouge I, Gibaud B, Le Goualher G, Collins DL, Evans A, Malandaln G, Ayache N, Christensen GE, et al. 2003. Retrospective evaluation of intersubject brain registration. IEEE Trans Med Imaging. 22:1120–1130.

Huster RJ, Westerhausen R, Kreuder F, Schweiger E, Wittling W. 2007. Morphologic asymmetry of the human anterior cingulate cortex. Neuroimage. 34:888–895.

Jenkinson M, Bannister P, Brady M, Smith S. 2002. Improved optimization for the robust and accurate linear registration and motion correction of brain images. Neuroimage. 17:825–841.

Jenkinson M, Smith S. 2001. A global optimisation method for robust affine registration of brain images. Med Image Anal. 5:143–156.

Jones AKP, Brown WD, Friston KJ, Qi LY, Frackowiak RSJ. 1991. Cortical and subcortical localization of response to pain in man using positron emission tomography. Proc R Soc Lond B Biol Sci. 244:39–44.

Kiehl KA, Liddle PF, Hopfinger JB. 2000. Error processing and the rostral anterior cingulate: an event-related fMRI study. Psychophysiology. 37:216–223.

Konishi S, Nakajima K, Uchida I, Sekihara K, Miyashita Y. 1998. No-go dominant brain activity in human inferior prefrontal cortex revealed by functional magnetic resonance imaging. Eur J Neurosci. 10: 1209–1213.

Koyama T, McHaffie JG, Laurienti PJ, Coghill RC. 2005. The subjective experience of pain: where expectations become reality. Proc Natl Acad Sci USA. 102:12950–12955.

Menon V, Adleman NE, White CD, Glover GH, Reiss AL. 2001. Error-related brain activation during a Go/NoGo response inhibition task. Hum Brain Mapp. 12:131–143.

Paus T, Tomaiuolo F, Otaky N, MacDonald D, Petrides M, Atlas J, Morris R, Evans AC. 1996. Human cingulate and paracingulate sulci: pattern, variability, asymmetry, and probabilistic map. Cereb Cortex. 6: 207–214.

Polli FE, Barton JJ, Cain MS, Thakkar KN, Rauch SL, Manoach DS. 2005. Rostral and dorsal anterior cingulate cortex make dissociable contributions during antisaccade error commission. Proc Natl Acad Sci USA. 102:15700–15705.

Ridderinkhof KR, Ullsperger M, Crone EA, Nieuwenhuis S. 2004. The role of the medial frontal cortex in cognitive control. Science. 306: 443–447.

Ridderinkhof KR, van den Wildenberg WPM, Segalowitz SJ, Carter CS. 2004. Neurocognitive mechanisms of cognitive control: the role of prefrontal cortex in action selection, response inhibition, performance monitoring, and reward-based learning. Brain Cogn. 56: 129–140.

Rubia K, Russell T, Overmeyer S, Brammer MJ, Bullmore ET, Sharma T, Simmons A, Williams SC, Giampietro V, Andrew CM, et al. 2001. Mapping motor inhibition: conjunctive brain activations across different versions of go/no-go and stop tasks. Neuroimage. 13: 250–261.

Schneider KA, Richter MC, Kastner S. 2004. Retinotopic organization and functional subdivisions of the human lateral geniculate nucleus: a high-resolution functional magnetic resonance imaging study. J Neurosci. 24:8975–8985.

Schwarzlose RF, Baker CI, Kanwisher N. 2005. Separate face and body selectivity on the fusiform gyrus. J Neurosci. 25:11055–11059.

Scouten A, Papademetris X, Constable RT. 2006. Spatial resolution, signal-to-noise ratio, and smoothing in multi-subject functional MRI studies. Neuroimage. 30:787–793.

Smith SM. 2002. Fast robust automated brain extraction. Hum Brain Mapp. 17:143–155.

Smith SM, Brady JM. 1997. Susan—a new approach to low level image processing. Int J Comput Vis. 23:45–78.

Stephan KE, Marshall JC, Friston KJ, Rowe JB, Ritzl A, Zilles K, Fink GR. 2003. Lateralized cognitive processes and lateralized task control in the human brain. Science. 301:384–386.

Talbot JD, Marrett S, Evans AC, Meyer E, Bushnell MC, Duncan GH. 1991. Multiple representations of pain in human cerebral-cortex. Science. 251:1355–1358.

Taylor SF, Martis B, Fitzgerald KD, Welsh RC, Abelson JL, Liberzon I, Himle JA, Gehring WJ. 2006. Medial frontal cortex activity and loss-related responses to errors. J Neurosci. 26:4063–4070.

Ullsperger M, von Cramon DY. 2004. Neuroimaging of performance monitoring: error detection and beyond. Cortex. 40:593–604.

Whalen PJ, Bush G, McNally RJ, Wilhelm S, McInerney SC, Jenike MA, Rauch SL. 1998. The emotional counting stroop paradigm: a functional magnetic resonance imaging probe of the anterior cingulate affective division. Biol Psychiatry. 44:1219–1228.

Woolrich MW, Behrens TEJ, Beckmann CF, Jenkinson M, Smith SM. 2004. Multilevel linear modelling for FMRI group analysis using Bayesian inference. Neuroimage. 21:1732–1747.

Woolrich MW, Ripley BD, Brady M, Smith SM. 2001. Temporal autocorrelation in univariate linear modeling of FMRI data. Neuroimage. 14:1370–1386.

Worsley KJ, Evans AC, Marrett S, Neelin P. 1992. A three-dimensional statistical analysis for CBF activation studies in human brain. J Cereb Blood Flow Metab. 12:900–918.

Yeung N, Botvinick MM, Cohen JD. 2004. The neural basis of error detection: conflict monitoring and the error-related negativity. Psychol Rev. 111:931–959.

Zysset S, Muller K, Lohmann G, von Cramon DY. 2001. Color-word matching stroop task: separating interference and response conflict. Neuroimage. 13:29–36.

Appendix 3

The Journal of Neuroscience, July 5, 2006 • 26(27):7129–7130 • 7129

Journal Club

Editor's Note: These short reviews of a recent paper in the *Journal*, written exclusively by graduate students or postdoctoral fellows, are intended to mimic the journal clubs that exist in your own departments or institutions. For more information on the format and purpose of the Journal Club, please see http://www.jneurosci.org/misc/ifa_features.shtml.

Parcellating the Medial Frontal Cortex: Evaluative and Cognitive Components of Performance Monitoring

Henry Lütcke

Max-Planck-Institut für Biophysikalische Chemie, Biomedizinische NMR Forschungs GmbH, 37070 Göttingen, Germany

Review of Taylor et al. (http://www.jneurosci.org/cgi/content/full/26/15/4063)

One of the hallmarks of human behavior is flexibility and a capacity to adapt to new situations. When external circumstances or internal goals change, behavior must be modified in such a way that new requirements are met. Cognitive control plays an instrumental role in overriding previously established and easily retrieved action patterns in favor of task-appropriate, yet novel and unlearned responses. As an example, imagine traveling from the United States or continental Europe to the United Kingdom. When crossing a street, you will now have to inhibit a highly overlearned and prepotent response to look first to the left, then to the right to initiate the appropriate opposite sequence of actions. Note that in this example, unchecked errors may have potentially disastrous consequences, highlighting the importance of cognitive control and error detection mechanisms in the real world.

There is now substantial evidence, mainly from functional magnetic resonance imaging (fMRI) and event-related potentials (ERPs) implicating the medial frontal cortex (MFC) as an important neural substrate of cognitive control mechanisms in the human brain (Ullsperger and von Cramon, 2004). Although activation of MFC is considered to be one of the most reliable neural correlates of cognitive effort, its functional significance is a matter of hot debate. Whereas initial evidence from ERP studies suggested that MFC [especially anterior cingulate cortex (ACC)] might serve as an error detector (Gehring et al., 1993), other experiments using fMRI indicated a broader function of this region in conflict monitoring (Carter et al., 1998). Furthermore, MFC activity might signify an emotional response to errors (Luu et al., 2003). Finally, substantial disagreement exists concerning the specific localization of activity within the region.

A recent study by Taylor et al. (2006) in *The Journal of Neuroscience* goes a long way toward resolving some of the open questions concerning MFC function. Using fMRI and an elegant experimental design, they were able to identify a region in MFC that selectively processes evaluative responses to errors. Furthermore, exhaustive analysis of the collected data based on single-subject results revealed surprising new insights into the localization of error- and conflict-related activations in MFC.

Taylor et al. (2006) presented subjects with strings of letters in which they were asked to identify the odd letter ("target") by either a right or left button press. To manipulate the degree of interference, distracter letters in a string could either be associated with the same ("low" interference) or opposite ("high" interference) button press. Crucially, the emotional valence of each trial was manipulated shortly before stimulus onset. In "gain" trials, subjects could win money if they identified the target within the deadline, whereas "loss" trials signified a financial penalty in case of incorrect response. Finally, during "neutral" trials, no money could be won or lost [Taylor et al. (2006), their Fig. 1 (http://www.jneurosci.org/cgi/content/full/26/15/4063/F1)]. Humans tend to avoid losses more than seek gains ("loss aversion"); thus, the authors reasoned that loss trials would be emotionally more engaging for subjects than gain or neutral trials. Unfortunately, only indirect evidence is provided in support of their logic. The majority of participants reported having tried harder on incentivized compared with neutral trials, and some subjects confirmed that they spent more effort on loss than gain trials. To ensure that loss-related errors did indeed elicit affective responses in subjects, physiological measures such as skin conductance should be reported.

For the purpose of data analysis, Taylor et al. (2006) subdivided the medial frontal cortex into three areas: posterior MFC (corresponding roughly to the pre-supplementary motor area (pre-SMA) and parts of dorsal ACC), mid-MFC (situated in the dorsal ACC) and rostral ACC (rACC) [Taylor et al. (2006), their Fig. 3*a–c* (http://www.jneurosci.org/cgi/content/full/26/15/4063/F3)]. To identify brain regions processing affective reactions to errors, activation attributable to loss errors was contrasted with hemodynamic responses after neutral trials. This strategy revealed a focus in the rACC that was not activated for "failure-to-gain"

Received May 24, 2006; revised May 26, 2006; accepted May 26, 2006.

Correspondence should be addressed to Henry Lütcke, Max-Planck-Institut für Biophysikalische Chemie, Biomedizinische NMR Forschungs GmbH, Am Fassberg 11, 37070 Göttingen, Germany. E-mail: hluetck@gwdg.de.

DOI:10.1523/JNEUROSCI.2196-06.2006

 0270-6474/06/267129-02$15.00/0

errors [Taylor et al. (2006), their Fig. 3*a*,*b* (http://www.jneurosci.org/cgi/content/full/26/15/4063/F3)].

To exclude a simple effect of motivation in rACC (remember that several subjects reported trying harder when an incentive was given), Taylor et al. (2006) compared correct and erroneous loss trials and confirmed that rACC was activated stronger after errors. Furthermore, they identified an area in mid-MFC that was activated stronger for incentivized correct responses (gain or loss) than for successful target identification on neutral trials [Taylor et al. (2006), their Fig. 3*f* (http://www.jneurosci.org/cgi/content/full/26/15/4063/F3)]. Such an activation pattern would be expected for brain regions associated with enhanced effort exerted during trials in which money could be won or lost. While rACC and mid-MFC seemed to be concerned with the emotional and motivational aspects of the experimental paradigm, posterior parts of the medial frontal cortex showed an altogether different pattern of activation. Although a cluster in the vicinity of pre-SMA also responded to errors, this region was much more active during the high interference condition (when target letters were incongruent to the distracters) compared with low interference trials. Moreover, posterior MFC activation was not contingent on incentive condition [Taylor et al. (2006), their Fig. 4 (http://www.jneurosci.org/cgi/content/full/26/15/4063/F4)]. Both error commission and high interference trials present instances of increased cognitive conflict. It therefore seems reasonable to assume that the pre-SMA cluster corresponds to a conflict monitoring module previously identified in ACC (Carter et al., 1998).

By devising an experimental paradigm that aimed at assessing subjects' affective responses, their motivational state, and the cognitive load of the task, Taylor et al. (2006) established that MFC, far from being a functionally homogenous structure, contains several distinct cortical modules. Their evidence suggests that although dorsal aspects are involved in cognitive components of performance monitoring, more rostral parts play a role in evaluative aspects of behavior.

These results, however, do not explain why several previous studies using cognitive interference tasks have reported activation foci that differ significantly from each other in their location along the dorsal–rostral MFC axis. To approach this issue, Taylor et al. (2006) evaluated activation maps of single subjects, rather than just the averaged group results. Amazingly, they found that individual foci for errors extended over the whole range of medial frontal cortex, clustering somewhat in dorsal and rostral parts [Taylor et al. (2006), their Fig. 5*b* (http://www.jneurosci.org/cgi/content/full/26/15/4063/F5)]. Correspondingly, subject-level analysis for cognitive conflict (high vs low interference) also revealed a substantial variability in cluster location, although more limited to the posterior part of the MFC [Taylor et al. (2006), their Fig. 5*a* (http://www.jneurosci.org/cgi/content/full/26/15/4063/F5)]. These striking results immediately suggest that discrepancies in the localization of error- or conflict-related processes between previous studies may actually be attributable to differential clustering of subjects' activation in the different samples, yielding incompatible group results. Even more importantly, these results call into question the very idea of a consistent cortical localization of higher cognitive functions for different individuals.

To summarize, Taylor et al. (2006) provided conclusive evidence for a functional heterogeneity of MFC. Whereas rACC is more concerned with evaluative components of error commission, posterior parts of this brain region seem to be specialized for monitoring and resolving cognitive conflict. Furthermore, the authors showed a surprising degree of variability in conflict and error processing between different subjects. Understanding the factors influencing this variability will be a major goal for future neuroimaging studies.

References

Carter CS, Braver TS, Barch DM, Botvinick MM, Noll D, Cohen JD (1998) Anterior cingulate cortex, error detection, and the online monitoring of performance. Science 280:747–749.

Gehring WJ, Goss B, Coles MGH, Meyer DE, Donchin E (1993) A neural system for error-detection and compensation. Psychol Sci 4:385–390.

Luu P, Tucker DM, Derryberry D, Reed M, Poulsen C (2003) Electrophysiological responses to errors and feedback in the process of action regulation. Psychol Sci 14:47–53.

Taylor SF, Martis B, Fitzgerald KD, Welsh RC, Abelson JL, Liberzon I, Himle JA, Gehring WJ (2006) Medial frontal cortex activity and loss-related responses to errors. J Neurosci 26:4063–4070.

Ullsperger M, von Cramon DY (2004) Neuroimaging of performance monitoring: error detection and beyond. Cortex 40:593–604.